A Co-Channel Interference Cancellation Technique using Orthogonal Convolutional Code

Yukitoshi Sanada
B.E., Keio University 1992

A Thesis Submitted in Partial Fulfillment of the
Requirement for the Degree of

MASTER OF APPLIED SCIENCE

in the Department of
Electrical and Computer Engineering

We accept this thesis as conforming
to the required standard

[redacted]

Dr. Qiang Wang, Supervisor
(Department of Electrical and Computer Engineering)

[redacted]

Dr. Vijay K. Bhargava, Departmental Member
(Department of Electrical and Computer Engineering)

[redacted]

Dr. Wendy Myrvold, Outside Member
(Department of Computer Science)

[redacted]

Dr. Hiroyuki Yashima, External Examiner
(Department of Infomation and Computer Siences, Saitama University)

Supervisor: Dr. Qiang Wang

ABSTRACT

In this thesis a new parallel co-channel interference cancellation technique which utilizes orthogonal convolutional codes is proposed and investigated.

In a spread spectrum multiple access environment, co-channel interference (CCI) limits the performance of the communication link. To remove this interference, several CCI cancellation techniques have been proposed, including those techniques which do not require the receiver to have knowledge of the cross-correlation between user sequences. These methods leave residual interference after the cancellation caused by errors on the initial decisions.

To improve the initial decisions and reduce the residual interference, the proposed scheme utilizes the error correcting capability of the orthogonal convolutional code. It is shown that the proposed CCI canceller offers an improvement in capacity by a factor of 1.5 ~ 3 as compared with a conventional canceller on AWGN channel and multipath Rayleigh fading channel. The proposed canceller works in the presence of residual interference due to imperfect cancellation. The proposed canceller also has a capacity improvement with the use of soft handoff in a multicell configuration.

Examiners:

[redacted]

Dr. Qiang Wang, Supervisor
(Department of Electrical and Computer Engineering)

[redacted]

Dr. Vijay Bhargava, Departmental Member
(Department of Electrical and Computer Engineering)

[redacted]

Dr. Wendy Myrvold, Outside Member
(Department of Computer Science)

[redacted]

Dr. Hiroyuki Yashima, External Examiner
(Department of Infomation and Computer Siences, Saitama University)

Table of Contents

List of Figures

List of Tables

Acknowledgments

I would like to express my sincere appreciation to, my supervisor, Professor Qiang Wang, whose guidance, support, and encouragement made my study fruitful, and I would also like to express my thanks to Professor Vijay K. Bhargava for his unfailing support in my research endeavors.

Thanks also to my colleagues in the Department of Electrical and Computer Engineering at the University of Victoria, especially Dr. Muzhong Wang, Mr. Greg Robertson, and Mr. Ron Kerr for stimulating discussions, proofreading the manuscript, and suggesting improvements.

Finally, special thanks are due to my mother, Emiko Sanada, who has been living by herself for almost three worrisome years filled with loneliness.

To My Parents

Chapter 1: Introduction

1.1 Background

The research described in this thesis is a part of a project to determined efficient methods for high rate packet transmission of integrated traffic over wireless cellular code division multiple access (CDMA) systems[1]. The integrated traffic compromises voice, video, and data traffic typical for multi-media services.

As the required bit error rate (BER) for multi-media communication was very low, present CDMA systems cannot support enough users. Therefore, a new co-channel interference cancellation technique is proposed in this thesis to increase a capacity of the CDMA system. The proposed cancellation technique utilizes the error correcting capability of orthogonal convolutional codes to accommodate more users than a conventional cancellation technique.

In this chapter, introduction of thesis, general concepts of a cellular CDMA system and multiuser detection are described.

1.2 General Concepts of Code Division Multiple Access

Recently direct sequence spread spectrum (SS/DS) systems have received a large amount of attention in wireless and cellular communication applications. One of the primary reasons is that SS/DS systems can provide the reliable communications with privacy and security even in multipath fading and a hostile jamming environment[2, Vol. 1].

Figure 1.1 shows the block diagram of a basic SS/DS system. The spreading circuit spreads the spectrum by modulating (multiplying) the digital data bits with a pseudo noise (PN) sequence of very high chip rate. Due to the high rate of the sequence, the bandwidth after the modulation is much wider than the bandwidth of the original information. The PN

sequence used in the SS/DS modulation is a unique code like white-noise which is assigned to each user in advance. At the receiver, multiplication of the received signal by the receiver's local PN sequence replica removes the spreading PN sequence multiplied at the transmitter, and thereby the original narrowband encoded data signal is demodulated.

The other reason for the popularity of DS/SS systems is the possibility of achieving a greater capacity per unit bandwidth (frequency utilization efficiency) with CDMA than with frequency division multiple access (FDMA) or time division multiple access (TDMA). A typical CDMA system is shown in Figure 1.2. In the CDMA system, a group of individual signals can be multiplexed onto a communication medium via a set of PN sequences. Each of PN sequences identifies a user. For example, suppose user 1 has the PN 1 and the user 2 through K have the PN 2 to PN K. If the receiver wants to listen to user 1, the receiver can despread only user 1's signal though it receives signals transmitted by all of the users. The receiver sees all the energy of user 1 and will experience interference from other users. This interference owing to other users is called co-channel interference (CCI). Unlike FDMA and TDMA capacities which are primarily bandwidth limited, CDMA capacity is CCI limited[3].

1.3 Cellular CDMA System

The original proposal for a cellular system was made by AT&T in 1968 in a submission to the FCC which resulted in Docket 18262 [4]. The basic objectives of the cellular system were to provide mobile telephone service nationally and to accommodate a large number of subscribers.

A single radio cell and the factors that dictate coverage are illustrated in Figure 1.3. The base station with which radio connection takes place is usually in a clear commanding position, and has an appropriate power, and a sensitive receiver with a low noise figure, minimal site noise, and usual antenna gain. The mobile station which denotes the radio

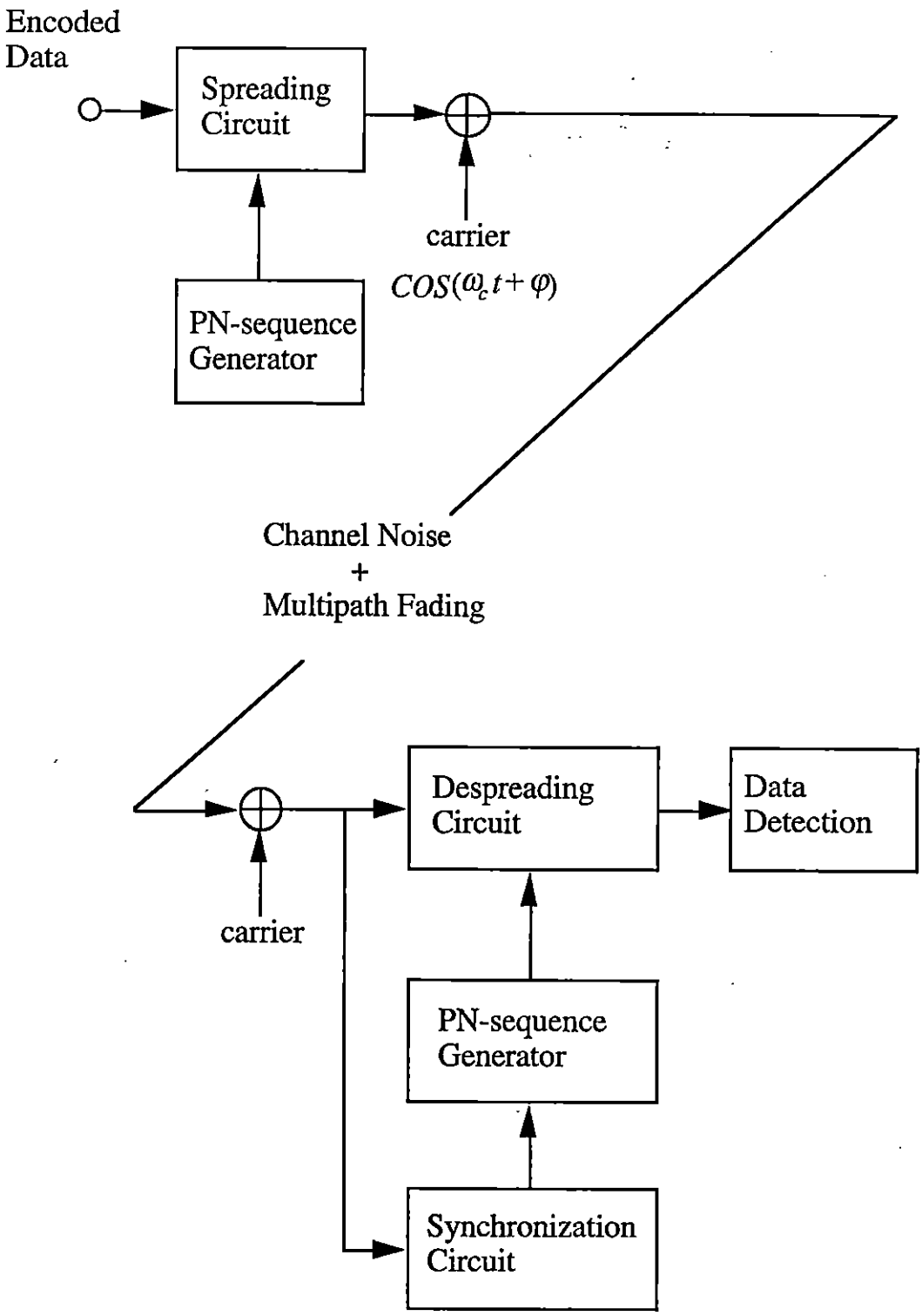

Figure 1.1 Block Diagram of a Basic SS/DS System.

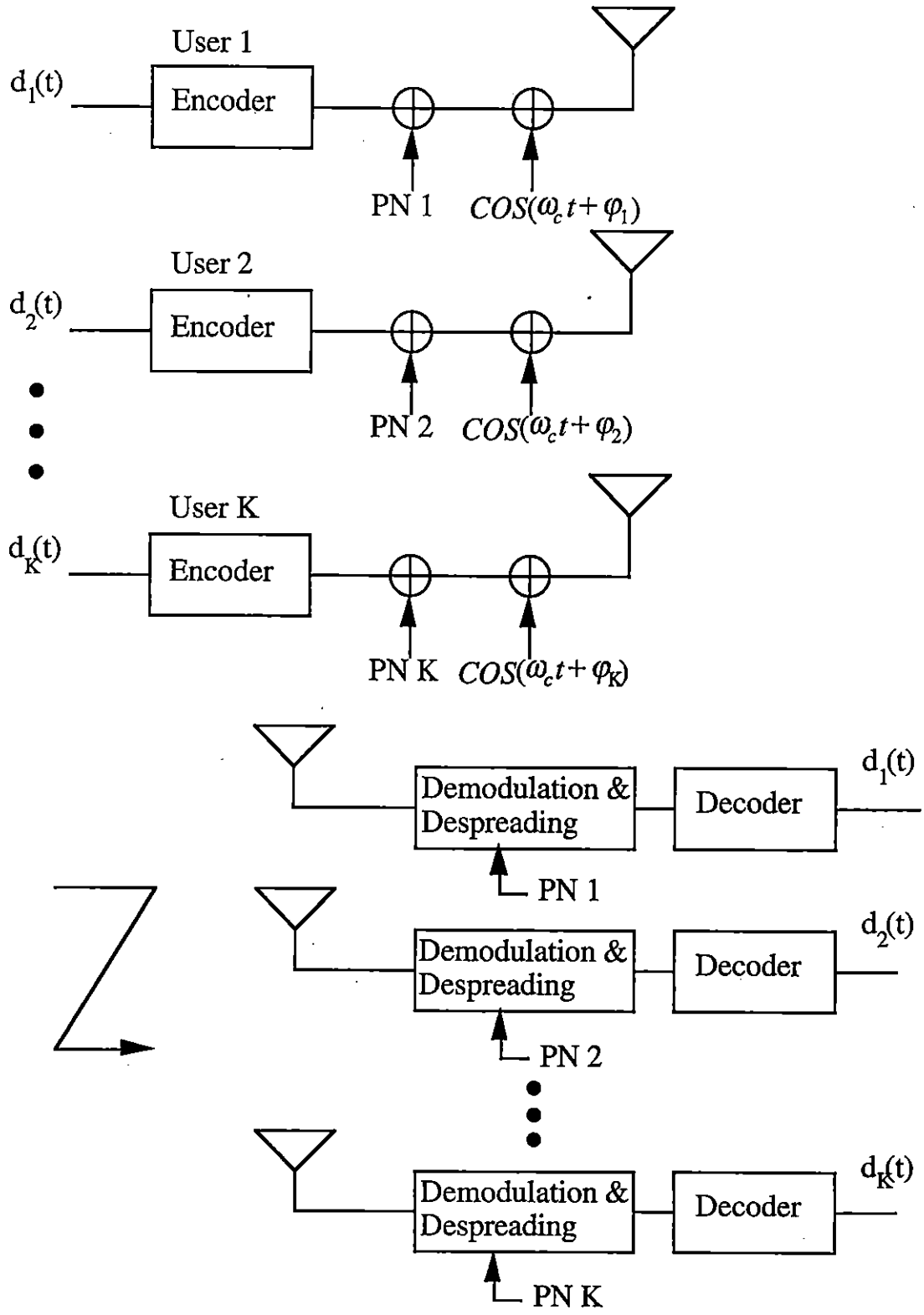

Figure 1.2 Block Diagram of a CDMA System.

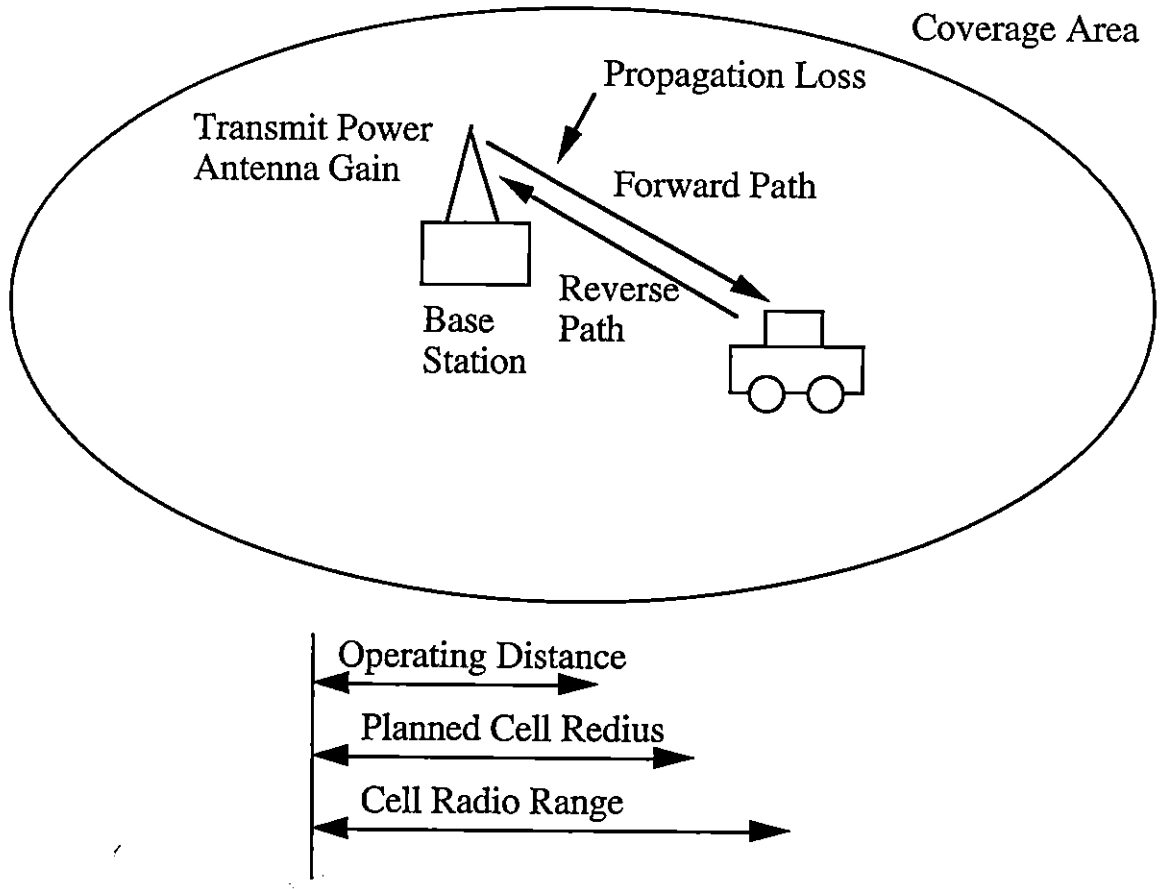

Figure 1.3 The Fundamental Radio Cell and Assosiated Parameters showing a Base Station and Mobile Station.

telephone, has limited transmitter power, especially in the portable mode, and an elementary antenna.

Basic elements of the cellular concept are cell splitting and frequency reuse. Regarding the cell splitting, the regular hexagonal shape is usually adopted for the economical reason. Suppose the worst case point is the point farthest from the nearest base station. If an equilateral triangle, a square, and a regular hexagon all have the same center-to-vertex distance, the hexagon has a substantially larger area. Consequently, to serve mobile stations in a given total coverage area, a hexagonal layout requires fewer cells,

hence fewer base stations. A system based on hexagonal cells therefore costs less than one with triangular or square cells, all other factors being equal.

Frequency reuse refers to the use of radio channels on the same carrier frequency to cover different areas which are separated from one another so that co-channel interference is not objectionable. The number of cells per cluster which uses different frequencies is called the frequency reuse factor. As an example, in the case of analog cellular system, the frequency reuse factor is 7.

In terms of the radio frequency usage, the CDMA system can be seen as a one-cell system since the same frequency is reused by all cells, and so the frequency reuse factor appears to be 1. When a service area consists of many cells, the channel capacity per CDMA cell decreases as a result of the excessive interference from other cells. However, CDMA cellular system can still achieve greater capacity than other digital cellular systems [5].

1.4 Multiuser Detection

To increase CDMA capacity, a detection scheme which utilizes received signals of multiple users has been developed for more than ten years. This detection scheme is called multiuser detection[6]. The optimum detector (minimum error probability detector) was proposed by Verdu[7], which consists of a matched filter front-end followed by a Viterbi algorithms. Although notable performance gains are obtained, the detector requires the signature waveforms and the received signal amplitudes of all users and its complexity grows exponentially with the number of users.

Suboptimum multiuser detectors whose complexities are less than the optimal multiuser detector have also been considered. In [8], sequential decoding is applied instead of the Viterbi algorithm as used in the optimal detector. In [9], [10], [11], and [12], the decorrelating detector, which multiplies the inverse cross-correlation matrix with the

matched filter outputs, has been investigated. In [13], the decorrelator is combined with a decision-feedback detector. Although these multiuser detectors show performance close to the optimum detector with reasonable computation, these detectors must calculate the inverse cross-correlation matrix. In [14], the minimum mean-square error (MMSE) detector was proposed, which calculates the inverse matrix adaptively. This detector outperforms the decorrelating detector when the background noise dominates the performance. However, it requires a training sequence. The requirement of training sequences in the multiuser detectors is really cumbersome. In [15][16], tentative-decision based multiuser detectors have been investigated. In a multistage structure, the first stage consists of a bank of conventional detectors. The second and third stages assume that the previous decisions are correct, calculate the co-channel interference (CCI) caused by undesired users' signals, and remove them from the correlator output of the desired user's signal.

1.5 IS-95 and CCI Cancellation

The multiuser detectors mentioned in Section 1.4 require the receiver to have , *a prior* or through training, the knowledge of the sequences' cross-correlation. Unfortunately, they are not useful if long PN sequences are used as signature sequences to separate the users' channels since the cross-correlation varies with different phases of the signature sequence. If the receiver has to calculate the cross-correlation for each symbol, the computational complexity grows exponentially with the number of users.

One example of a CDMA system which employs long PN sequences is specified in IS-95 (North American Digital Cellular Standard)[17]. Figure 1.4 is the structure of the reverse link (mobile to base station) transmitter. The data is encoded by the rate 1/3 orthogonal convolutional code of the constraint length 9 [18]. The coded symbols are interleaved and then 6 symbols are assigned to one orthogonal code. Then the orthogonal

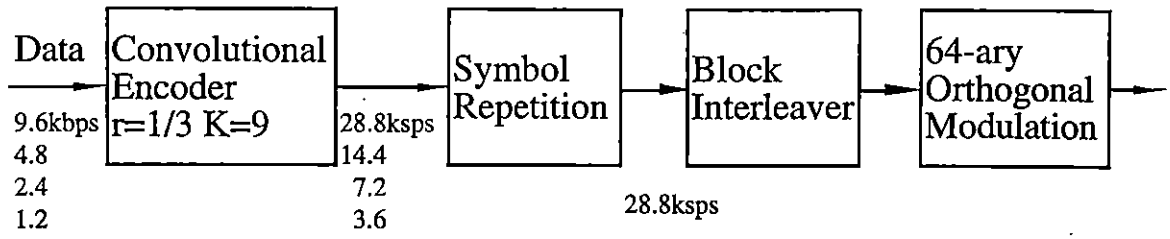

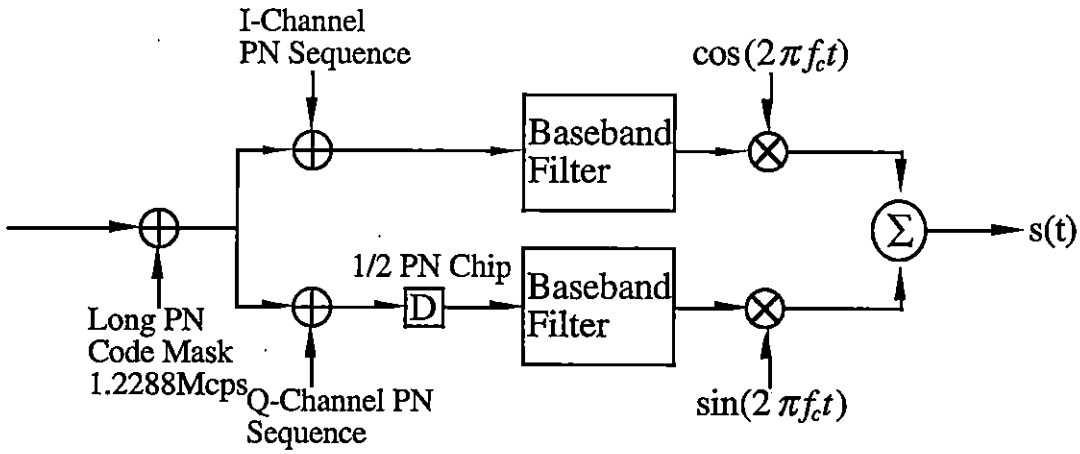

Figure 1.4 Structure of the Reverse Link Transmitter specified by IS-95.

sequence is multiplied by the part of I, Q long PN sequences and modulated using Offset-QPSK (OQPSK).

If a multiuser detector is implemented in the base station, it should not require the knowledge of the sequences' cross-correlation. Multiuser detection methods which do not use the knowledge of the sequences' cross-correlation and whose complexity grows only linearly with the number of users, have also been proposed [19], [20]. In [20], users are detected all at once while in [19] they are detected successively. In these methods the receiver reconstructs other users' transmitted signals by using initial decisions about other users' signals. These receivers then use the estimates (reconstructed signals) to remove CCI from the composite received signal. These methods do not require the knowledge of the cross-correlation between the spreading codes. However, there is residual interference due to symbol errors in the initial decision [21], [22]. The performance of the canceller depends on the performance of the initial decision. Therefore, it is desirable to improve the accuracy of the initial decision.

In this thesis, a parallel CCI cancellation technique which utilizes orthogonal convolutional codes is proposed. In this method, received signals are both demodulated and decoded. Then the resulting bit streams are re-encoded and re-spread to be subtracted from the composite received signals. On account of the error correcting capability of orthogonal convolutional codes, the residual interference is decreased. In other words, the proposed canceller makes one initial decision over several symbols. Thus, the BER performance can be improved. Since decoding of the orthogonal convolutional codes increases the processing delay, this system is primarily for data communications.

It is at least theoretically interesting to note that a scheme proposed in 1990 by Viterbi [23] combining the successive CCI cancellation with an orthogonal convolutional code has been shown to be able to achieve the Shannon capacity. The implementation complexity of this scheme for successively decoding signals of all users remains to be a

concern, especially at high data rate. In addition, it requires very accurate power control to make all the users have equitable performance.

1.6 Thesis Outline

This thesis consists of five chapters. This chapter, Chapter 1, has presented the general concepts of CDMA and multiuser detection. In Chapter 2, the concepts of the conventional and the proposed CCI cancellers are described. Chapter 2 also introduces the structure of orthogonal convolutional codes, which is an important element of the proposed canceller. In Chapter 3, performance of both cancellers on an additive white Gaussian noise (AWGN) channel is derived. Simulation results and theoretical performance results are shown. Chapter 4, shows the performances of the cancellers on a multipath Rayleigh fading channel. Finally, conclusions are presented in Chapter 5.

Chapter 2: Co-Channel Interference Cancellation Techniques

2.1 Orthogonal Convolutional Codes

2.1.1 Encoder

The orthogonal convolutional code, which is used in the CDMA system specified by IS-95 and is the key element of the proposed cancellation technique, was first introduced by Trumpis[18] for an *M-ary* channel. Instead of employing *M-ary* channels, *M-ary* orthogonal codes are applied for the CDMA system. These rate 1 *M-ary* convolutional codes are analogous to rate $1/\log_2 M$ binary convolutional codes.

The encoder shown in Figure 2.1 is a linear finite-state machine consisting of a n_A-stage binary shift resister and $\log_2 M$ modulo-2 adders connected to the shift register stages.

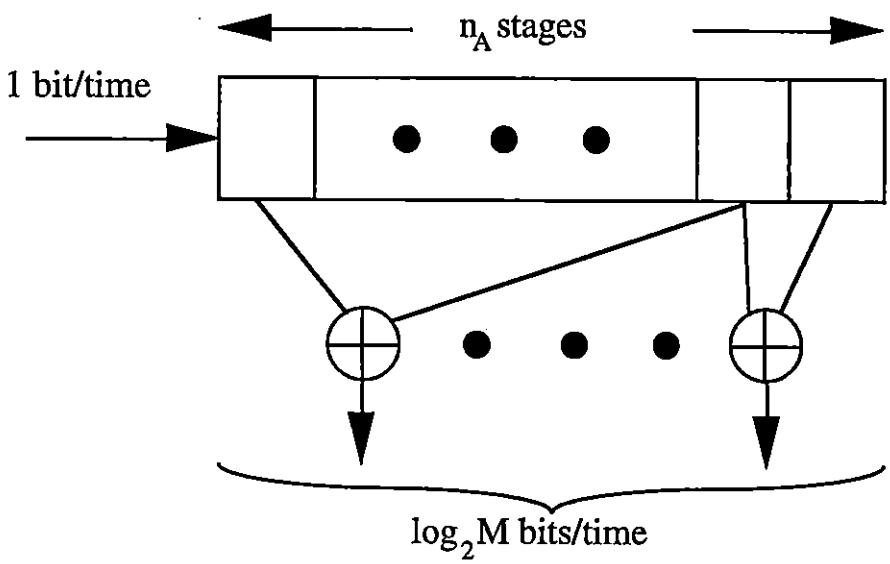

Figure 2.1 The General Rate 1, Constraint Length n_A, *M-ary* Convolutional Encoder.

The binary input data is shifted through the register one bit at a time. After each shift the contents of the register stages are combined as determined by the connections to form a binary (log_2M)-tuple. The encoding equations in matrix form are given by

$$v = uG \tag{2.1}$$

where u is the information sequence, v is the output sequence, and G is the generator matrix given by

$$\mathbf{G} = \begin{bmatrix} \mathbf{G_0} & \mathbf{G_1} & \mathbf{G_2} & \cdots & \mathbf{G_{n_A-1}} & & \\ & \mathbf{G_0} & \mathbf{G_1} & \mathbf{G_2} & \cdots & \mathbf{G_{n_A-1}} & \\ & & \ddots & & & & \ddots \\ & & & \ddots & & & \end{bmatrix} \tag{2.2}$$

where each $\mathbf{G}_\ell$ is a (log_2M) by i submatrix whose entries are

$$\mathbf{G}_\ell = \left[g_\ell^{(1)} \quad g_\ell^{(2)} \quad \cdots \quad g_\ell^{(\log_2 M)} \right] \tag{2.3}$$

where $g_\ell^{(i)}$ is 1 if there is a tap from i-th register to the ℓ-th modulo-2 adder, and is 0 other wise.

The (log_2M)-tuple corresponds to one of the *M-ary* orthogonal codewords generated by the Walsh function (*8-ary* orthogonal codewords are shown in Table 2.1)[17].

	0	1	2	3	4	5	6	7
0	0	0	0	0	0	0	0	0
1	0	1	0	1	0	1	0	1
2	0	0	1	1	0	0	1	1
3	0	1	1	0	0	1	1	0
4	0	0	0	0	1	1	1	1
5	0	1	0	1	1	0	1	0
6	0	0	1	1	1	1	0	0
7	0	1	1	0	1	0	0	1

Table 2.1 8-ary Orthogonal Codewords

2.1.2 State Diagram and Minimum Distance

The state of the encoder is defined as the contents of the left-most n_A-1 stages of the shift register, making the total number of states equal to 2^{n_A-1}. When encoding, the shift register makes transitions from one state to another with every new input bit. These transitions are expressed by a state diagram. An example of an encoder and its state diagram is shown in Figure 2.2. X_0, X_1, X_2, X_3, and X_0' are assumed to be different states of the encoder. Every transition is labeled by the function N^iD^j where i=0 or 1 if the input bit is 0 or 1, and j=0 or 1 if the code symbol is zero or nonzero.

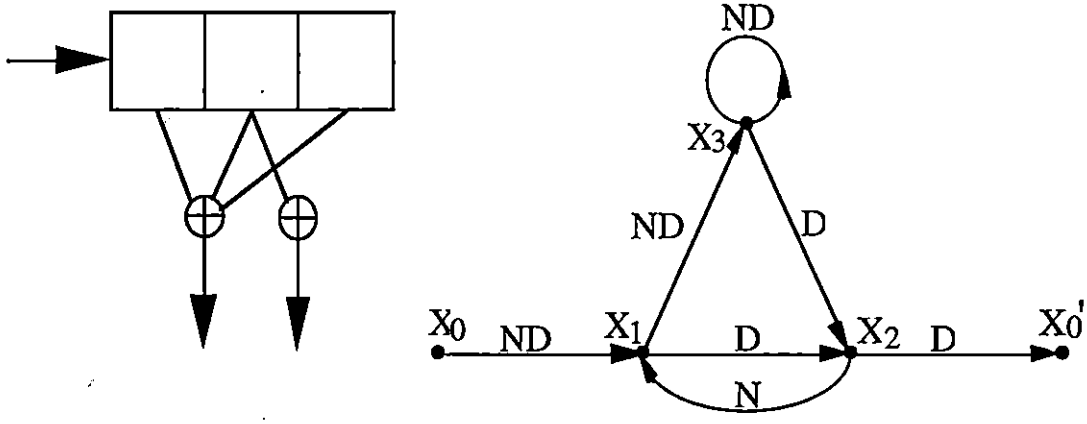

Figure 2.2 Example of a 4-ary Encoder and its State Diagram.

An important concept in coding is the distance between codewords. Define the distance between two codewords as the number of *M-ary* symbol positions in which they disagree. The performance of coding depends on the decoder and the distance property of the code. The minimum distance from the state X_0 to the state X_0' is called the code's free distance, d_{free}.

2.1.3 Transfer Function and Performance Bound

The distance properties and the error rate performance of a convolutional code can be obtained from its state diagram. The state diagram shown in Figure 2.2 will be used to

demonstrate the method for obtaining the distance properties of an orthogonal convolutional code. From Figure 2.2,, the four state equations are obtained;

$$X_1 = NDX_0 + NX_2 \quad , \tag{2.4}$$

$$X_2 = DX_1 + DX_3 \quad , \tag{2.5}$$

$$X_3 = NDX_1 + NDX_3 \quad , \tag{2.6}$$

$$X_0' = DX_2 \quad . \tag{2.7}$$

The transfer function for the code is defined as $T(D,N)=X_0'/X_0$. By solving the state equation given above, the transfer function is

$$T(D,N) = \frac{ND^3}{1-2ND} \quad . \tag{2.8}$$

The series form is then

$$T(D,N) = ND^3 + 2N^2D^4 + 4N^3D^5 + \ldots + 2^{d-3}N^{d-2}D^d + \ldots \quad . \tag{2.9}$$

Now define the general form of the transfer function by

$$T(D,N) = \sum_{d=d_{free}}^{\infty} A_d(N) D^d \tag{2.10}$$

where $A_d(N)$ is a polynomial in N of the form

$$A_d(N) = a_{d1}N + a_{d2}N^2 + \ldots + a_{d\ell_d}N^{\ell_d} \quad . \tag{2.11}$$

The general term in (2.10) has the following interpretation. For the given code there are $a_{d\ell_d}$ codewords (called paths) that leave the X_0 state via an input 1 and return to X_0' for the first time at some later point; these codewords have distance d and are produced by input sequence with ℓ_d 1's. The total number of paths which have distance d is $A_d = A_d(N)|_{N=1}$. This function is used to calculate the upper bound of the error probability. Suppose that the maximum likelihood decoder (Viterbi decoder) is used and that Pd is the probability of choosing an incorrect path. Then, the probability of bit error is bounded by[18]

$$Pb < \sum_{d=d_{free}}^{\infty} Pd \left. \frac{\partial A_d(N)}{\partial N} \right|_{N=1} = \sum_{d=d_{free}}^{\infty} B_d \cdot Pd \quad . \tag{2.12}$$

2.2 Co-Channel Interference Cancellation Techniques

2.2.1 Conventional Cancellation Technique

The conventional CCI cancellation technique mentioned in this thesis was proposed by Kohno for a power line CDMA LAN[20]. Its characteristics were investigated by Tachikawa on the AWGN channel[21][22].

Figure 2.3 shows a model of a receiver using the conventional parallel CCI canceller with user 1 as the reference user. Here, perfect chip synchronization for every user is assumed. It is also assumed that the information data is encoded by an orthogonal convolutional code. In this method, as shown in Figure 2.3, every user's received signals are first despread and decorrelated with a bank of correlators. Then the most probable orthogonal sequence is selected for each user. Utilizing these initial decisions, the selected sequences for each user are then re-spread with delay, attenuation , and phase shift. The re-modulated signals are removed from the composite received signal. After that, user 1's signal is despread, decorrelated, de-interleaved and decoded based on the orthogonal convolutional code employed.

When an error in the initial decision arises, the CCI cancellation process actually doubles the interference power since the canceller adds another interference signal instead of canceling one. Thus, the performance of the canceller depends on the performance of the initial decision.

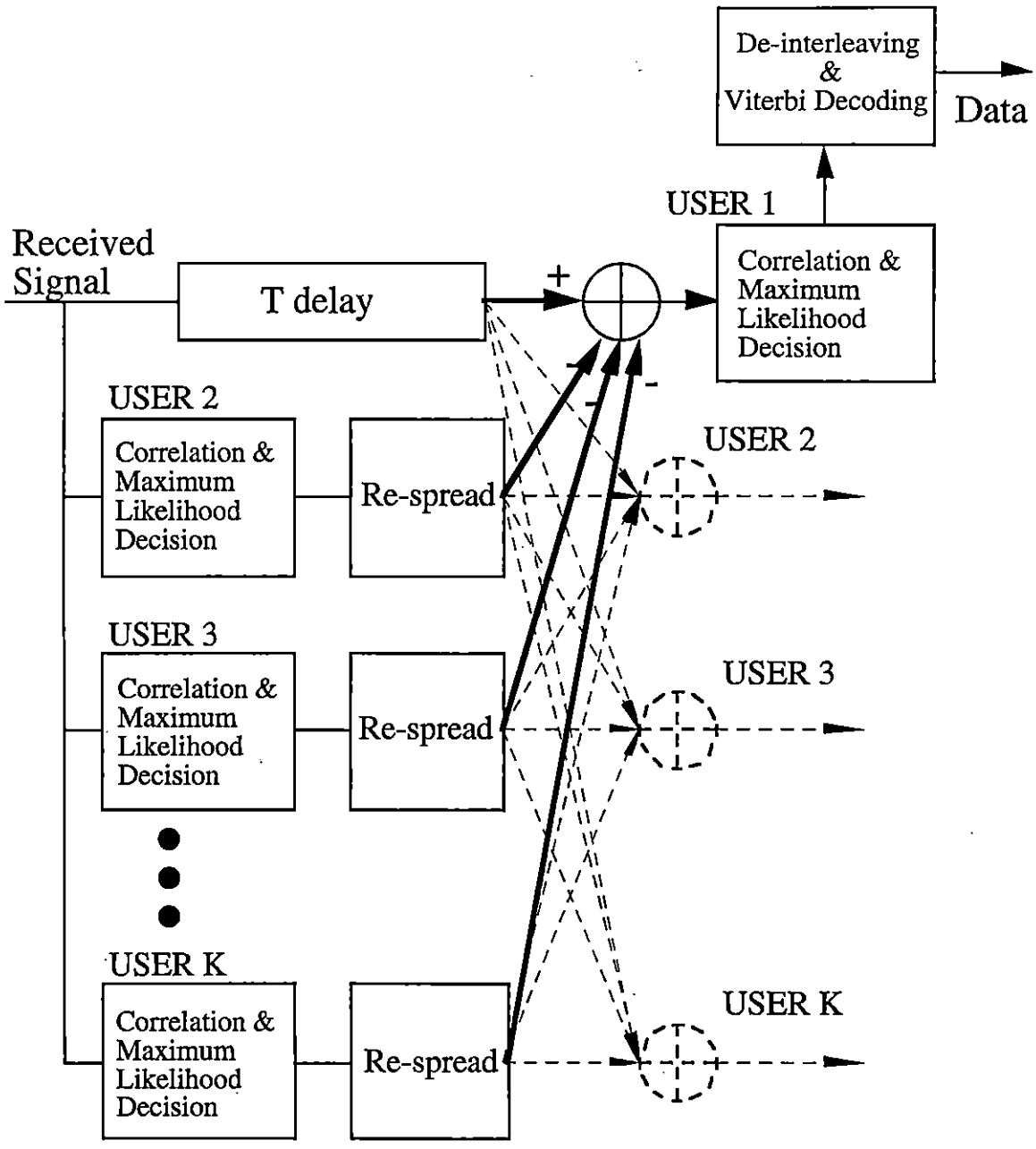

Figure 2.3 Model of a Receiver using the Conventional CCI Canceller.

2.2.2 Proposed Cancellation Technique

Now a new parallel CCI canceller using an orthogonal convolutional code is presented. As mentioned above, the performance of the CCI canceller depends on the initial decision. To reduce the error probability of the initial decision, the proposed system utilizes the error correcting capability of orthogonal convolutional codes.

Figure 2.4 is a model of a receiver using the proposed canceller. After the maximum likelihood decision on the sequence, the proposed canceller de-interleaves coded symbols and then decodes the orthogonal convolutional code using a Viterbi decoder. The decoded data is then re-encoded, assigned to one orthogonal sequence, interleaved, and re-spread by the long PN sequence. During the process, on the other hand, the received signal is put in the memory. The memory size equals the interleaving size. After the re-spreading, in the same manner as the conventional canceller, signals of user *2* to K are removed from the composite received signal extracted from the memory. After the other users are removed from the composite signal, user *1* 's signal is despread, decorrelated, de-interleaved, and decoded.

It is noted that Viterbi decoders needed in the proposed scheme are already in the conventional CCI cancellation scheme where each user has a Viterbi decoder. If the required processing delay is not acceptable with the reuse of the same Viterbi decoder after CCI cancellation, one can solve the problem by employing two Viterbi decoders per user (if transmissions of packets are considered, which may tolerate a relatively long delay, and quite often, the receiver may not be busy for receiving consecutive packets). Later it will be shown that, for the same performance, the complexity of each decoder may be reduced by more than a factor of four so that the overall complexity is still reduced.

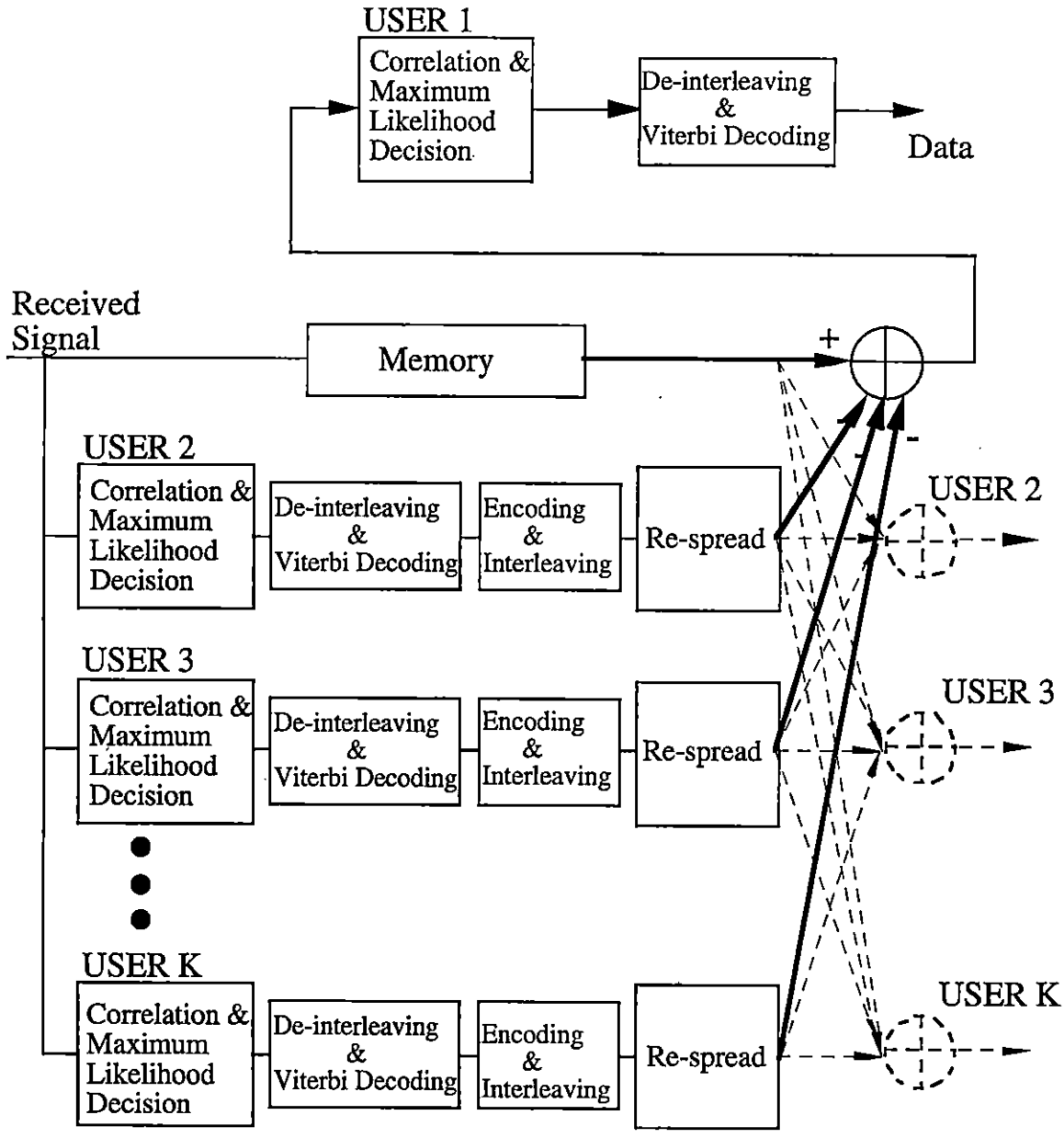

Figure 2.4 Model of a Receiver using the Proposed CCI Canceller.

2.3 Summary

In this chapter, the conventional and the new parallel CCI cancellation techniques were presented. First, the orthogonal convolutional codes employed in the CDMA system specified by IS-95 were depicted. The upper bound of the error performance was obtained from the transfer function of the code. Next, the model of the receiver using the conventional CCI canceller was described. It was pointed out that the performance of the cancellers depended on the performance of the initial decision. The new CCI canceller using the orthogonal convolutional code was then proposed.

Chapter 3: Performances on an AWGN Channel

3.1 System Model

In this chapter, the performances of both the conventional and the proposed CCI cancellers on an AWGN channel are derived. For simplicity, we focus on a base-band asynchronous CDMA system.

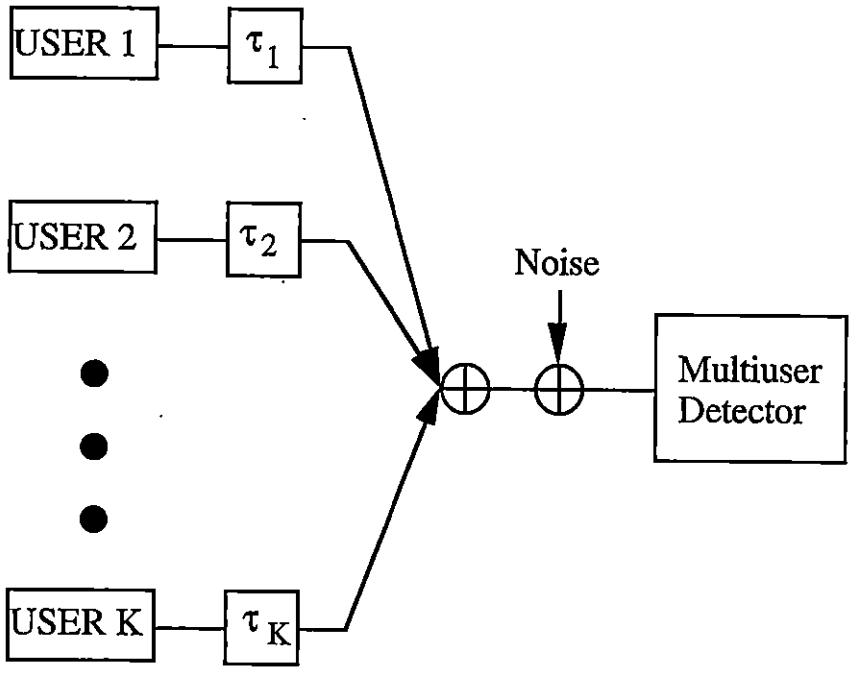

Figure 3.1 Model of an Asynchronous CDMA System.

Figure 3.1 shows a model of an asynchronous CDMA system with K transmitting users and a multiuser detector. Each user encodes its data using an orthogonal convolutional code. Assume that the code rate is $1/m$ ($M = 2^m$) and the constraint length is n_A. Depending on the output of the convolutional code, one of M orthogonal sequences is chosen by the orthogonal convolutional encoder as shown in Figure 3.2. The resulting

orthogonal sequences are then interleaved and combined with a part of the long PN sequence which is unique for each user and separates one user from another in the direct sequence spreading. The processing gain $Gp = T_s / T_c$ where T_s is the symbol duration and T_c is the chip duration of the PN sequence. The received signal of the k-th user is

$$S_k(t) = \sqrt{P_k} W^r(t - \tau_k) C_k(t - \tau_k) + n(t) \tag{3.1}$$

where $W^r(t)$ is one of the orthogonal sequences referred to as the r-th symbol, $r = 1,...,M$, $C_k(t)$ is the long PN sequence for the k-th user whose period is much larger than Gp[17], P_k is the signal power for the k-th user (for simplicity, it is subsequently assumed that $P_k = P$ for all k), τ_k is the time delay for the k-th user ($0 \le \tau_k \le T_s$) and $n(t)$ is the AWGN with power spectral density $N_o / 2$(W/Hz)

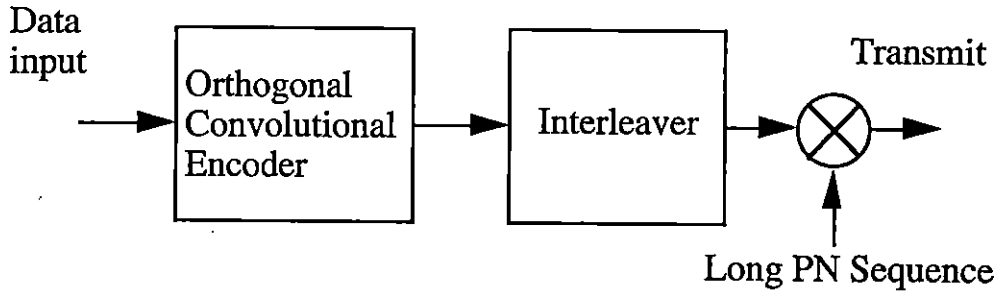

Figure 3.2 Transmitter Structure.

3.2 Performance Analysis

3.2.1 Conventional CCI Canceller

To analyze the performance of the conventional CCI canceller shown in Figure 2.3, it is assumed that all the users' sequences are independent and randomly distributed, and that the chip pulse shape is rectangular.

The signal-to-noise ratio SNR_{c1} after correlation with user 1's sequence at the receiver is given by

$$SNR_{c1} = \frac{1}{\frac{1}{3Gp^3}\sum_{i=2}^{K} r_{1k} + \frac{N_o}{2E_s}} \tag{3.2}$$

where r_{1k} is the average interference parameter between the user *1* and user *k* and $E_s = PT_s$ is the energy per symbol[24]. When the sequences are assumed as random sequences, the average of r_{1k} becomes the constant value $2Gp^2$[21][22]. Therefore, the SNR after the correlation is

$$SNR_{c1} = \frac{1}{\frac{2(K-1)}{3Gp} + \frac{N_o}{2E_s}} \quad . \tag{3.3}$$

The denominator of Equation (3.3) corresponds to approximation of the CCI as AWGN. The validity of this approximation will be shown later through simulation. The error probability of the initial decision is the probability that the *r*-th sequence correlator output U_r is smaller than any of the other sequences' outputs U_i ($i=1,...,M,\ i\neq r$) and is given by[21][22][25]

$$\begin{aligned} Pe_c &= 1 - \int_{-\infty}^{\infty} P(U_1 < U_r, U_2 < U_r, \cdots, U_M < U_r | U_r) p(U_r) dU_r \\ &= 1 - \frac{1}{\sqrt{2\pi}} \int_{-\infty}^{\infty} \exp(\frac{-u^2}{2}) \{1 - Q(u + \sqrt{SNR_{c1}})\}^{M-1} du \\ &\leq (M-1) \cdot Q\left(\sqrt{SNR_{c1}}\right) \end{aligned} \tag{3.4}$$

where

$Q(t)$: standard Gaussian upper cumulative distribution function

$$Q(t) = \frac{1}{\sqrt{2\pi}} \int_t^{\infty} \exp\left(\frac{-x^2}{2}\right) dx \quad . \tag{3.5}$$

When an error in the initial decision arises, the CCI cancellation process actually doubles the interference power since the canceller adds the another interference signal instead of canceling it. Figure 3.3 shows the residual interference caused by the *k*-th user. It is assumed that errors occur independently with the probability Pe_c on two adjacent symbols of *k*-th user. The average interference to symbol *n* of user *1* caused by symbol *n-1* of user *k* is

$$2Pe_c\left(\frac{T'}{T_s}\right)\frac{2}{3Gp} \tag{3.6}$$

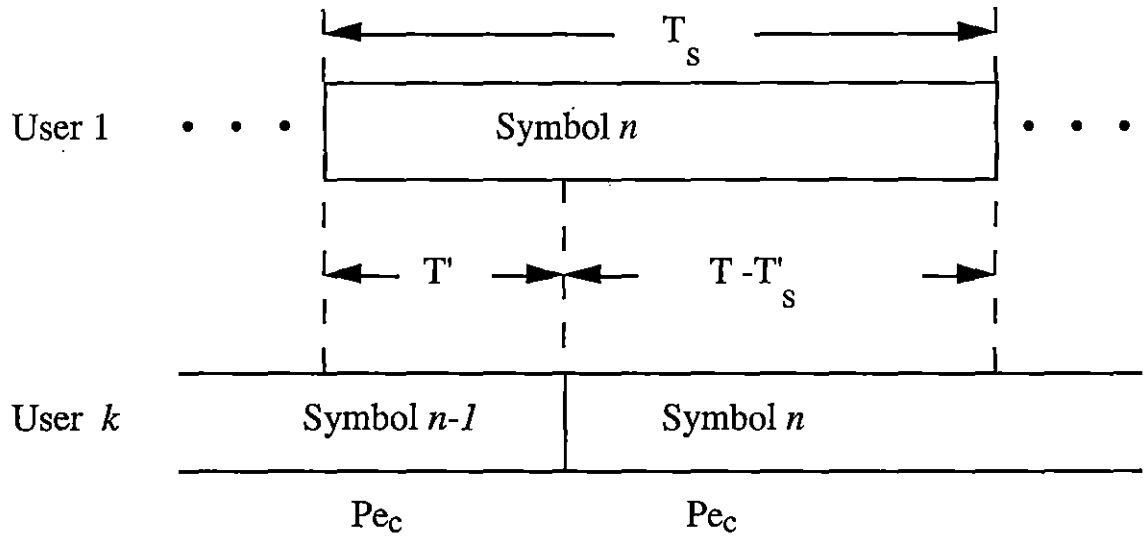

Figure 3.3 Residual Interference caused by the User *k*.

where T' is shown in Figure 3.3. Similarly, the average interference caused by symbol *n* of user *k* is

$$2Pe_c\left(\frac{T_s - T'}{T_s}\right)\frac{2}{3Gp} \quad . \tag{3.7}$$

From Equations (3.6) and (3.7), the average total interference to symbol *n* of user *1* caused by symbol *n-1* and *n* of user *k* is

$$2Pe_c\left(\frac{T'}{T_s} + \frac{T_s - T'}{T_s}\right)\frac{2}{3Gp} = 2Pe_c\frac{2}{3Gp} \quad . \tag{3.8}$$

There are *K-1* interfering users. Thus, the signal-to-noise ratio after the CCI cancellation is

$$SNR_{c2} = \frac{1}{2Pe_c\dfrac{2(K-1)}{3Gp} + \dfrac{N_o}{2E_s}} \quad . \tag{3.9}$$

From Equation (3.9), it is clear that the SNR after the cancellation is dependent on the error probability of the initial decision.

Here, it is assumed that the receiver can estimate an accurate value of the received signal power *P*. The upper bound on the bit error probability using a soft decision Viterbi decoder can be obtained as[18][26][27]

$$Pb_c < \sum_{d=d_{free}}^{\infty} B_d \cdot Pd_c \tag{3.10}$$

where

Pd_c: probability of selecting the incorrect path[18],

$$P_d = Q\left(\sqrt{\frac{d \cdot SNR_{c2}}{2}}\right) \quad ; \tag{3.11}$$

B_d: total number of nonzero information bits on all weight d paths[26];

d_{free}: minimum free distance.

If the weight spectra B_d is known from d_{free} to infinity in Equation (3.10), the upper bound can be calculated. However, the bound becomes looser as the BER becomes worse. Quite often, the first few terms in Equation (3.10) are used to get a performance approximation of the canceller. The first four terms are used as the approximation for both the conventional and the new CCI cancellation schemes in order to make a fair comparison.

3.2.2 Proposed CCI Canceller

All assumptions are the same as for the conventional canceller presented in Section 3.2.1. The number of symbol errors caused by choosing a wrong path after re-encoding is the distance between the coded sequence arising from the wrong path in the state diagram and the coded sequence along the correct path (For example, the number of symbol errors is four in Figure 3.4.). There are A_d paths which cause d symbol errors after the re-encoding and the probability with which the Viterbi decoder chooses a wrong path with the distance d is

$$Pd_{n1} = Q\left(\sqrt{\frac{d \cdot SNR_{n1}}{2}}\right) \tag{3.12}$$

where

$$SNR_{n1} = \frac{1}{\frac{2(K-1)}{3Gp} + \frac{N_o}{2E_s}} \tag{3.13}$$

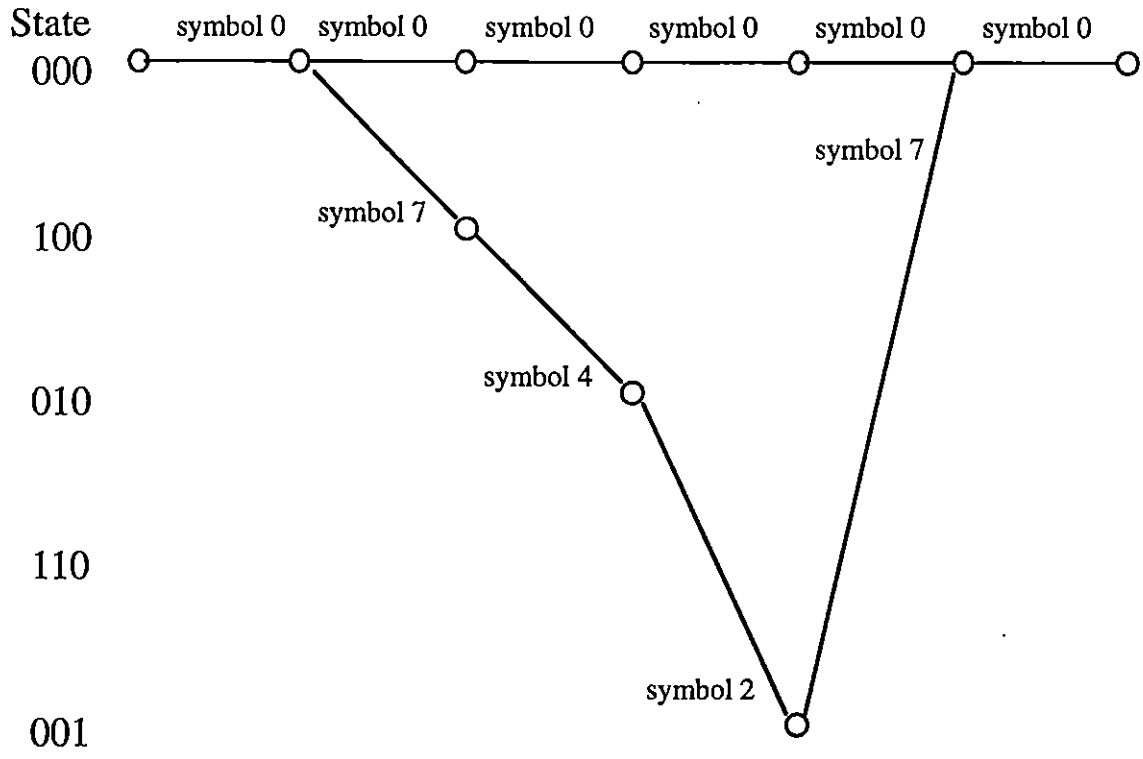

Figure 3.4 Symbol Errors caused by a Wrong Path,
Code Rate=1/3, Constraint Length=4.

Then the average symbol error probability caused by one user after the re-encoding is

$$Pe_n = \sum_{d=d_{free}}^{d_{free}+3} d \cdot A_d \cdot Pd_{n1} \quad . \tag{3.14}$$

Therefore, the signal-to-noise ratio after the cancellation is

$$SNR_{n2} = \frac{1}{2Pe_n \frac{2(K-1)}{3Gp} + \frac{N_o}{2E_s}} \quad . \tag{3.15}$$

From SNR_{n2}, the approximate error probability after cancellation is

$$Pb_n \approx \sum_{d=d_{free}}^{d_{free}+3} B_d \cdot Pd_{n2} \tag{3.16}$$

where Pd_{n2} is obtained from SNR_{n2} ,

$$Pd_{n2} = Q\left(\sqrt{\frac{d \cdot SNR_{n2}}{2}}\right) \quad . \tag{3.17}$$

3.2.3 Performance Improvement

From Equations (3.10) and (3.16), the performance improvement of the proposed canceller over the conventional canceller comes from the difference between SNR_{c2} and SNR_{n2}. This difference is due to the error correction capability of the orthogonal convolutional codes.

From Equations (3.9) and (3.15), the SNR difference after the cancellation is

$$\begin{aligned} SNR_{n2} - SNR_{c2} &= \frac{1}{2Pe_n \frac{2(K-1)}{3Gp} + \frac{N_o}{2E_s}} - \frac{1}{2Pe_c \frac{2(K-1)}{3Gp} + \frac{N_o}{2E_s}} \\ &= \frac{2\alpha(Pe_c - Pe_n)}{(2\alpha Pe_n + \beta)(2\alpha Pe_c + \beta)} \end{aligned} \tag{3.18}$$

where

$$\alpha = \frac{2(K-1)}{3Gp} \; ; \tag{3.19}$$

$$\beta = \frac{N_o}{2E_s} \quad . \tag{3.20}$$

From Equations (3.4) and (3.14),

$$\begin{aligned} Pe_c - Pe_n &\approx (M-1)\cdot Q\left(\sqrt{SNR}\right) - \sum_{d=d_{free}}^{d_{free}+3} d \cdot A_d \cdot Pd_{n1} \\ &= (M-1)\cdot Q\left(\sqrt{SNR}\right) - \sum_{d=d_{free}}^{d_{free}+3} d \cdot A_d \cdot Q\left(\sqrt{\frac{d \cdot SNR}{2}}\right) \end{aligned} \tag{3.21}$$

where

$$SNR = \frac{1}{\alpha + \beta} \quad . \tag{3.22}$$

If the SNR is large, the first term of Equation (3.14) dominates Pe_n. Therefore,

$$Pe_c - Pe_n \approx (M-1)\cdot Q\left(\sqrt{SNR}\right) - d_{free} \cdot A_{d_{free}} \cdot Q\left(\sqrt{\frac{d_{free} \cdot SNR}{2}}\right) \quad . \tag{3.23}$$

When $Pe_c - Pe_n \geq 0$, the proposed canceller shows better performance than the conventional canceller. This means

$$\frac{M-1}{d_{free} \cdot A_{d_{free}}} \geq \frac{Q\left(\sqrt{\frac{d_{free} \cdot SNR}{2}}\right)}{Q\left(\sqrt{SNR}\right)} \qquad (3.24)$$

As the constraint length of the orthogonal convolutional code increases and d_{free} increases, the numerator of the right side of Equation (3.24) decreases exponentially. Thus, the proposed canceller shows performance improvement in lower SNR with the orthogonal convolutional code of larger constraint length. The performance improvement of the proposed canceller can also be shown through Equation (3.18) where the numerator increases and the denominator decreases with the constraint length of the orthogonal convolutional code.

3.3 Results

Suppose that each time delay τ_i $(i=1,2,...,K)$ can be known perfectly[21][22]. It is also assumed that the processing gain Gp is 128 and coding rate is 1/3 (8-ary orthogonal convolutional code) with optimum generator polynomials given in Table 3.1 [17][18].

Figure 3.5 shows the BER performance of the orthogonal convolutional code on the AWGN channel. In the figure, the points are the simulation results and the lines are the theoretical performance calculated from the Gaussian approximation with the first four terms of Equation (3.10). In Figure 3.5, the results for constraint length n_A of 4, 7, and 9 are shown. As the simulated points are close to the theoretical values with $d=d_{free}\sim d_{free}+3$, it is concluded that the approximation is appropriate.

Figures 3.6 and 3.7 also compare the simulation results with the theoretical performance for three schemes: with no CCI canceller, with the conventional canceller, and with the proposed canceller. The points are the simulation results and the lines are the theoretical performance calculated with the assumptions described in Section 3.2.1.

Constraint Length	Polynomials (Octal)		
3	4 5 6		
4	4-ary	8-ary	16-ary
	12 15	1 1 1 3 1 5	11, 13 14, 15
5	2 3 3 3 2 6		
6	4 5 6 7 5 6		
7	1 1 4 1 5 6 1 3 3		
9	5 5 7 6 6 3 7 1 1		

Ex. Constraint Length 4
8-ary Optimum Code

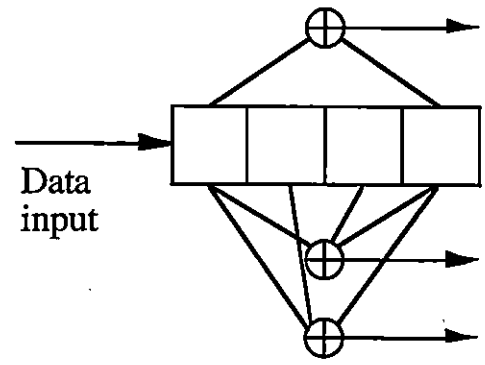

Table 3.1 Generator Polynomials of an Orthogonal Convolutional Code.

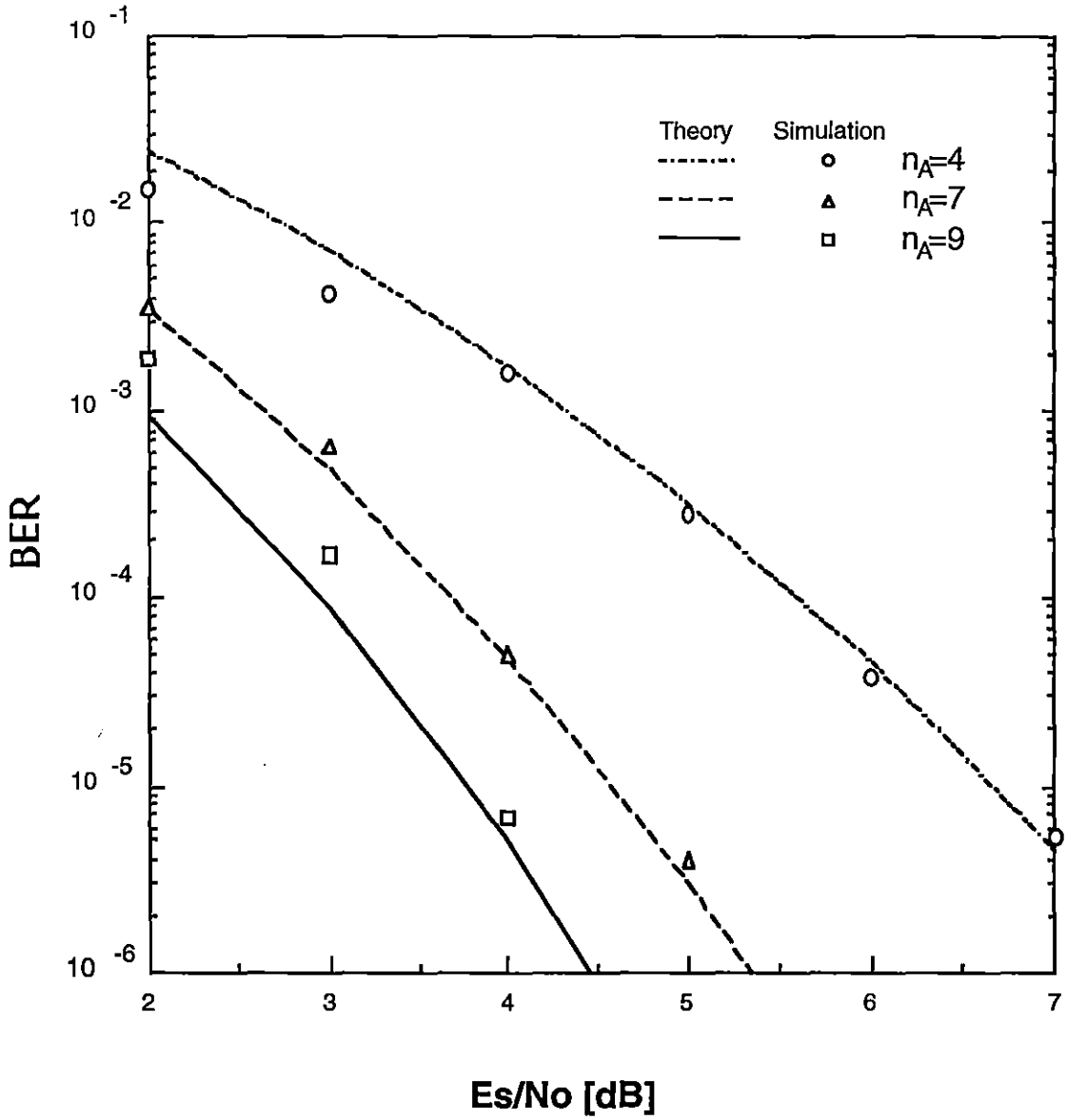

Figure 3.5 Performance of the Orthogonal Convolutional Code, Number of Users=1, Code Rate=1/3.

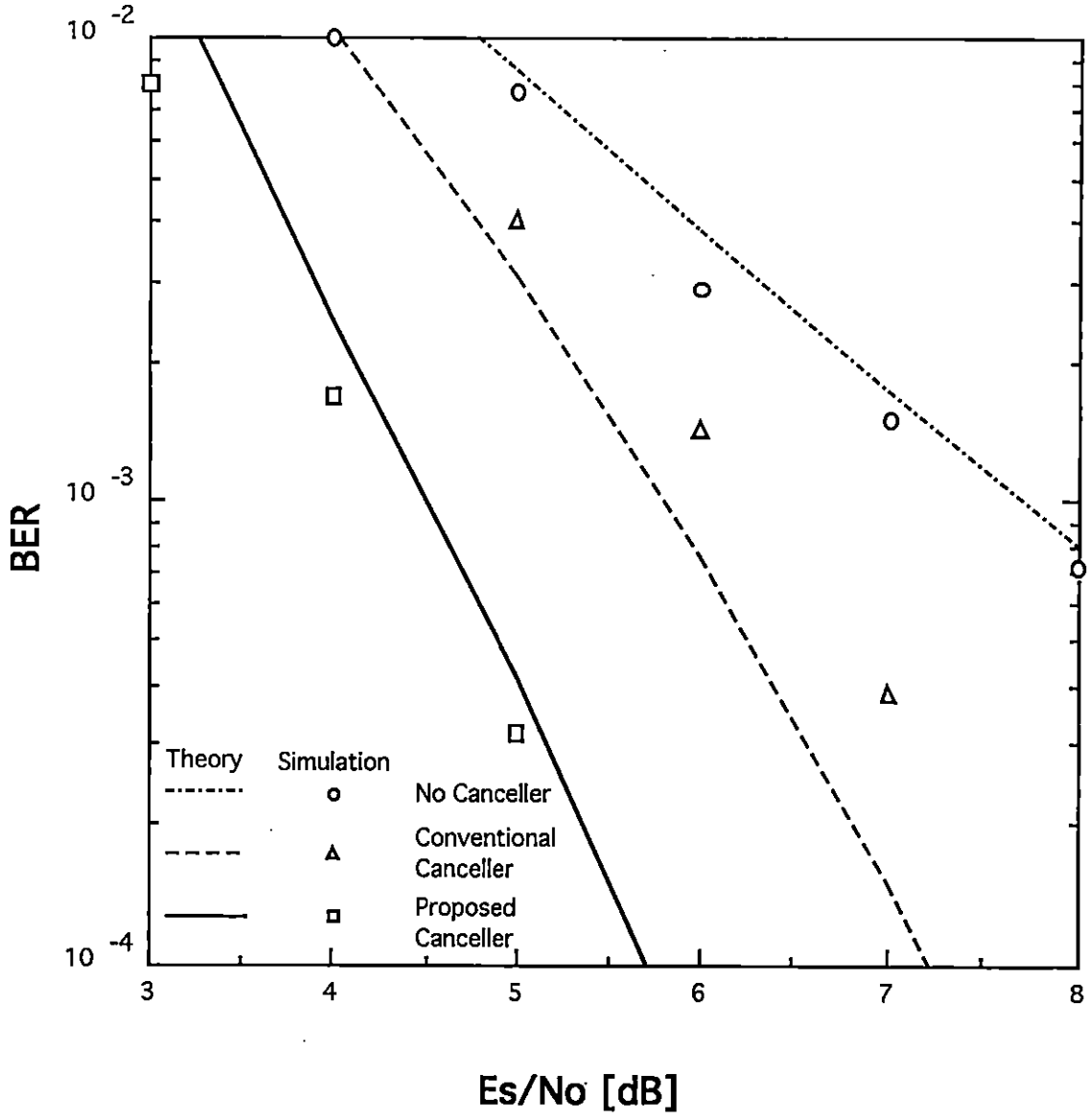

Figure 3.6 BER vs. Es/No,

Number of Users=20, Code Rate=1/3,
Constraint Length=4.

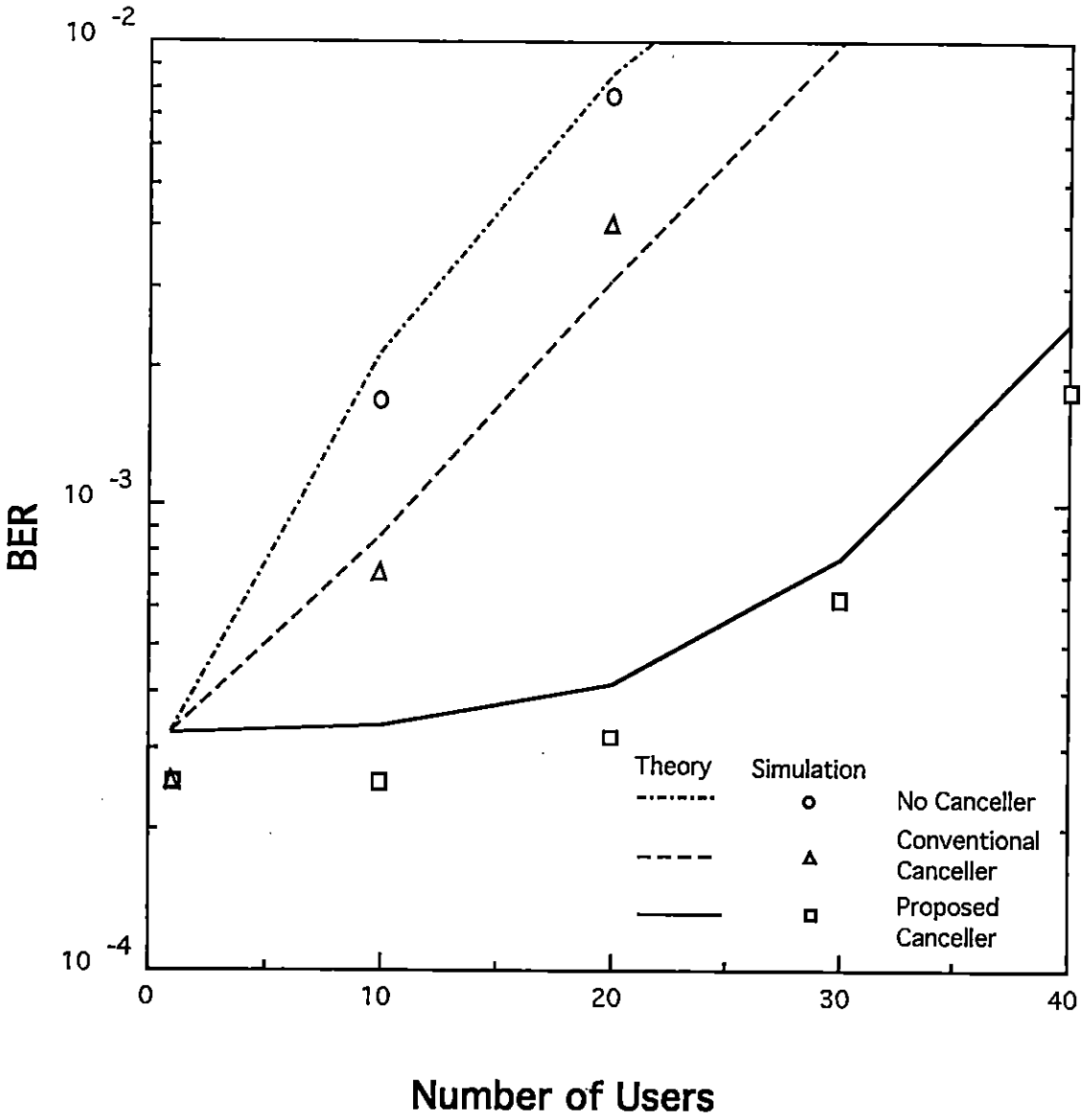

Figure 3.7 BER vs. Number of Users,

Es/No=5dB, Code Rate=1/3,
Constraint Length=4.

The simulation assumes asynchronous CDMA and 8 samples per chip so that $\tau_k = iT_c / 8$ ($i=0,1,...,7$). The interleaver whose size is 12 symbols × 14 symbols is employed to assure symbol errors are independent. The performance without a canceller is calculated by Equations (3.10) and (3.11) with SNR_{c1} replacing SNR_{c2}. Since the simulated points are close to the theoretical values, it is once again confirmed that the approximations in Section 3.2.1 are acceptable.

In Figures 3.8 to 3.15, the performances without a canceller, with the conventional canceller and with the proposed canceller are presented. Figure 3.8 shows the system SNR vs. E_s / N_o with a constraint length of 7. The number of users which transmit the signal at the same time is K. The system SNR is the SNR just before the final maximum likelihood decision (after the cancellation), which is SNR_{c2} or SNR_{n2}. Thus, the difference between these two SNR as shown in Figure 3.9 is the CCI which cannot be removed by the canceller. From Figure 3.9, it is clear that the proposed canceller cancels more CCI and provides better SNR than the conventional canceller when the E_s / N_o is not too low. Especially when K=20, the proposed canceller removes most of the CCI and provides a nearly interference free signal for the final maximum likelihood decision. However, if K is 60 and E_s / N_o is less than 5 dB, then the re-encoding process produces too much interference. Thus, in this case, the proposed canceller is inferior to the conventional canceller.

Figures 3.10, 3.11, and 3.12 show the BER vs. E_s / N_o with a constraint length of 4, 7, and 9. When K=20 (the number of users which transmit a signal at the same time), the performance of the proposed canceller is very close to the performance with K=1 and superior to the conventional canceller by 1 dB at BER=10^{-3} and 2 dB at BER=10^{-5}. If K=60, the difference between the BER of the two methods is much larger than the K=20 case in favor of the proposed canceller. For example, using a constraint length nine code, the difference is more than 6 dB for K=60 at BER=10^{-5}. The performance difference

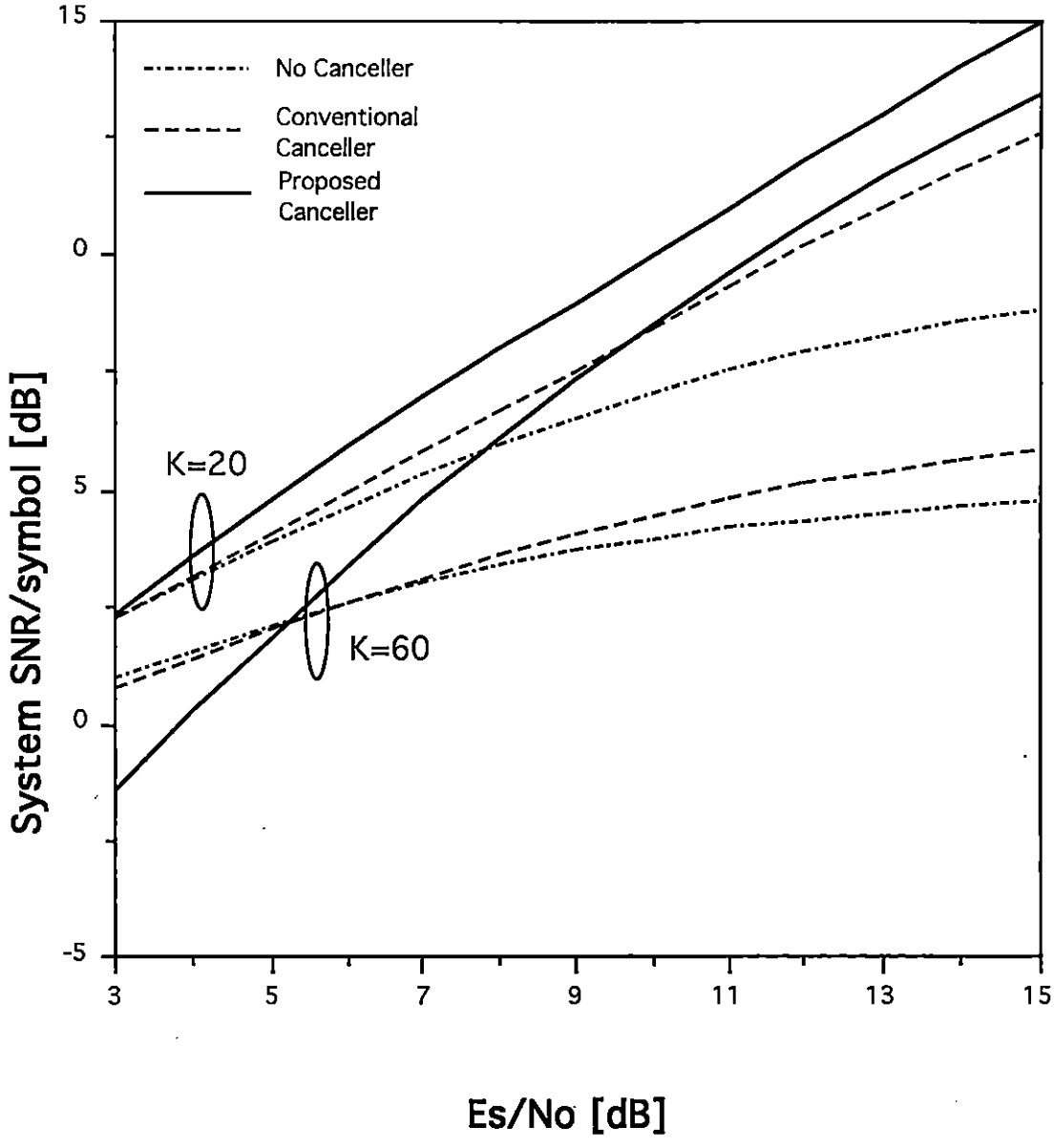

Figure 3.8 System SNR vs. Es/No,

Code Rate=1/3, Constraint Length=7.

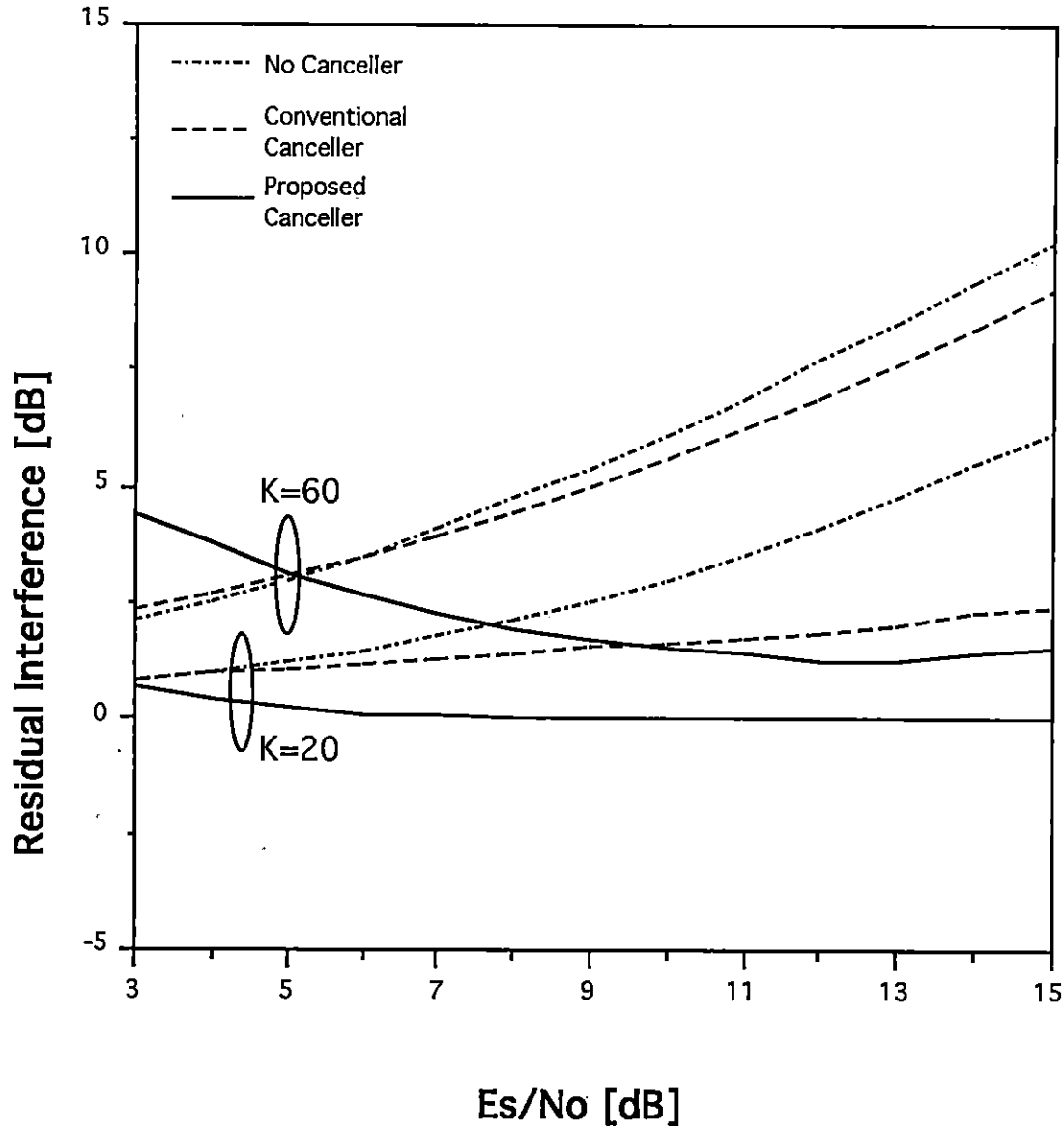

Figure 3.9 Residual Interference vs. Es/No,
Code Rate=1/3, Constraint Length=7.

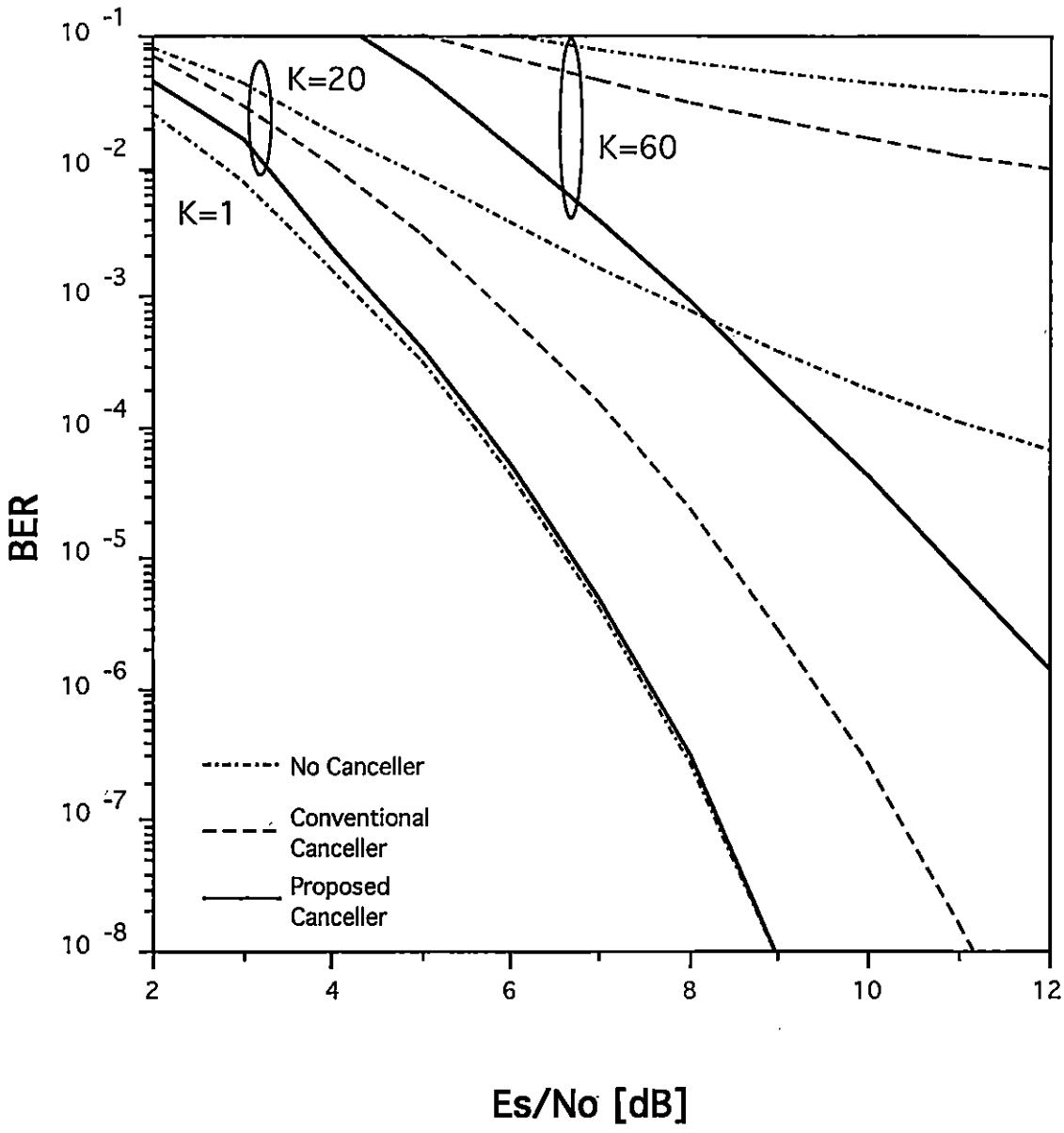

Figure 3.10 BER vs. Es/No,

Code Rate=1/3, Constraint Length=4.

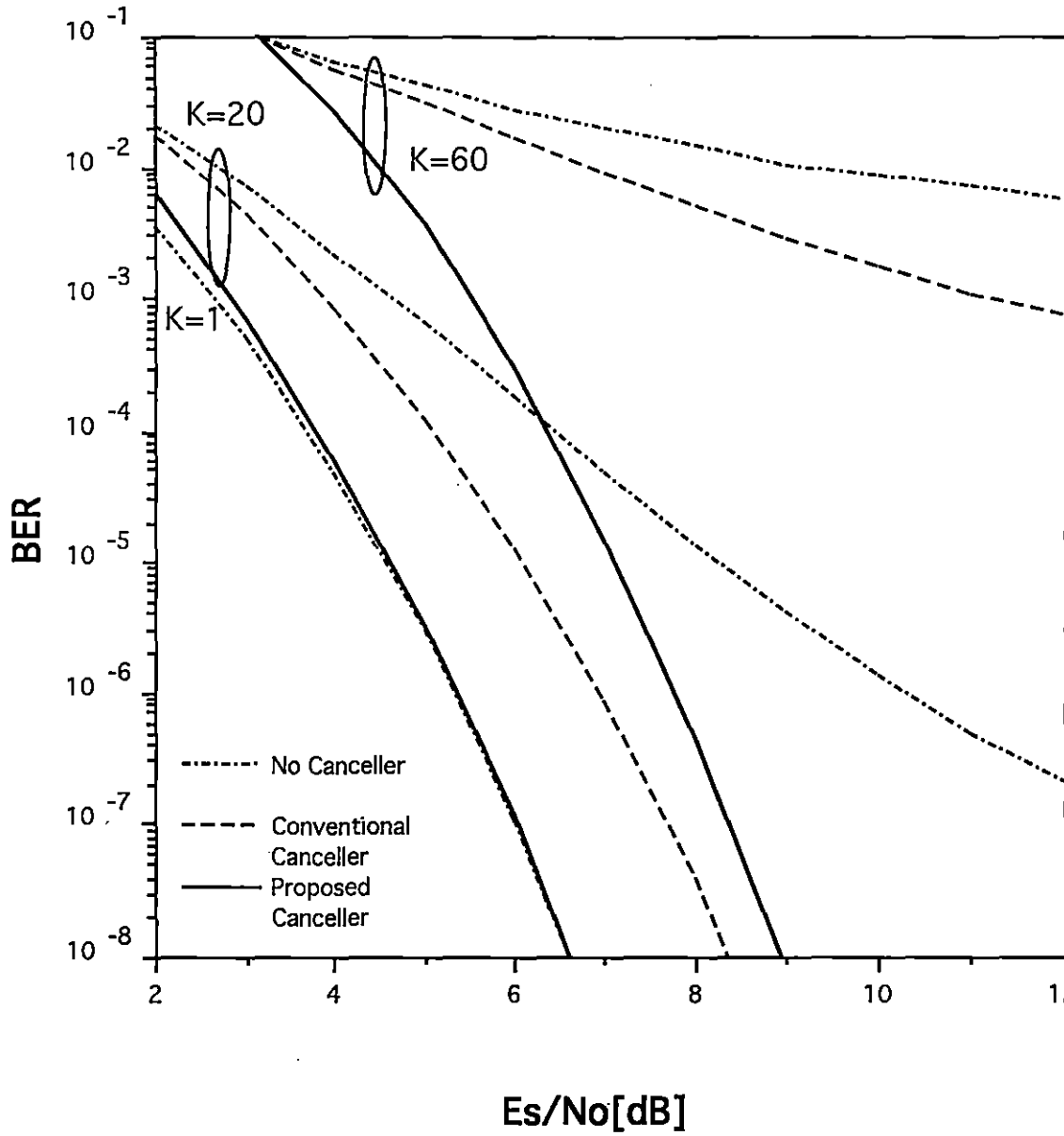

Figure 3.11 BER vs. Es/No,

Code Rate=1/3, Constraint Length=7.

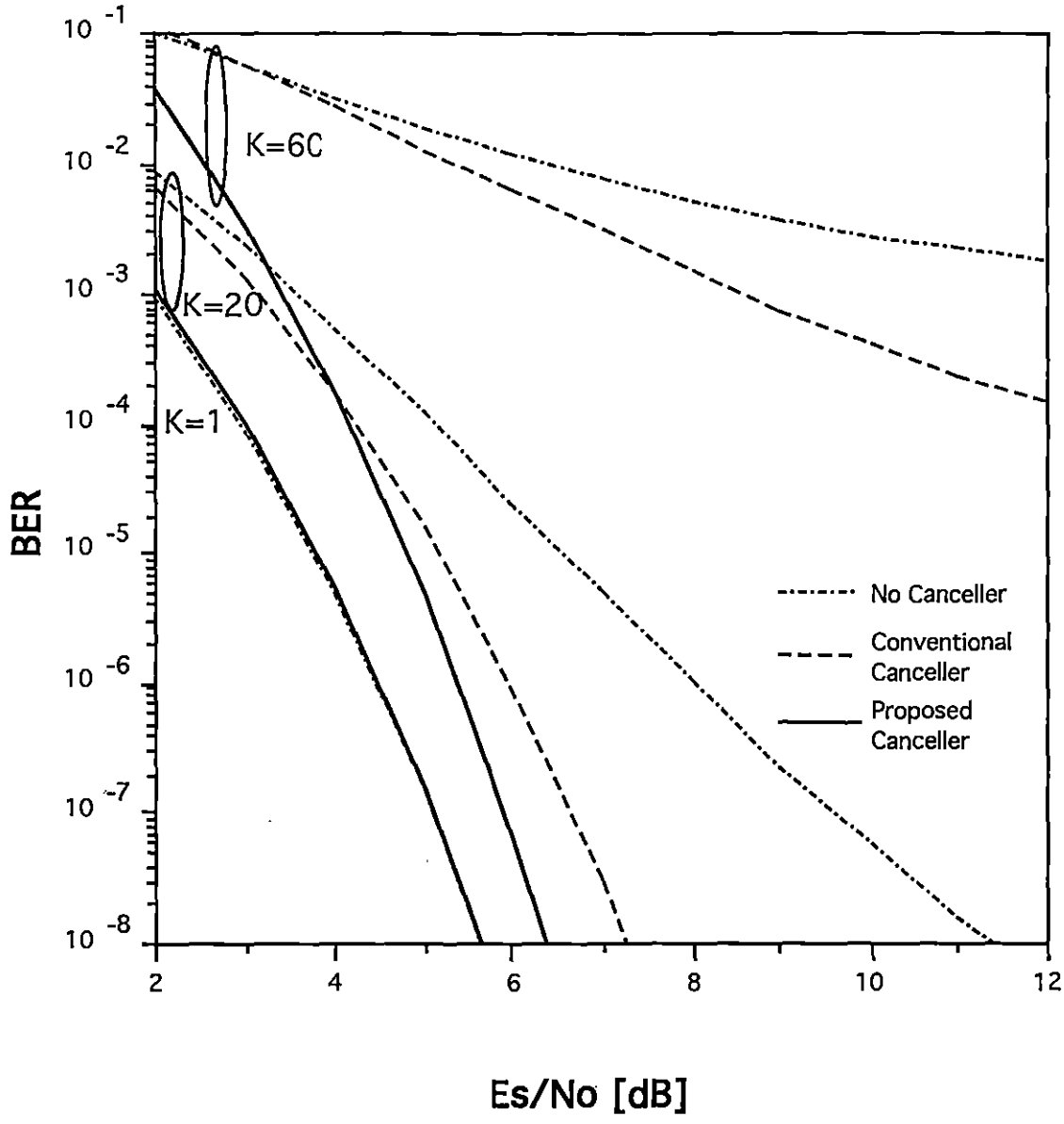

Figure 3.12 BER vs. Es/No,

Code Rate=1/3, Constraint Length=9.

increases as the constraint length becomes longer. This result is due to the fact that a convolutional code with a longer constraint length has more powerful error correcting capability which makes the initial decision more accurate. Therefore the canceller should use a orthogonal convolutional code which has a large constraint length .

Figures 3.13, 3.14, and 3.15 show the BER vs. number of users. It is shown that the number of simultaneous users at BER=10^{-3} improves by a factor of two to three when E_s / N_o is 5 dB, and one and a half to two when E_s / N_o is 10 dB as compared to the conventional canceller. It has also been shown that up to about 40 users, the proposed CCI canceller has a performance which is near to the performance without interference. As can be seen from these figures, as the constraint length is longer, the performance improves.

Figure 3.16 shows BER versus constraint length of the orthogonal convolutional codes. From this figure, it is clear that even though the conventional canceller does not work well when K=60, the proposed canceller works quite effectively. Also if the receiver uses a longer constraint length code, the performance improvement of the proposed canceller is larger, especially when K is large.

The proposed cancellation scheme can also be viewed as an effective way of reducing the system implementation complexity. For example, for K =20 and required BER<10^{-3}, from Figure 3.16, the conventional canceller requires the code constraint length equal to 6, while the proposed canceller requires the constraint length equal to 4. This represents a factor of four reduction in the complexity of the Viterbi decoder for doing add-compare-select (ACS) operation. The complexity of the ACS operation is basically proportional to the number of states in the state diagram which is equal to 2^{n_A-1}[26, pp. 337] (In this case, the complexity for the ACS circuit reduces from 2^5 to 2^3). Also the size of the path memory is reduced as the required decoding depth is reduced[27]. Recall that the number of Viterbi decoders could be doubled in order to shorten the delay. The overall

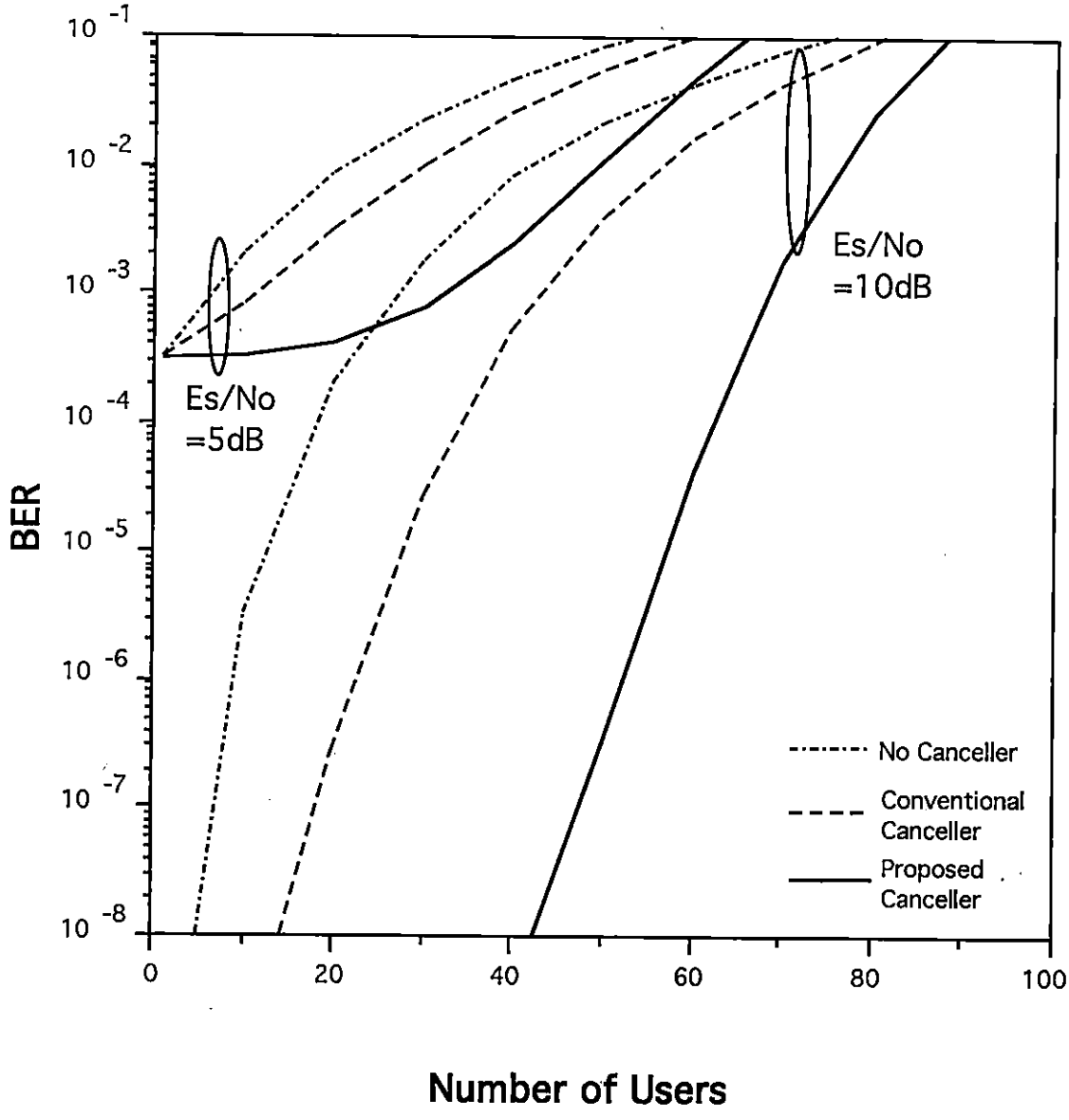

Figure 3.13 BER vs. Number of Users,
Code Rate=1/3, Constraint Length=4.

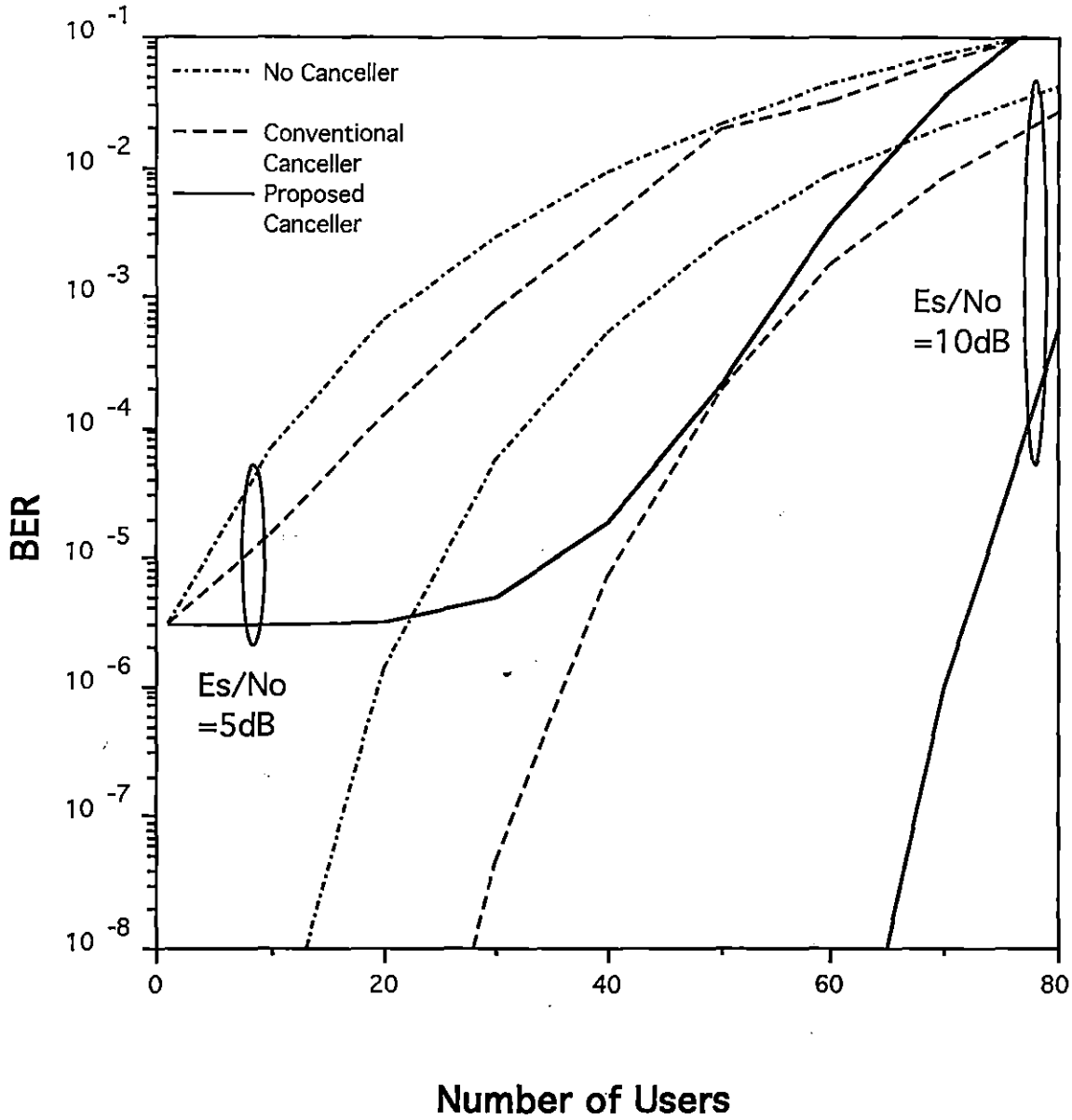

Figure 3.14 BER vs. Number of Users,

Code Rate=1/3, Constraint Length=7.

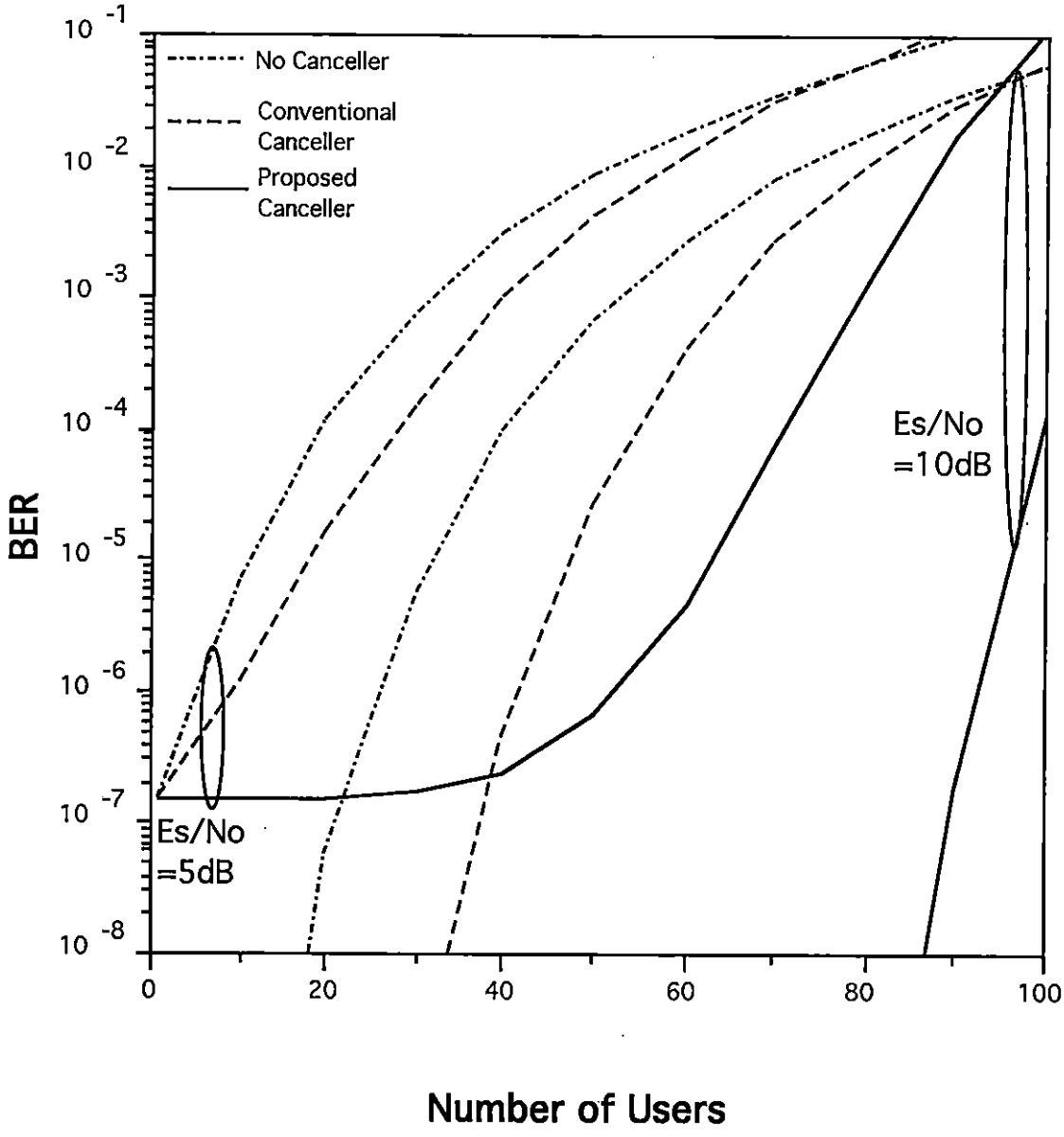

Figure 3.15 BER vs. Number of Users,
Code Rate=1/3, Constraint Length=9.

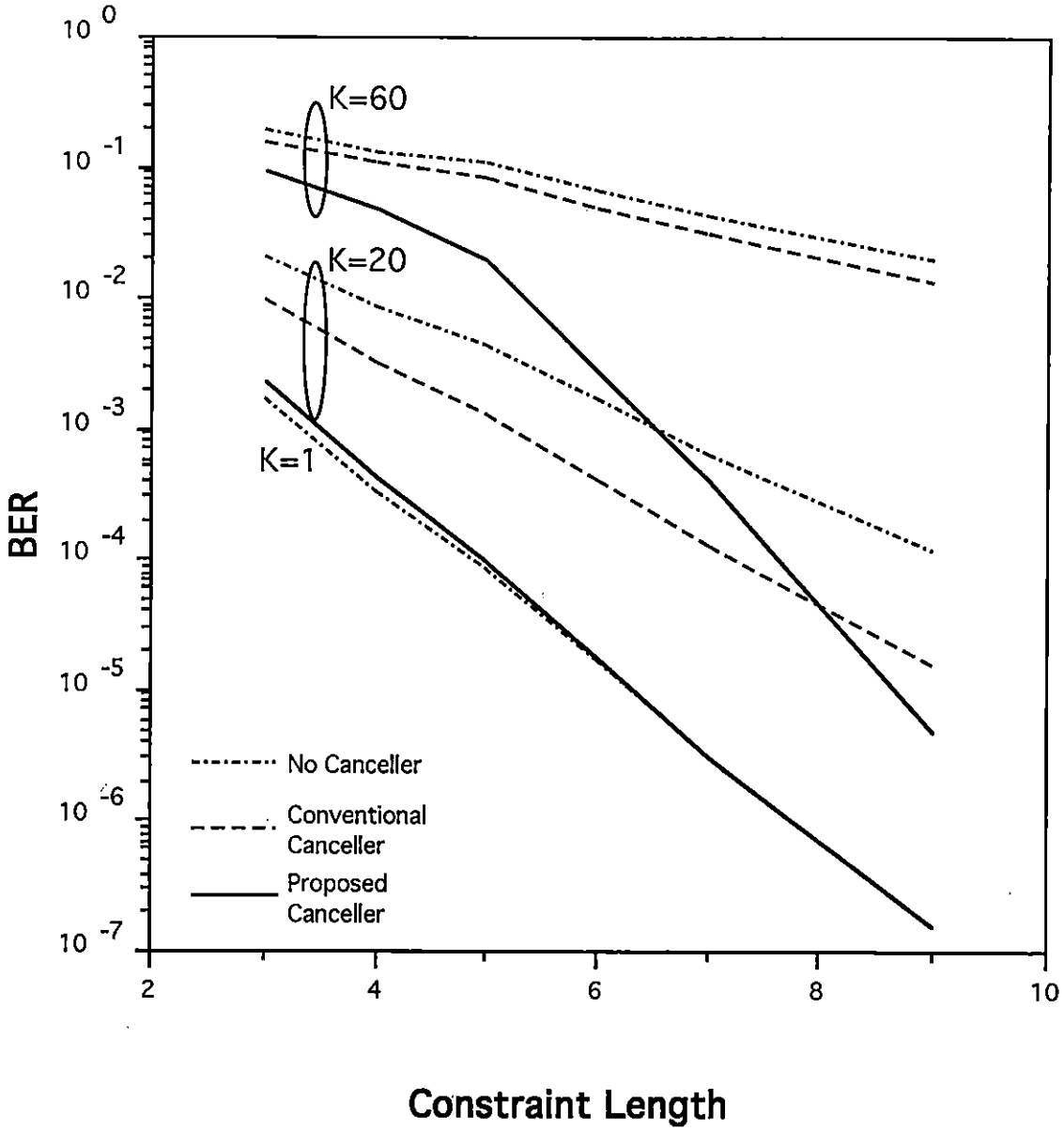

Figure 3.16 BER vs. Constraint Length,
Es/No=5dB, Code Rate=1/3 .

complexity is still reduced by a factor of two when an additional Viterbi decoder is included.

Figure 3.17 shows the BER versus code rate with a constraint length of 4. The generator polynomials of the codes with the rate 1/2, 1/3, and 1/4 are given in Table 3.1. The performance with the proposed canceller improves as the code rate reduces since it takes full advantage of the better distance structure of a lower rate code. For the conventional canceller, it is interesting to note the existence of the optimum code rate at 1/3. This is because, from Equation (3.4), the error probability of the initial decision increases with the same SNR per symbol as M increases while the conventional canceller itself does not perform error correction. Therefore, even though a code with larger M has a better distance structure, the conventional canceller makes more symbol errors and the performance becomes worse when the code rate is less than 1/3. The performance with the proposed canceller improves because the error probability of the initial decision is lowered with better codes.

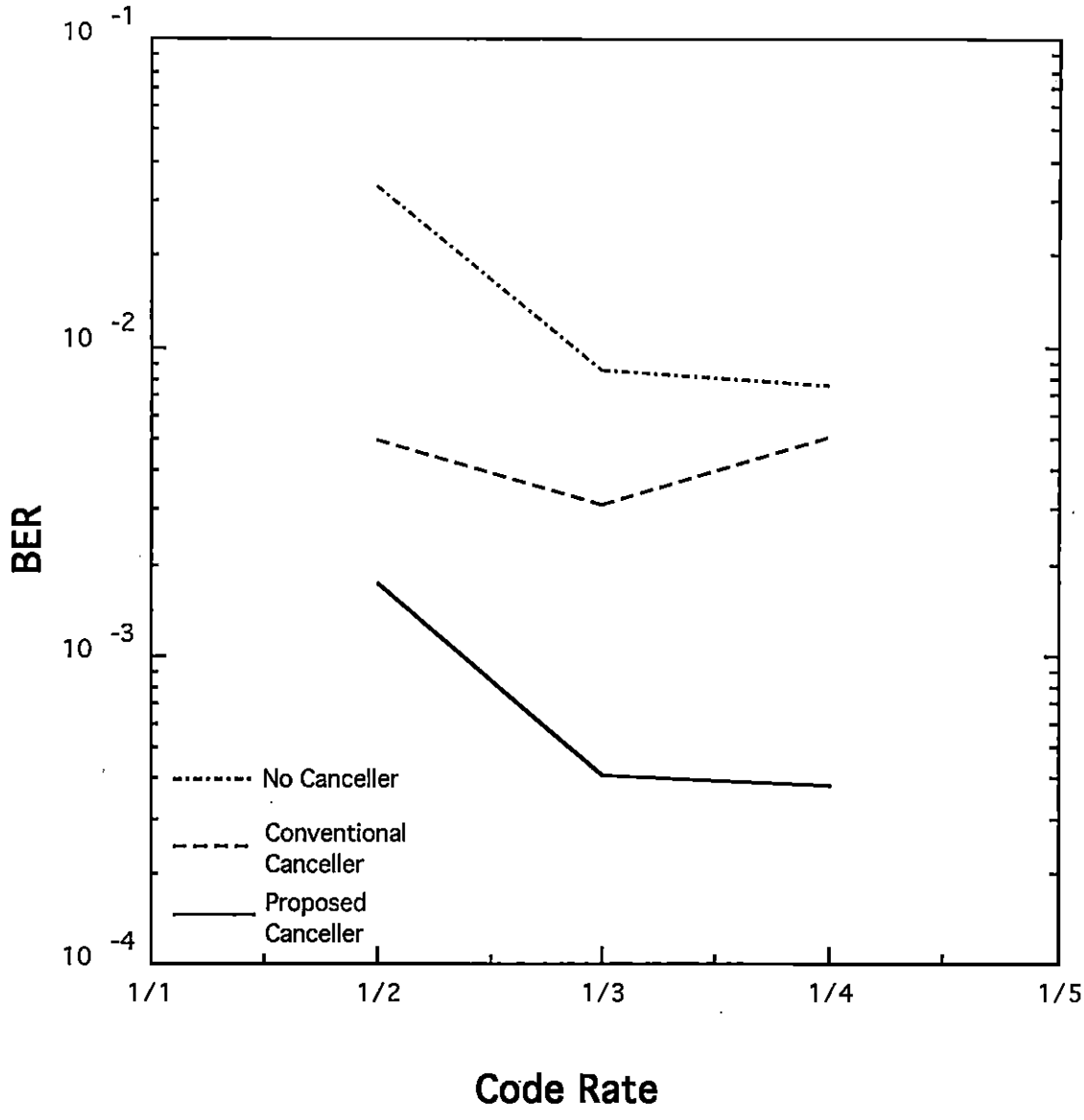

Figure 3.17 BER vs. Code Rate,

Number of Users=20, Es/No=5dB,
Constraint Length=4.

3.5. Summary

In this chapter, the performance of the proposed CCI canceller on an AWGN channel was shown. The performance of the proposed canceller was computed and compared with the conventional canceller. It was shown that the proposed canceller offered one and a half to three times higher user capacity than the conventional canceller. Up to about 40 users, the proposed CCI canceller canceled nearly all multiuser interference. It was also shown that the canceller could significantly benefit from the use of a code with a large constraint length. For the same performance, the proposed canceller could effectively reduce the decoding complexity. Employing low rate codes, the performance of the proposed canceller improves while the performance with the conventional canceller might not.

Chapter 4: Performance on a Multipath Rayleigh Fading Channel

4.1 System Model

In this chapter, the performances of both the conventional and the proposed CCI cancellers on a multipath Rayleigh fading channel are derived. The transmitter structure is the same as the one specified by IS-95. We also consider a multicell environment in this chapter.

The system model is based on [28] and extended to a multipath Rayleigh fading channel. There are K active users in a cell. Each user encodes their data using the orthogonal convolutional code as shown in Figure 4.1.

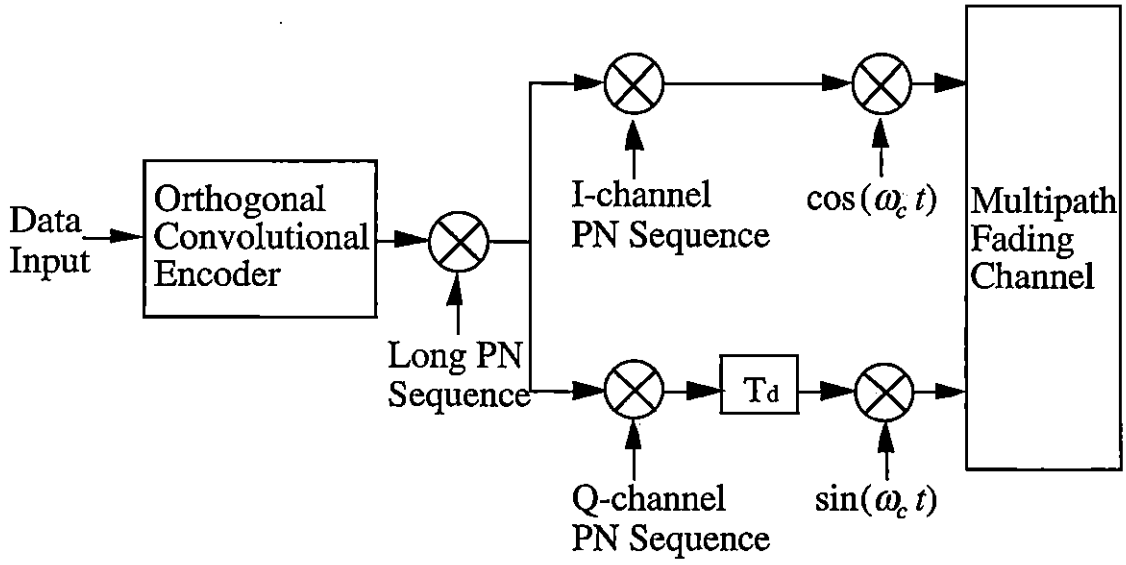

Figure 4.1 Transmitter Structure.

As in Chapter 3, the code rate and the constraint length are defined as $1/m$ ($M = 2^m$) and n_A, respectively. Depending on the output of the convolutional code, one of M orthogonal

sequences is chosen. Then the resulting orthogonal sequence is combined with long PN sequences which separate the users' channels and modulated using Offset-QPSK (OQPSK). The transmitted OQPSK signal of the i-th user during one symbol interval T_s is

$$\begin{aligned}\tilde{s}_i(t) = \{&\sqrt{P}W^r(t)c_i(t)p_I(t) \\ &+ j\sqrt{P}W^r(t-T_d)c_i(t-T_d)p_Q(t-T_d)\}\exp(-j\omega_c t) \qquad 0 \le t \le T_s\end{aligned} \tag{4.1}$$

where $c_i(t)$ is the long PN sequence for the i-th user, $p_I(t)$, $p_Q(t)$ are the PN sequences for the I and Q channels, T_d is the time offset which is equal to $T_c / 2$, and T_c is the chip interval. The processing gain $Gp = T_s / T_c$ where T_s is the symbol duration.

For wireless communications, there may be many propagation paths between a transmitter and a receiver due to the radio waves reflections from surrounding obstacles. If the signal written in Equation (4.1) is transmitted over a multipath channel, the resulting signal $y(t)$ at the receiver is the sum of delayed, phase-shifted, and attenuated versions of the input signal. The received signal for the i-th user can be written as

$$y_i(t) = \mathrm{Re}\left[\sum_{j=1}^{L_i} g_{ij}^*(t-\tau_{ij})\tilde{s}_i(t-\tau_{ij})\right] \tag{4.2}$$

where L_i is the number of paths for the i-th user's channel, τ_{ij} and $g_{ij}(t)$ are the delay and complex gain coefficients, respectively, for the j-th path for the i-th user, and the asterisk denotes complex conjugation. The complex gain coefficients are defined as

$$g_{ij}(t) = \gamma_{ij}(t)\exp(j\phi_{ij}) \tag{4.3}$$

where $\gamma_{ij}(t)$ and ϕ_{ij} account for the attenuation and phase shift, respectively. $\gamma_{ij}(t)$ is Rayleigh distributed[29] and ϕ_{ij} is an uniform random variable in $[0, 2\pi)$.

In a single cell CDMA cellular system with K users, the signal arriving at the base station receiver is

$$r(t) = \mathrm{Re}\left[\sum_{i=1}^{K}\sum_{j=1}^{L_i} g_{ij}^*(t-\tau_{ij})\tilde{s}_i(t-\tau_{ij})\right] + n(t) \tag{4.4}$$

where $n(t)$ is additive white Gaussian noise with zero mean and spectral density $N_o / 2$. At the output of the receiver bandpass filter with a bandwidth of $B (\approx 1 / T_c)$, $n(t)$ becomes a narrowband noise that can be represented by

$$n(t) = n_c(t)\cos\omega_c t + n_s(t)\sin\omega_c t \tag{4.5}$$

where $n_c(t)$ and $n_s(t)$ are independent lowpass Gaussian processes with zero mean and variance $N_o B$.

Figure 4.2 shows the receiver structure.

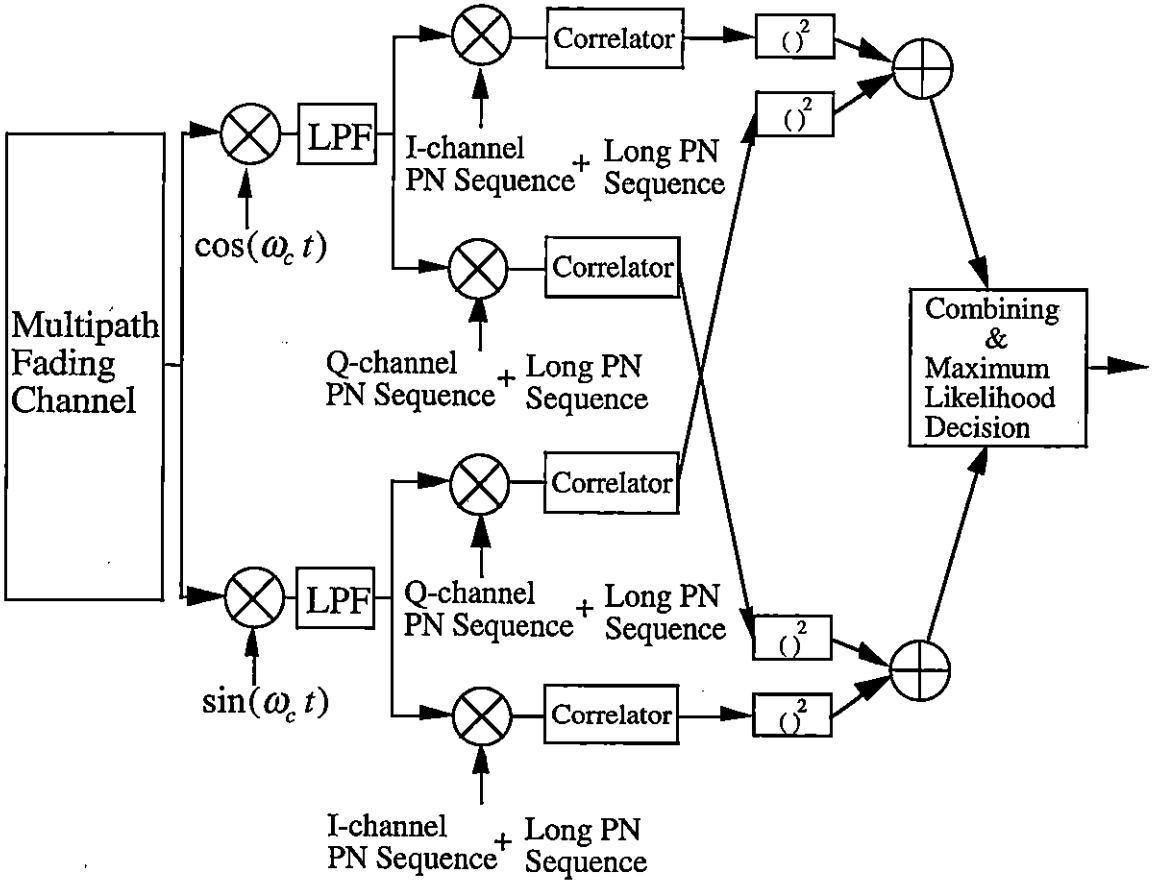

Figure 4.2 Receiver Structure.

At the output of the lowpass filter (LPF) of the upper path (I-channel),

$$\begin{aligned} d_I(t) &= LPF\left[r(t)\cos\omega_c t\right] \\ &= \sum_{i=1}^{K}\sum_{j=1}^{L_i}\gamma_{ij}(t-\tau_{ij})\{\sqrt{P}W^r(t-\tau_{ij})c_i(t-\tau_{ij})p_I(t-\tau_{ij})\frac{\cos\theta_{ij}}{2} \\ &+\sqrt{P}W^r(t-T_d-\tau_{ij})c_i(t-T_d-\tau_{ij})p_Q(t-T_d-\tau_{ij})\frac{\sin\theta_{ij}}{2}\}+\frac{n_c(t)}{2} \end{aligned} \tag{4.6}$$

where $\theta_{ij}=\phi_{ij}-\omega_c\tau_{ij}$. Also for the lower path (Q-channel),

$$\begin{aligned} d_Q(t) &= LPF\left[r(t)\sin\omega_c t\right] \\ &= \sum_{i=1}^{K}\sum_{j=1}^{L_i}\gamma_{ij}(t-\tau_{ij})\{-\sqrt{P}W^r(t-\tau_{ij})c_i(t-\tau_{ij})p_I(t-\tau_{ij})\frac{\sin\theta_{ij}}{2} \\ &+\sqrt{P}W^r(t-T_d-\tau_{ij})c_i(t-T_d-\tau_{ij})p_Q(t-T_d-\tau_{ij})\frac{\cos\theta_{ij}}{2}\}+\frac{n_s(t)}{2} \end{aligned} \tag{4.7}$$

For the I-channel, the output of the m-th correlator for the real (I) part of the λ-th path of the κ-th user is

$$\begin{aligned} Z_{I,I}^{\kappa\lambda}(m) &= \frac{1}{\sqrt{T_s}}\int_0^{T_s} d_I(t)c_\kappa(t-\tau_{\kappa\lambda})p_I(t-\tau_{\kappa\lambda})W^m(t-\tau_{\kappa\lambda})dt \\ &= \int_0^{T_s}\gamma_{\kappa\lambda}(t-\tau_{\kappa\lambda})\sqrt{\frac{P}{T_s}}W^r(t-\tau_{\kappa\lambda})W^m(t-\tau_{\kappa\lambda})\frac{\cos\theta_{\kappa\lambda}}{2}dt \\ &+ I_{I,I}^{\kappa\lambda,\kappa\lambda}+I_{I,I}^{\kappa\lambda,\kappa j}+I_{I,I}^{\kappa\lambda,ij}+N_{I,I}^{\kappa\lambda} \end{aligned} \tag{4.8}$$

where $I_{I,I}^{\kappa\lambda,\kappa\lambda}$, $I_{I,I}^{\kappa\lambda,\kappa j}$, $I_{I,I}^{\kappa\lambda,ij}$, and $N_{I,I}^{\kappa\lambda}$, which are given in Appendix A, represent the self path interference, interference due to the other paths, interference due to the other users and thermal noise due to the real (I) part of the path, respectively. Due to the quadrature nature of the PN sequences, the self path interference are small compared to the other interference (Appendix A). In this case, the I-channel correlator output becomes

$$Z_{I,I}^{\kappa\lambda}(m)=\begin{cases}\tilde{\gamma}_{\kappa\lambda}\sqrt{E_s}\dfrac{\cos\theta_{\kappa\lambda}}{2}+N_{I,I}^{\kappa\lambda}+I_{I,I}^{\kappa\lambda,\kappa j}+I_{I,I}^{\kappa\lambda,ij} & m=r \\ N_{I,I}^{\kappa\lambda}+I_{I,I}^{\kappa\lambda,\kappa j}+I_{I,I}^{\kappa\lambda,ij} & m\neq r\end{cases} \tag{4.9}$$

where $\tilde{\gamma}_{\kappa\lambda}$ is the average attenuation of $\gamma_{\kappa\lambda}(t)$ over the symbol period. Similarly, the output of the m-th correlator for the imaginary (Q) part of the λ-th path of the κ-th user $d_{I,Q}^{\kappa\lambda}$ is

$$Z_{I,Q}^{\kappa\lambda}(m)=\begin{cases}\tilde{\gamma}_{\kappa\lambda}\sqrt{E_s}\dfrac{\sin\theta_{\kappa\lambda}}{2}+N_{I,Q}^{\kappa\lambda}+I_{I,Q}^{\kappa\lambda,\kappa j}+I_{I,Q}^{\kappa\lambda,ij} & m=r\\ N_{I,Q}^{\kappa\lambda}+I_{I,Q}^{\kappa\lambda,\kappa j}+I_{I,Q}^{\kappa\lambda,ij} & m\neq r\end{cases} \tag{4.10}$$

where $I_{I,Q}^{\kappa\lambda,\kappa j}$, $I_{I,Q}^{\kappa\lambda,ij}$, and $N_{I,Q}^{\kappa\lambda}$ are the interference due to the other paths, interference due to the other users, and thermal noise due to the imaginary (Q) part of the path, respectively. Also the output of the Q-channel correlator becomes

$$Z_{Q,I}^{\kappa\lambda}(m)=\begin{cases}-\tilde{\gamma}_{\kappa\lambda}\sqrt{E_s}\dfrac{\sin\theta_{\kappa\lambda}}{2}+N_{Q,I}^{\kappa\lambda}+I_{Q,I}^{\kappa\lambda,\kappa j}+I_{Q,I}^{\kappa\lambda,ij} & m=r\\ N_{Q,I}^{\kappa\lambda}+I_{Q,I}^{\kappa\lambda,\kappa j}+I_{Q,I}^{\kappa\lambda,ij} & m\neq r\end{cases} \tag{4.11}$$

where $I_{Q,I}^{\kappa\lambda,\kappa j}$, $I_{Q,I}^{\kappa\lambda,ij}$, and $N_{Q,I}^{\kappa\lambda}$ are the interference due to the other paths, interference due to the other users, and thermal noise due to the real (I) part of the path, respectively, and

$$Z_{Q,Q}^{\kappa\lambda}(m)=\begin{cases}\tilde{\gamma}_{\kappa\lambda}\sqrt{E_s}\dfrac{\cos\theta_{\kappa\lambda}}{2}+N_{Q,Q}^{\kappa\lambda}+I_{Q,Q}^{\kappa\lambda,\kappa j}+I_{Q,Q}^{\kappa\lambda,ij} & m=r\\ N_{Q,Q}^{\kappa\lambda}+I_{Q,Q}^{\kappa\lambda,\kappa j}+I_{Q,Q}^{\kappa\lambda,ij} & m\neq r\end{cases} \tag{4.12}$$

where $I_{Q,Q}^{\kappa\lambda,\kappa j}$, $I_{Q,Q}^{\kappa\lambda,ij}$, and $N_{Q,Q}^{\kappa\lambda}$ are the interference due to the other paths, interference due to the other users, and thermal noise due to the imaginary (Q) part of the path, respectively. Due to the square-law combining, the decision variable for the κ-th user is

$$S^{\kappa}(m)=\sum_{j=1}^{L_\kappa}\{[Z_{I,I}^{\kappa j}(m)+Z_{Q,Q}^{\kappa j}(m)]^2+[Z_{I,Q}^{\kappa j}(m)-Z_{Q,I}^{\kappa j}(m)]^2\} \tag{4.13}$$

From [28][30][31] and Appendix A, the average SNR for the λ-th path of the κ-th user after the correlation is,

$$SNR_{\kappa\lambda}=\frac{\bar{\gamma}_{\kappa\lambda}E_s}{\dfrac{2\left(\sum_{i=1}^{K}\sum_{j=1}^{L_i}\bar{\gamma}_{ij}E_s-\bar{\gamma}_{\kappa\lambda}E_s\right)}{3Gp}+N_o} \tag{4.14}$$

For simplicity, L_i is set to L for all i. It is also assumed all fading paths have equal mean strength, i.e., $\bar{\gamma}_{ij}$ is 1 for all i and j. With these assumptions, the SNR per path becomes

$$SNR = \frac{E_s}{\frac{2(K \cdot L - 1)E_s}{3Gp} + N_o} \quad . \tag{4.15}$$

4.2 Performance Analysis

4.2.1 Conventional Canceller

To emphasize the performance difference of the conventional and the proposed canceller, a simple case is considered. To analyze the performance of the conventional CCI canceller, it is assumed that the interference from the other users is Gaussian distributed, the chip pulse shape is rectangular, the chip synchronization is perfect, and that the canceller can estimate the phase shift, the attenuation, and the delay perfectly. If the parameters are not accurately estimated, the performance of all cancellers will degrade[16][32] and this is shown in Section 4.2.3.

The error probability of the initial decision on the orthogonal sequence is given by[25, pp. 745]

$$Pe_c = 1 - \int_0^{\infty} \frac{U^{L-1} e^{\frac{-U}{1+SNR_{c1}}}}{(1+SNR_{c1})^L (L-1)!} \left(1 - e^{-U} \sum_{h=0}^{L-1} \frac{U^h}{h!}\right)^{M-1} dU \tag{4.16}$$

where SNR_{c1} is the signal-to-noise ratio after the first correlation given in Equation (4.15) and is given by

$$SNR_{c1} = \frac{E_s}{\frac{2(K \cdot L - 1)E_s}{3Gp} + N_o} \quad . \tag{4.17}$$

When errors in the initial decisions arise, the CCI canceller doubles the interference power[21][22]. Similar to Equation (3.9), the signal-to-noise ratio after the CCI cancellation is

$$SNR_{c2} = \frac{E_s}{2Pe_c \frac{2(K-1) \cdot LE_s}{3Gp} + \frac{2(L-1)E_s}{3Gp} + N_o} \quad . \tag{4.18}$$

Here, it is assumed that the receiver can estimate received signal power accurately. Then the upper bound on the bit error rate using a soft decision Viterbi decoder can be obtained as[25]

$$Pb_{c2} \approx \sum_{d=d_{free}}^{d_{free}+3} B_d Pd_c(d,L) \tag{4.19}$$

where

$Pd_c(d,L)$: probability of selecting an incorrect path(Appendix B)

$$Pd_c(d,L) = {p_c}^{dL} \sum_{h=0}^{dL-1} \binom{dL-1+h}{h} (1-p_c)^h \quad ; \tag{4.20}$$

p_c : probability of error for square-law combining between orthogonal sequences

$$p_c = \frac{1}{2+SNR_{c2}} \quad ; \tag{4.21}$$

B_d: total number of nonzero information bits on all weight d paths[18][26];

d_{free} : minimum free distance.

4.2.2 Proposed CCI Canceller

All of the assumptions are the same as those for the conventional canceller, which were presented in Section 4.2.1. Suppose there are A_d paths which cause d symbol errors after the re-encoding and the probability with which the Viterbi decoder chooses the wrong path with the distance d is

$$Pd_{n1}(d,L) = {p_{n1}}^{dL} \sum_{h=0}^{dL-1} \binom{dL-1+h}{h} (1-p_{n1})^h \tag{4.22}$$

where

$$p_{n1} = \frac{1}{2+SNR_{n1}} \quad ; \tag{4.23}$$

$$SNR_{n1} = \frac{E_s}{\frac{2(K \cdot L-1)E_s}{3 \cdot Gp} + N_o} \quad . \tag{4.24}$$

Then the average symbol error probability after the re-encoding caused by one user is

$$Pe_n \approx \sum_{d=d_{free}}^{d_{free}+3} d \cdot A_d \cdot Pd_{n1}(d,L) \quad . \tag{4.25}$$

The signal-to-noise ratio after the cancellation is

$$SNR_{n2} = \frac{E_s}{2Pe_n \frac{2(K-1)LE_s}{3Gp} + \frac{2(L-1)E_s}{3Gp} + N_o} \quad . \tag{4.26}$$

From SNR_{n2}, the approximate error rate after the cancellation can be obtained by an equation similar to Equation (4.19), that is

$$Pb_{n2} \approx \sum_{d=d_{free}}^{d_{free}+3} B_d Pd_{n2}(d,L) \tag{4.27}$$

where $Pd_{n2}(d,L)$ is obtained by substituting SNR_{n2} into Equations (4.20) and (4.21) instead of SNR_{c2}

$$Pd_{n2}(d,L) = {p_{n2}}^{dL} \sum_{h=0}^{dL-1} \binom{dL-1+h}{h} (1-p_{n2})^h \quad ; \tag{4.28}$$

$$p_{n2} = \frac{1}{2+SNR_{n2}} \quad . \tag{4.29}$$

4.2.3 Imperfect Cancellation

In Sections 4.2.1 and 4.2.2, it is assumed that the canceller can estimate the phase shift, the attenuation, and the delay perfectly. However, there are always estimation errors on these parameters due to the noise or the co-channel interference. Therefore, even though the canceller reconstructs correct signals after the initial decisions, it might not remove the co-channel interference completely. There is residual interference caused by imperfect cancellation.

Suppose a fraction β of canceled CCI power is left in the composite signal. For the conventional canceller, the average number of canceled users is $(K-1)(1-Pe_c)$, so the SNR after the cancellation is

$$SNR_{c2}(\beta) = \frac{E_s}{2Pe_c \frac{2(K-1)LE_s}{3Gp} + \frac{2\beta(K-1)(1-Pe_c)LE_s}{3Gp} + \frac{2(L-1)E_s}{3Gp} + N_o}. \tag{4.30}$$

For the proposed canceller, the average number of canceled users is given by $(K-1)(1-Pe_n)$, so the SNR after the cancellation is

$$SNR_{n2}(\beta)=\frac{E_s}{2Pe_n\frac{2(K-1)LE_s}{3Gp}+\frac{2\beta(K-1)(1-Pe_n)LE_s}{3Gp}+\frac{2(L-1)E_s}{3Gp}+N_o}. \quad (4.31)$$

Substituting $SNR_{c2}(\beta)$ and $SNR_{n2}(\beta)$ into Equations (4.19) and (4.27), the approximate error rate after the cancellation can be obtained.

4.2.4 Intercell Interference and Soft Handoff

In previous sections, a single cell configuration is assumed. In this section, I now consider a multicell configuration, consisting of a cluster of seven cells as presented in Fig 4.3. Each cell is divided into three sectors. Due to the sectorization, the interference at the base station comes from only two adjacent cells. Based on the assumptions of perfect power control, wave propagation with path loss proportional to the 4th power of the distance, and K uniformly distributed users in a sector, the intercell interference energy from one of the adjacent cells is[33]

$$I_{mul}(d_mR)=2E_{ts}\cdot 3K\cdot\left[2\cdot {d_m}^2\ln\left(\frac{{d_m}^2}{{d_m}^2-1}\right)-\frac{4\cdot {d_m}^4-6\cdot {d_m}^2+1}{2({d_m}^2-1)^2}\right] \quad (4.32)$$

where d_mR is the distance between the base stations (in this case d_m=2), and E_{ts} is the total symbol energy defined as LE_s. Therefore, in Equation (4.15), the SNR per path becomes

$$SNR=\frac{E_s}{\frac{2(K\cdot L-1)E_s}{3\cdot Gp}+2\cdot\frac{2I_{mul}(2R)}{3\cdot Gp}+N_o}. \quad (4.33)$$

If soft handoff is employed, mobiles close to cell boundaries might transmit to two base stations. Suppose the handoff probability is P_{off}[34], the period of the soft handoff is short, and the mobiles which are in the soft handoff process transmit their signals with energy E_{ts} to the base stations, the number of users using the soft handoff can be considered as

$$K'=\lfloor(1+P_{off})K\rfloor \quad (4.34)$$

where $\lfloor X \rfloor$ is the nearest integer less than or equal to X. Also, the intercell interference decreases to

$$I'_{mul}(2R) = I_{mul}(2R) - E_{ts}\lfloor P_{off}K \rfloor \quad . \tag{4.35}$$

The performance of the CCI cancellers can be calculated by adding the intercell interference term and replacing K with K'. Therefore the path SNR after the cancellation for the conventional canceller is

$$SNR'_{c2} = \frac{E_s}{2Pe'_c \frac{2(K'-1)LE_s}{3Gp} + \frac{2(L-1)E_s}{3Gp} + 2 \cdot \frac{2I'_{mul}(2R)}{3Gp} + N_o} \tag{4.36}$$

where Pe'_c is calculated by Equations (4.16) and (4.17) with SNR_{c1} replacing SNR given by Equation (4.33). Also, for the proposed canceller the path SNR after the cancellation is

$$SNR'_{n2} = \frac{E_s}{2Pe'_n \frac{2(K'-1) \cdot LE_s}{3Gp} + \frac{2(L-1)E_s}{3Gp} + 2 \cdot \frac{2I'_{mul}(2R)}{3Gp} + N_o} \tag{4.39}$$

where Pe'_n is calculated by Equations (4.22), (4.23), (4.24), and (4.25) with SNR_{n1} replacing SNR given by Equation (4.33).

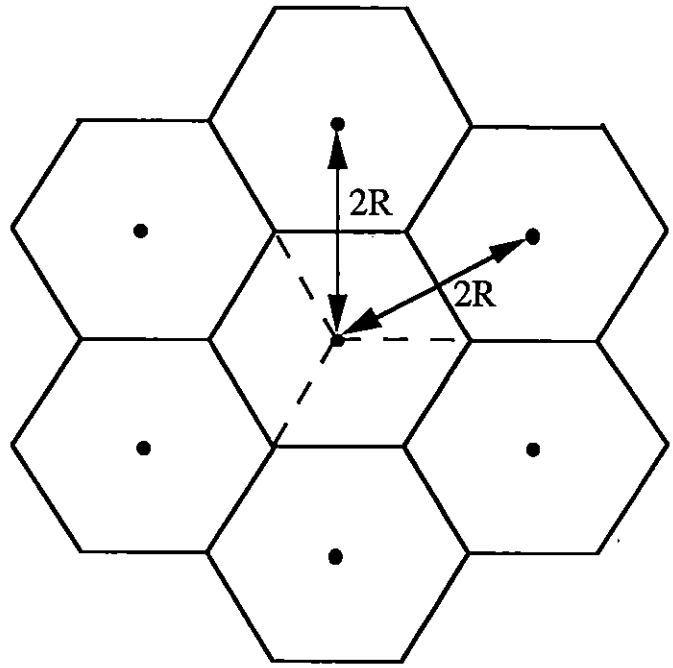

Figure 4.3 Multicell Configuration.

4.3 Results

The following results assume ideal interleaving. The processing gain *Gp* is set to 128 and the coding rate is 1/3 (8-ary orthogonal convolutional code) with optimum generator polynomials given in Table 3.1.

Figure 4.4 and 4.5 show the BER performance of the convolutional orthogonal code on the multipath Rayleigh fading channel. In these figures, the points are the simulation results and the line is the theoretical performance calculated from the approximation with the first four terms of Equation (4.19). The results for the number of paths equal to 1 and 3 are shown in Figures 4.4 and 4.5, respectively. As the simulated points are close to the theoretical values with $w = d_{free}$ to $d_{free}+3$, the approximation is appropriate.

In Figures 4.6 to 4.18, the performances without a canceller, with the conventional canceller and with the proposed canceller are presented for different conditions. The performance without a canceller is calculated by Equations (4.19), (4.20), and (4.21) with SNR_{c1} replacing SNR_{c2}. Figures 4.6 and 4.7 show the system SNR vs. SNR/symbol with the number of paths equal to 1 and 3, respectively. The number of users which transmit at the same time is denoted by *K*. The system SNR is the SNR just before the final maximum likelihood decision (after the cancellation), defined as $L \cdot SNR_{c2}$ or $L \cdot SNR_{n2}$. The SNR per symbol is the SNR without the CCI, which is defined as $E_{ts} / N_o = LE_s / N_o$. Thus the difference between these two SNR's as shown in Figures 4.8 and 4.9 is the CCI which cannot be removed by the canceller. From Figures 4.8 and 4.9, it is clear that the proposed canceller cancels more CCI and provides a better SNR than the conventional canceller when the SNR per symbol is not too low. Especially when *K*=20, the proposed canceller removes most of the CCI and provides a nearly interference free signal for the final maximum likelihood decision. Also the proposed canceller works very well when there are multiple paths on the channel which cause more CCI. In Figure 4.9, when *K*=20, the

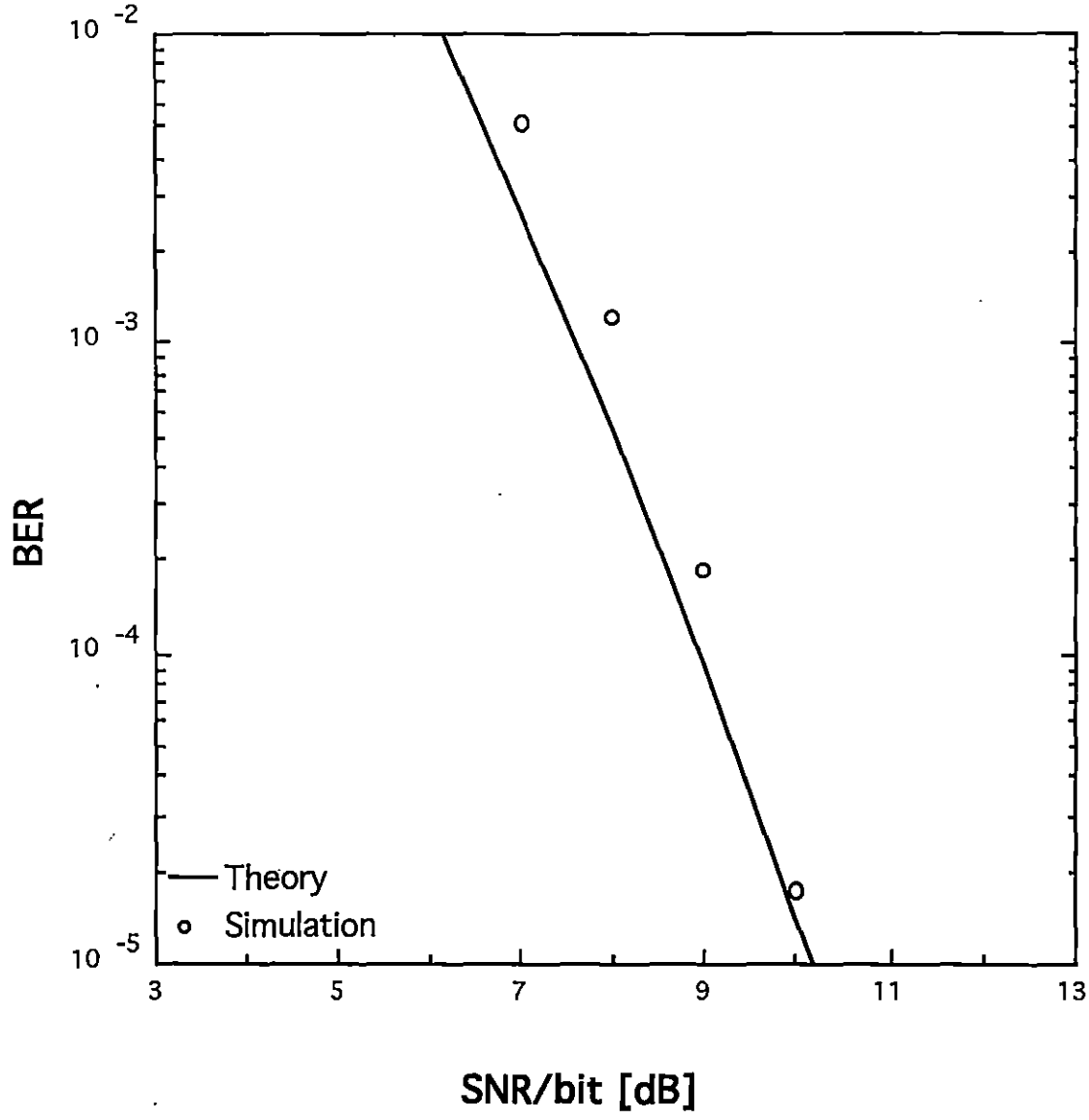

Figure 4.4 Performance of Orthogonal Convolutional Code,

Number of Paths=1, Code Rate=1/3,
Constraint Length=9.

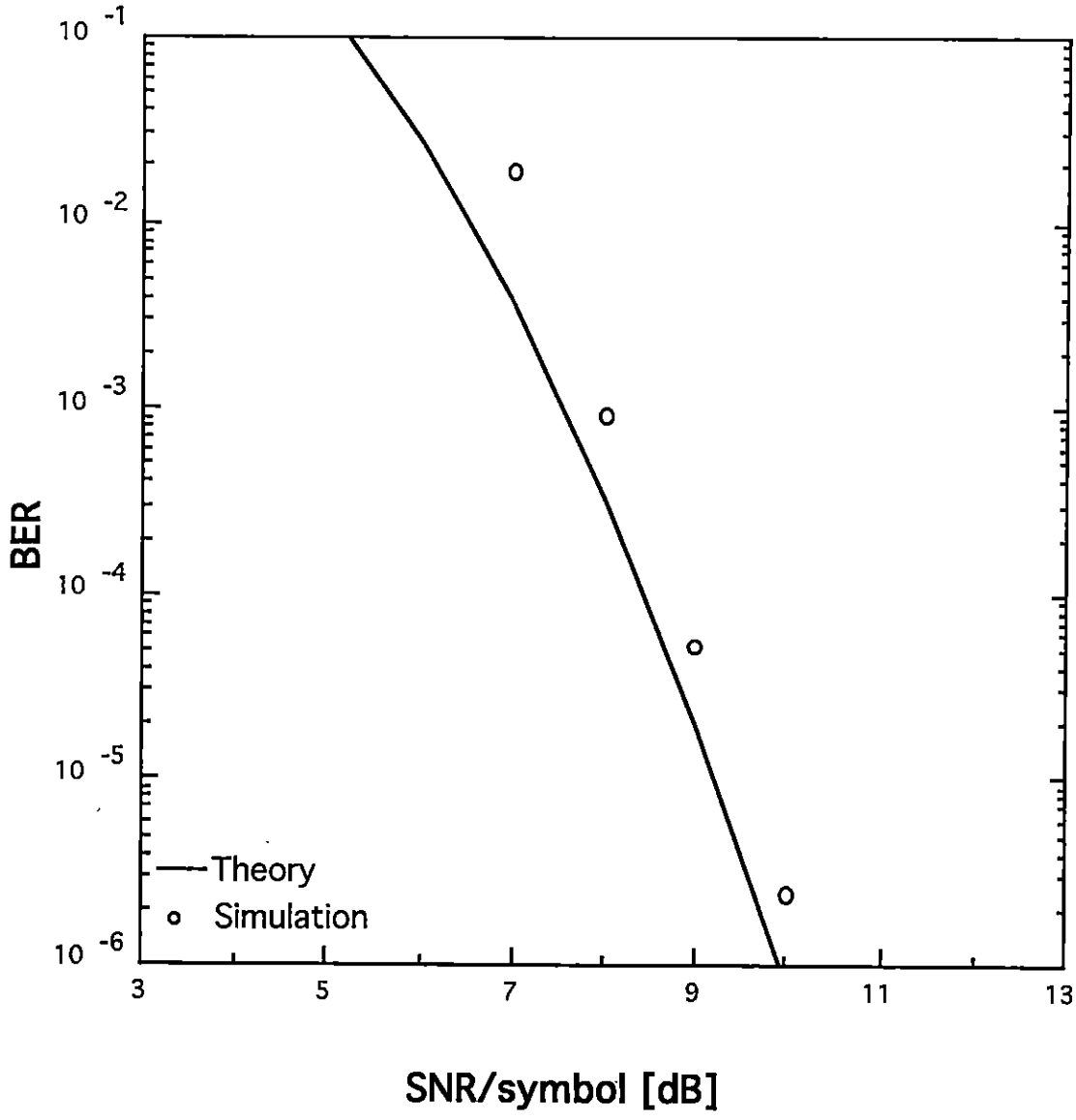

Figure 4.5 Performance of Orthogonal Convolutional Code,

Number of Paths=3, Code Rate=1/3,
Constraint Length=9.

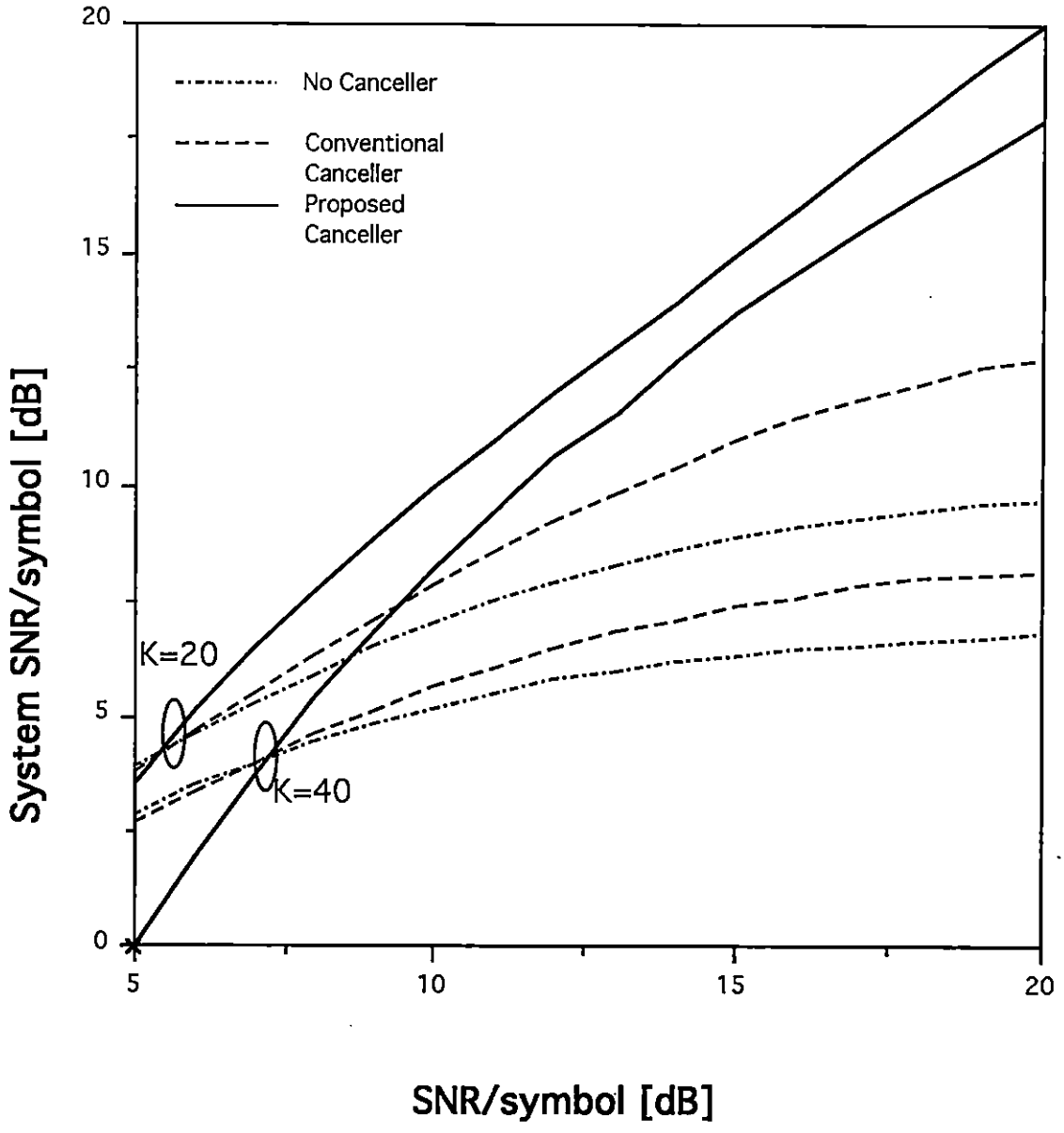

Figure 4.6 System SNR vs. SNR/symbol,

Number of Paths=1, Code Rate=1/3,
Constraint Length=9.

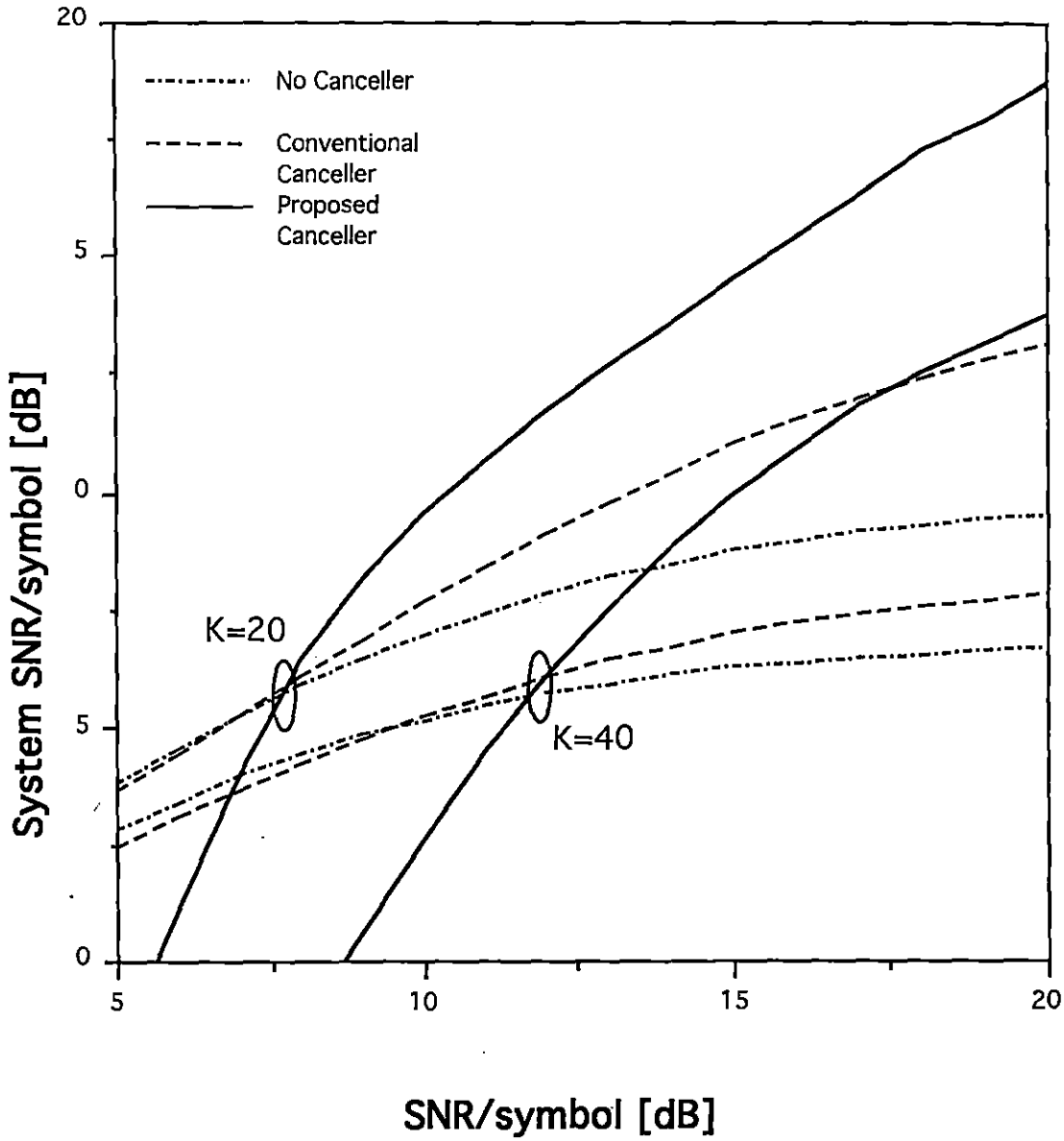

Figure 4.7 System SNR vs. SNR/symbol

Number of Paths=3, Code Rate=1/3,
Constraint Length=9.

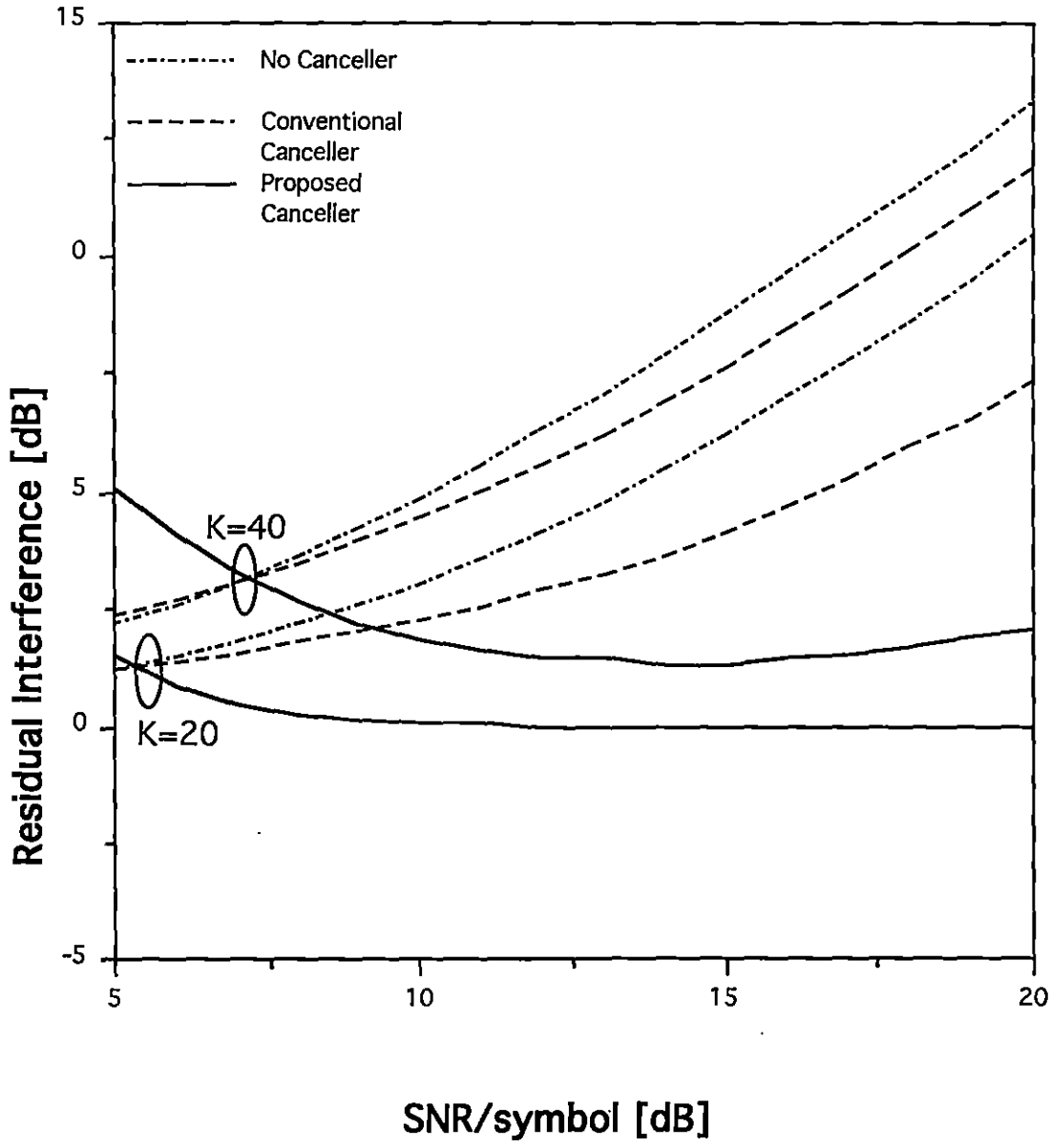

Figure 4.8 Residual Interference vs. SNR/symbol,

Number of Paths=1, Code Rate=1/3,
Constraint Length=9.

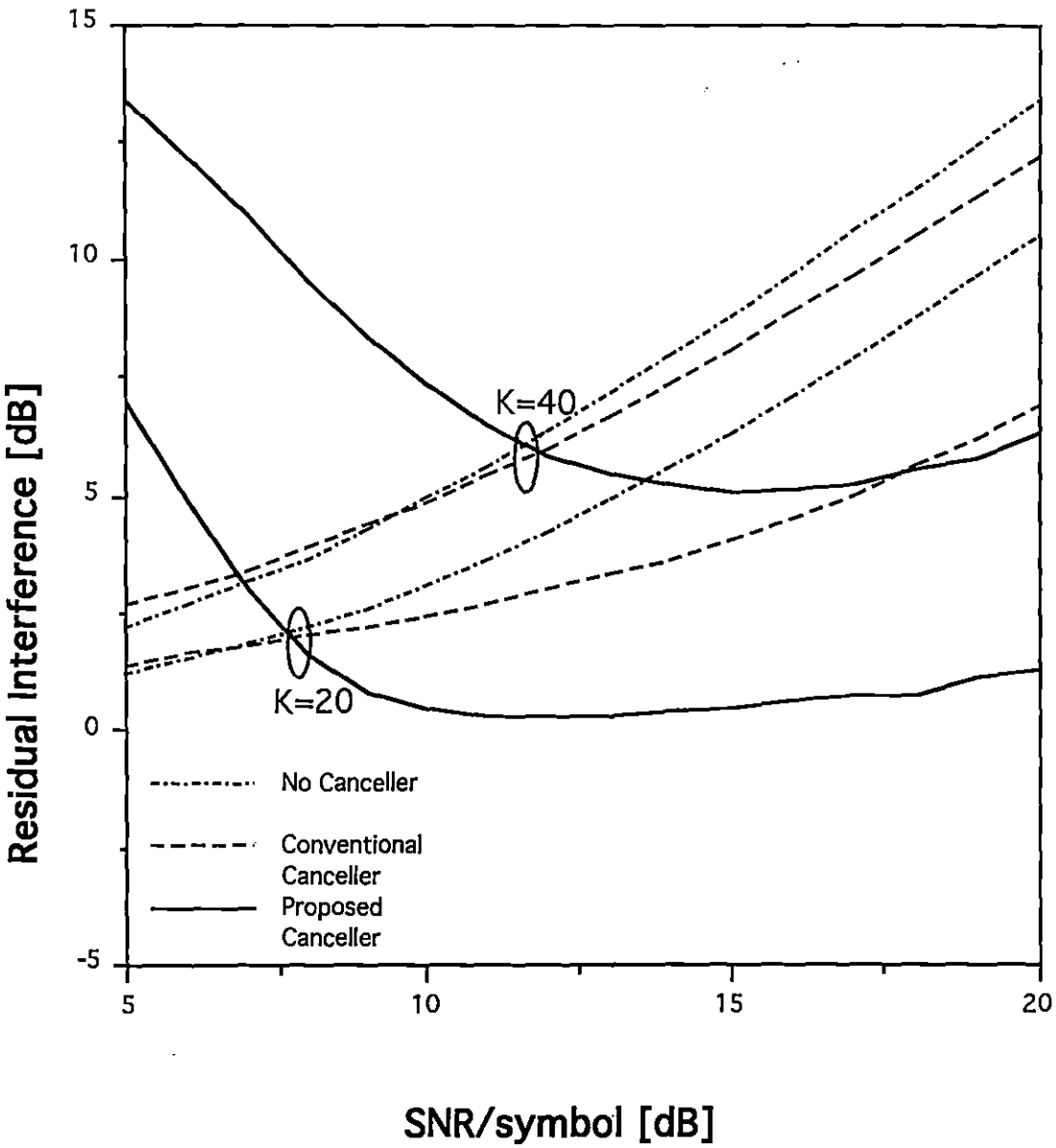

Figure 4.9 Residual Interference vs. SNR/symbol,
Number of Paths=3, Code Rate=1/3,
Constraint Length=9.

system SNR of the conventional canceller does not improve in the high SNR per symbol area since the CCI dominates the accuracy of the initial decisions. On the other hand, the proposed canceller improves the system SNR as the SNR per symbol becomes larger. However, if K is 40, there are 3 paths, and the SNR per symbol is less than 12 dB, then the re-encoding process produces too much interference. Thus, in this case, the proposed canceller is inferior to the conventional canceller.

Figures 4.10 and 4.11 show the BER vs. SNR per symbol with the number of paths equal to 1 and 3, respectively. When K=20, the performance of the proposed canceller is very close to the performance with K=1 and superior to the conventional canceller by 2 dB with 1 path and by 1 dB with 3 paths at BER=10^{-3} . If K=40, the difference between the BER of the two methods is much larger than the K=20 case. For example, for constraint length 9, with 1 path, and at BER=10^{-3}, the difference is more than 6 dB as seen in Figure 4.10.

Figures 4.12 and 4.13 show the BER vs. the number of users for 1 and 3 paths, respectively. It is shown that the number of simultaneous users at BER=10^{-3} increases by a factor of one and a half to three with the new canceller as compared with the conventional canceller. It is also clear that up to about 20 users the proposed canceller removes almost all of the CCI when the SNR per symbol equals 10 dB as the error floor due to thermal noise is observed.

Figures 4.14 and 4.15 show the BER vs. the constraint length of the convolutional code for 1 and 3 paths, respectively. From the results, a significant performance improvement can be obtained by using a longer constraint length, especially when K is large. As the constraint length becomes longer, the BER decreases linearly. Therefore the canceller should use a orthogonal convolutional code which has a large constraint length.

As discussed in Chapter 3, the proposed cancellation scheme can also be viewed as an effective way of reducing the system implementation complexity even on the multipath

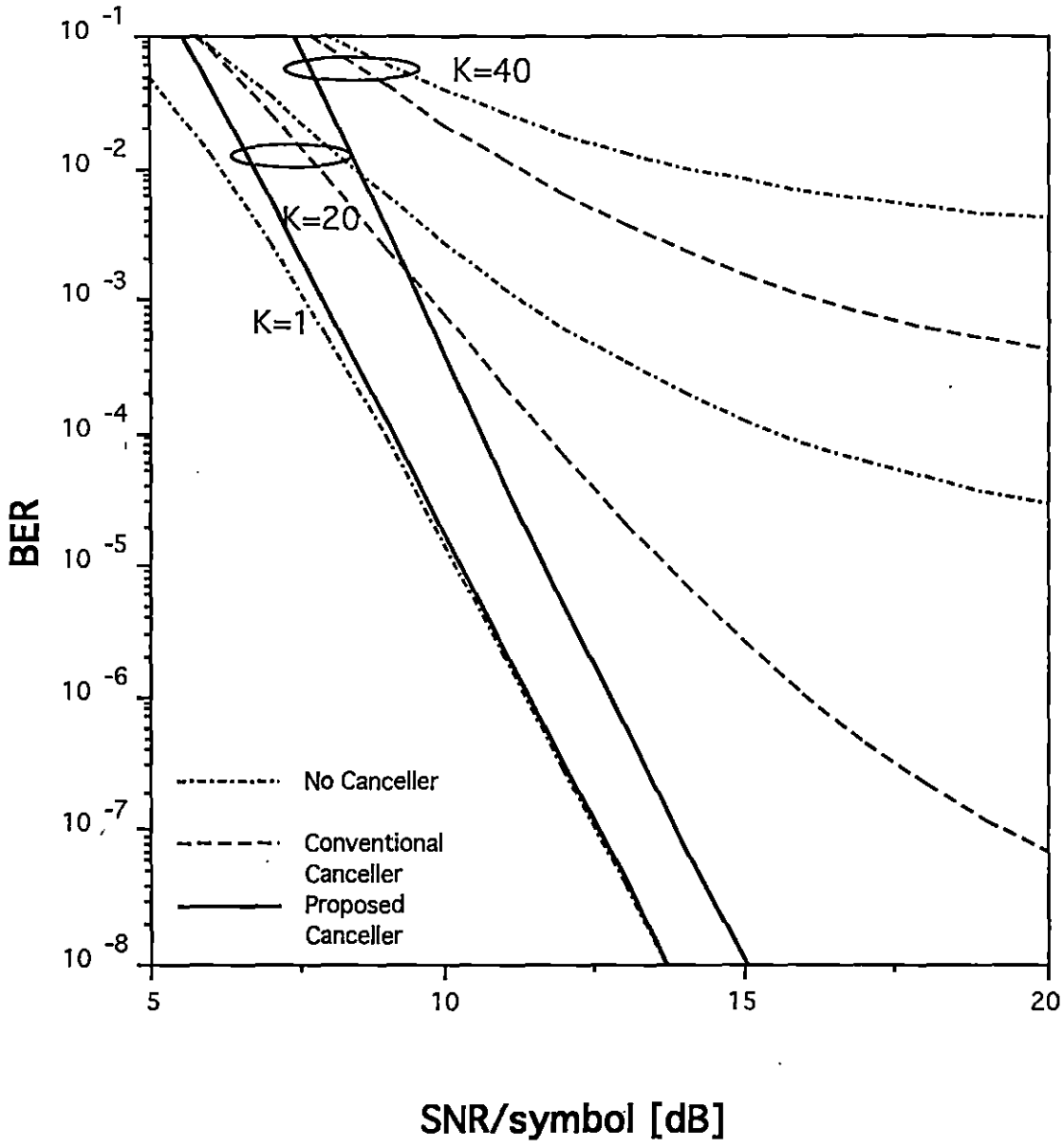

Figure 4.10 BER vs. SNR/symbol,

Number of Paths=1, Code Rate=1/3,
Constraint Length=9.

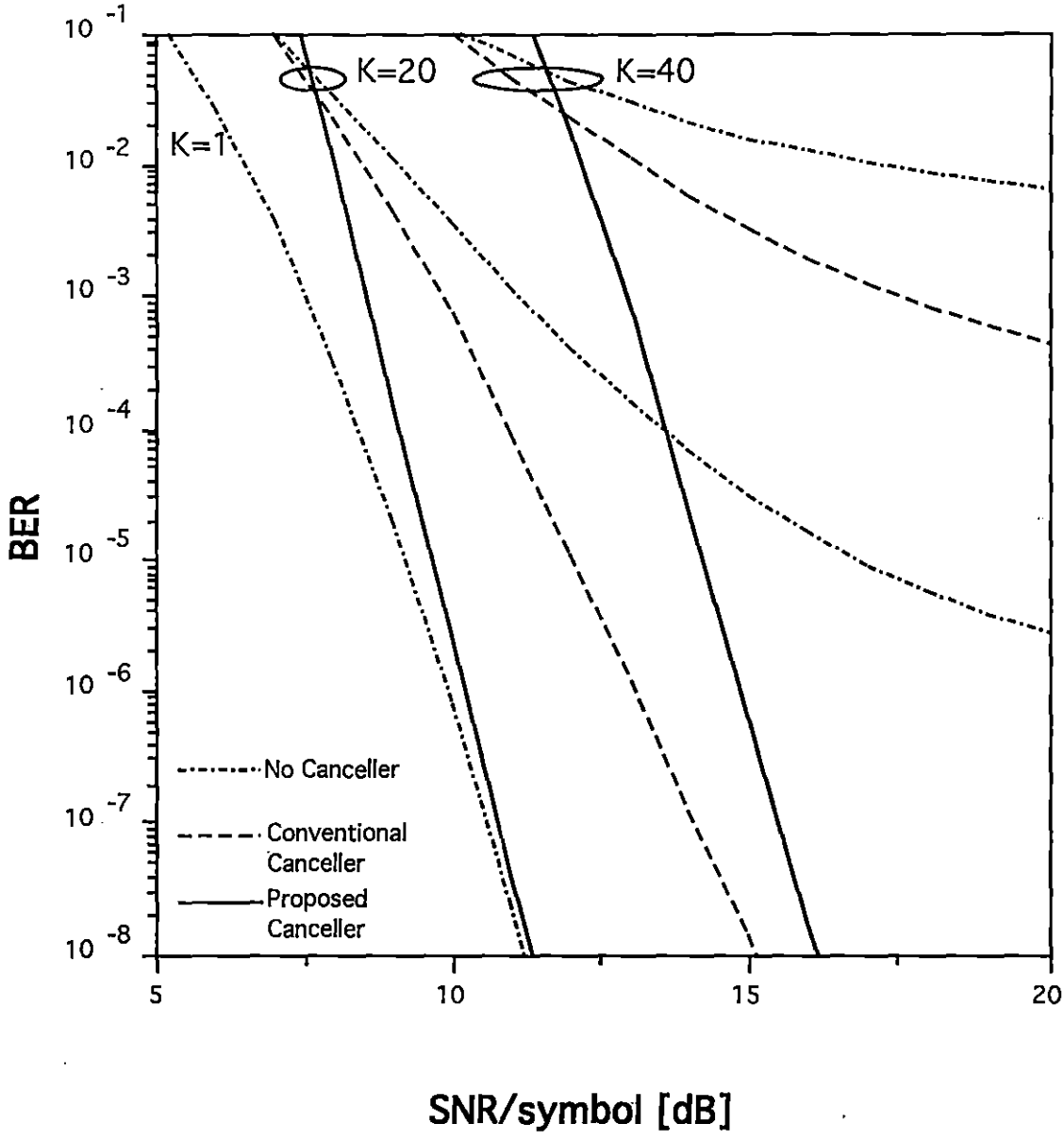

Figure 4.11 BER vs. SNR/symbol,

Number of Paths=3, Code Rate=1/3,
Constraint Length=9.

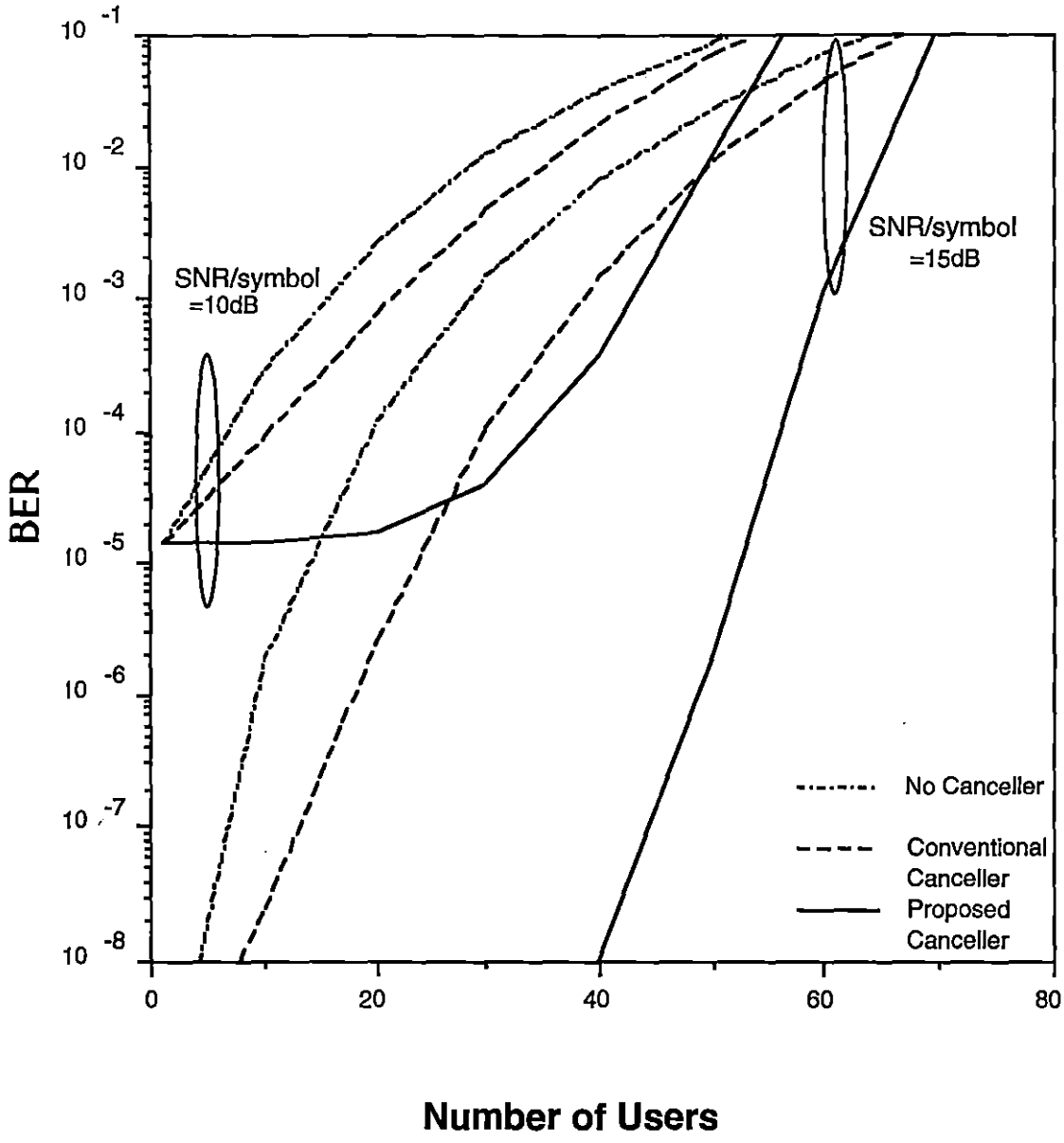

Figure 4.12 BER vs. Number of Users,

Number of Paths=1, Code Rate=1/3,
Constraint Length=9.

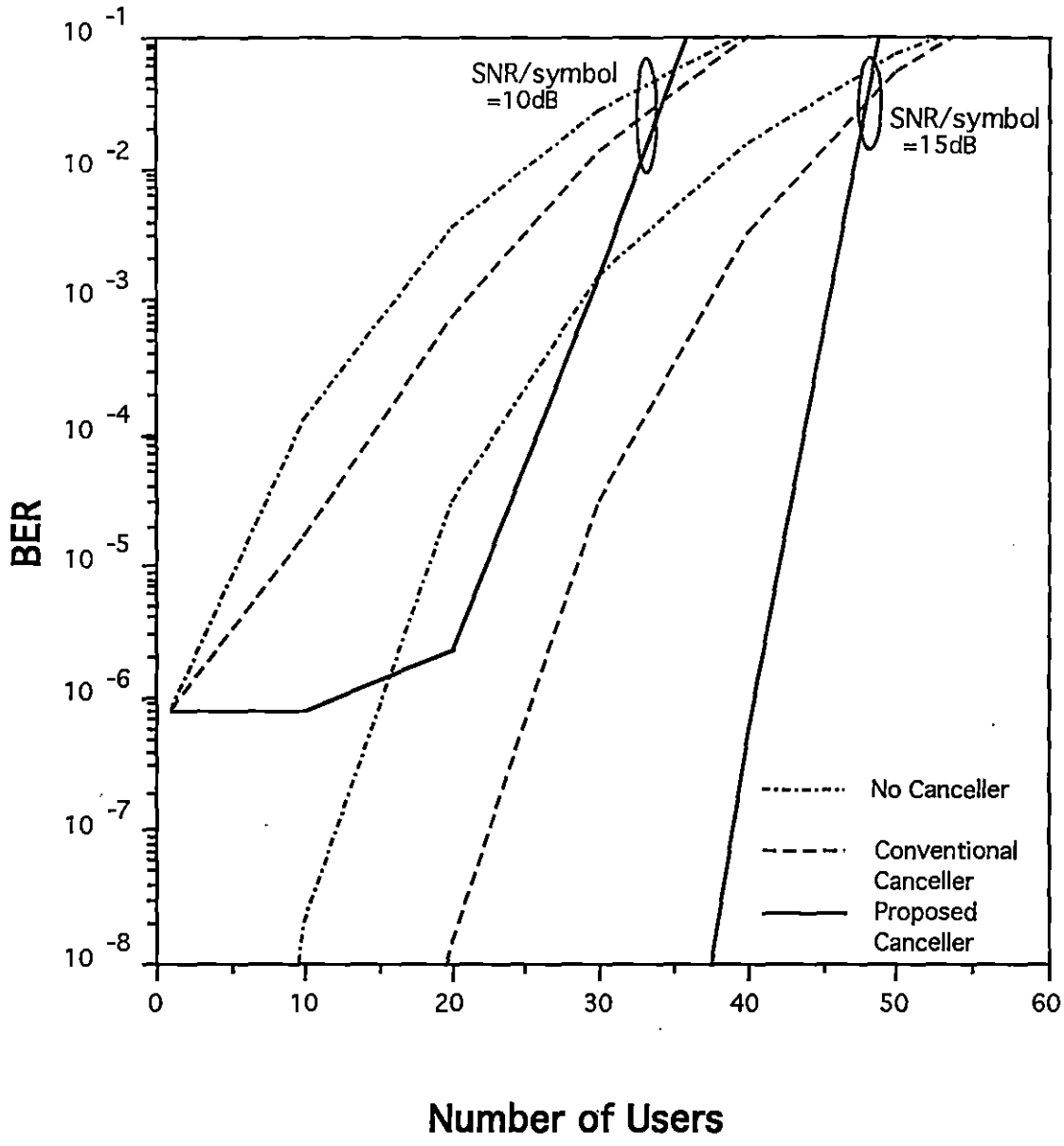

Figure 4.13 BER vs. Number of Users,

Number of Paths=3, Constraint Length=9,
Code Rate=1/3.

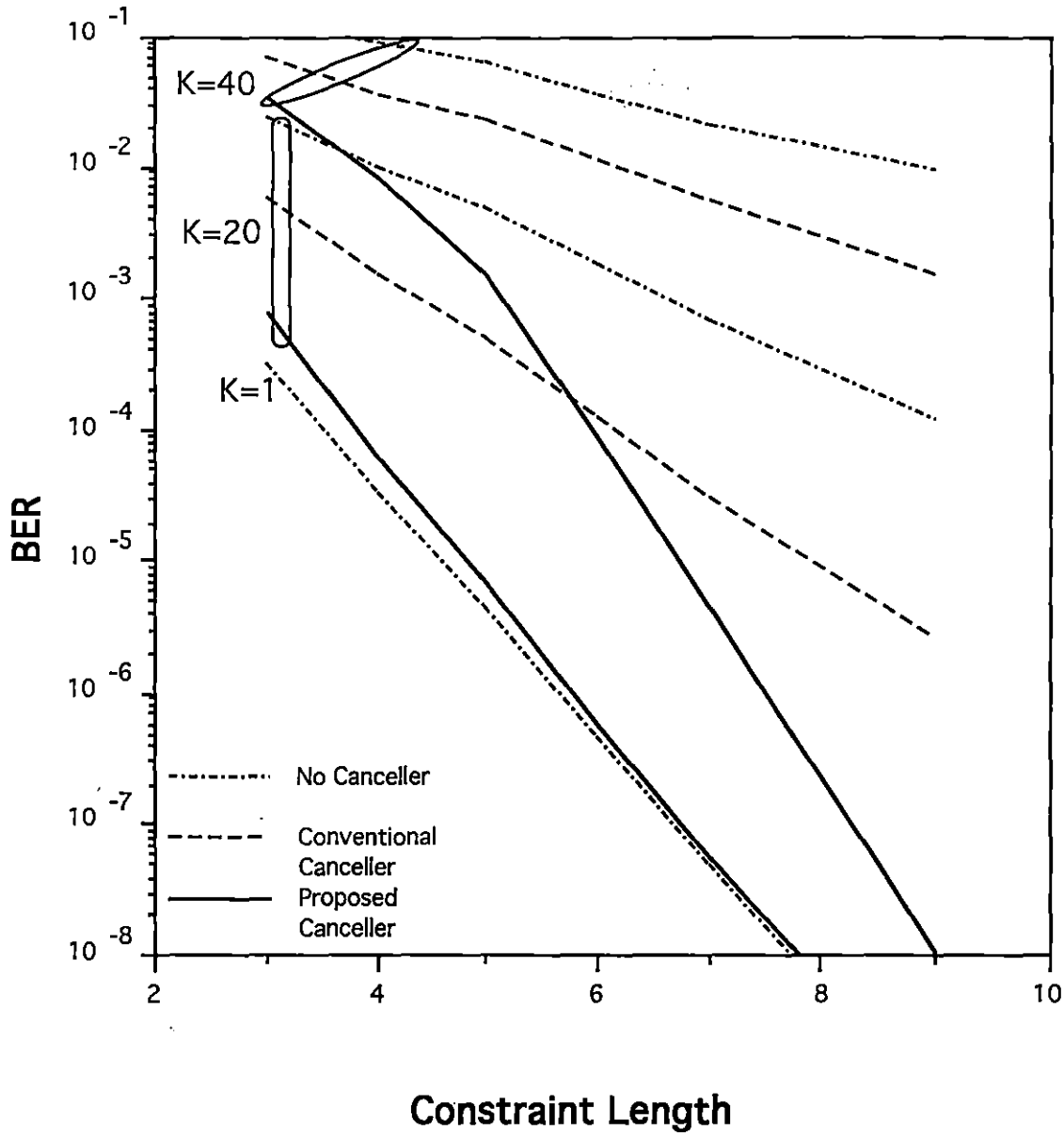

Figure 4.14 BER vs. Constraint Length,

Number of Paths=1, SNR/symbol=15dB
Code Rate=1/3.

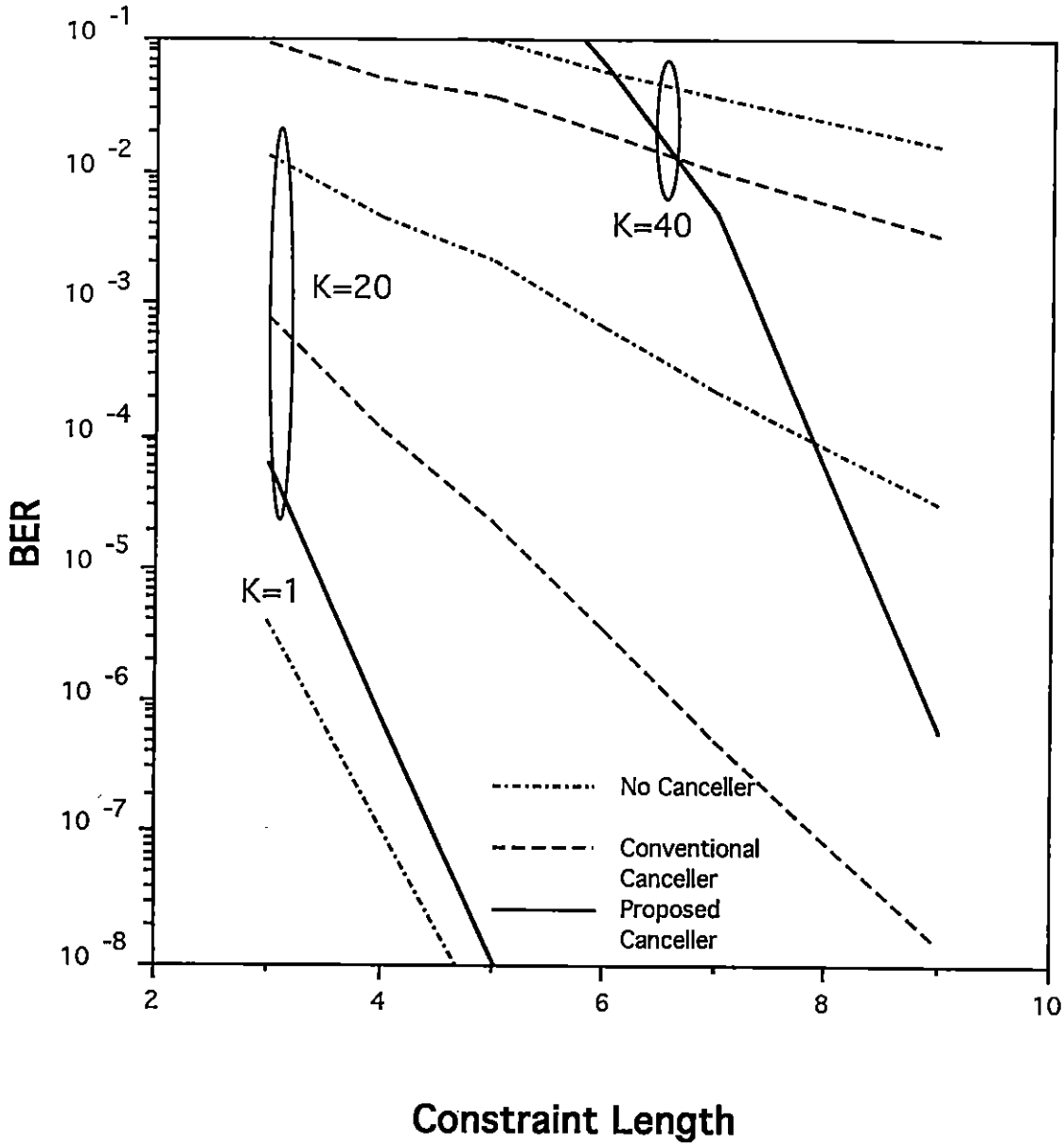

Figure 4.15 BER vs. Constraint Length,

Number of Paths=3, SNR/symbol=15dB,
Code Rate=1/3.

Rayleigh fading channel. For example, for K=20 and required BER<10^{-3}, from Figure 4.14, the conventional canceller requires the code constraint length equal to 5, while the proposed canceller requires the constraint length equal to 3. This represents more than a factor of four reduction in Viterbi decoding complexity. Even if the number of Viterbi decoders is doubled as mentioned in Section 2.2.2, the overall complexity is reduced by more than a factor of two.

Figure 4.16 shows the BER vs. number of paths which are available for the square-law combining. When K is 20, the BER of both cancellers improves as the number of paths increases from 1 to 2. However, if the number of paths further increases, the performance deteriorates, and the proposed canceller is affected more than the conventional canceller when the number of paths is more than 5. When K is 40, as the number of paths increases, the BER becomes worse, as there is too much interference due to too many paths, and the low SNR produces more symbol errors in the decoding process.

Figures 4.17 and 4.18 show the BER performance in the presence of imperfect cancellation for 1 and 3 paths. The estimation error β is the fraction of canceled signal power which is left in the composite signal. There is almost no influence of the estimation error on both the conventional and the proposed cancellers when $\beta<10^{-2}$ and both cancellers work well until $\beta=10^{-1}$. From these results, it is concluded that CCI cancellers are useful even with the estimation error.

Figures 4.19 and 4.20 show the BER vs. the number of users with the estimation error for 1 and 3 paths, respectively. It is clear that the number of simultaneous users with estimation error $\beta=10^{-1}$ is almost the same as the no estimation error for both the conventional canceller and the proposed canceller. Therefore, the proposed canceller is effective and better than the conventional canceller in the presence of the interference caused by imperfect cancellation.

Figures 4.21 and 4.22 show the BER performance for the multicell situation and the effects of the cancellation with the soft handoff and 1 and 3 paths per channel. The number of users per sector is the number of users which transmit in one sector at the same time. Though the handoff probability P_{off} depends on many parameters, P_{off} is set to 0.087 following reference [34] as an example. It is shown that the combination of the soft handoff and the proposed canceller improves the capacity while the conventional canceller does not make any substantial difference in the capacity. The reason is that if the number of users per sector is small, very few users utilize the soft handoff. Therefore the effect of the canceller is not significant as it does not cancel signals from adjacent cell mobiles which are not in soft handoff to the reference cell. On the other hand, if there are a large number of users per sector, the conventional canceller does not work well. In this case, even though some mobiles outside the cell transmit to the base station during soft handoff, the conventional canceller might not cancel the interference from them. Since the proposed canceller still works with a large number of users in the low BER region, it shows the capacity improvement with the use of the soft handoff.

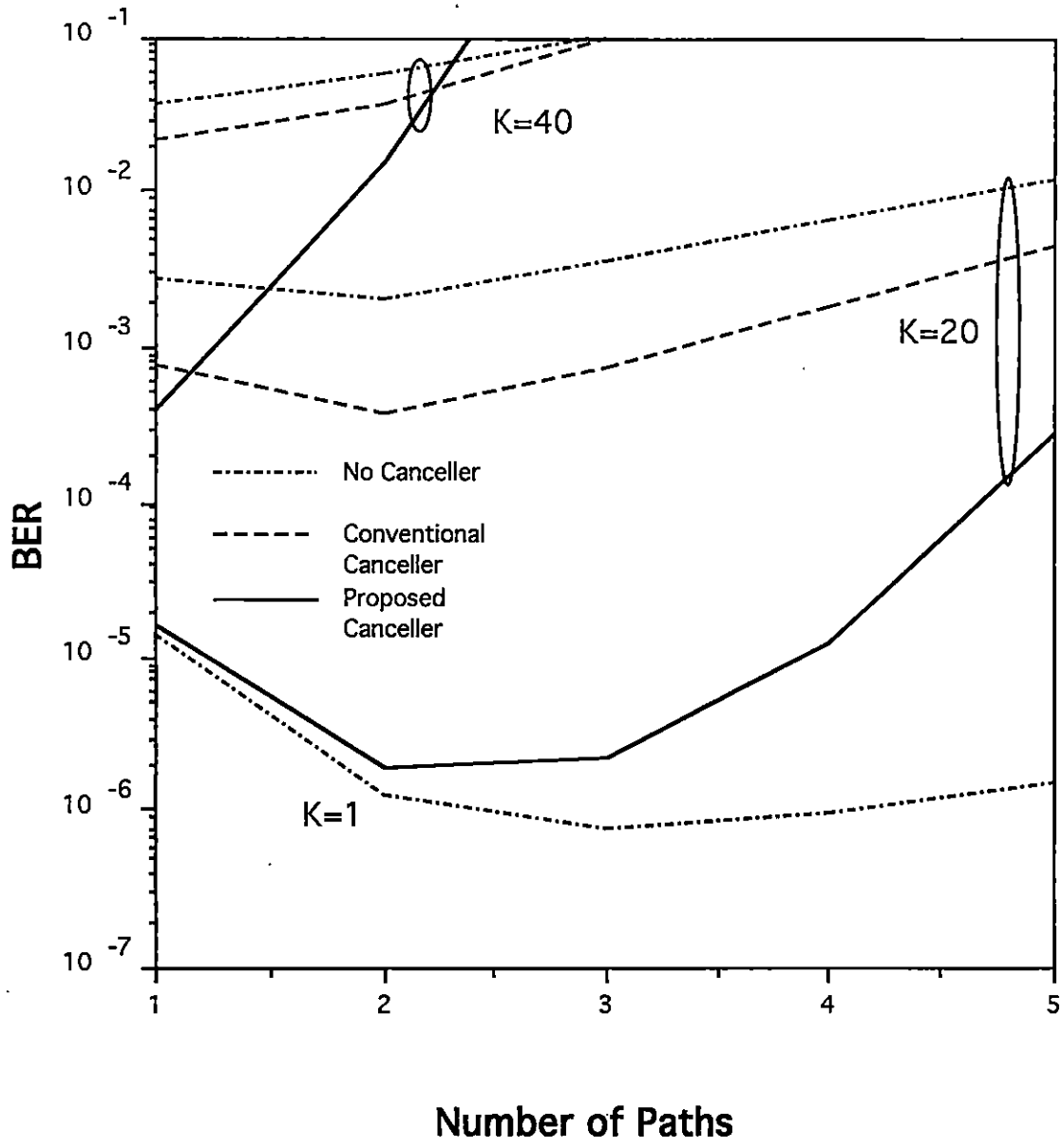

Figure 4.16 BER vs. Number of Paths,
SNR/symbol=15dB, Code Rate=1/3,
Constraint Length=9.

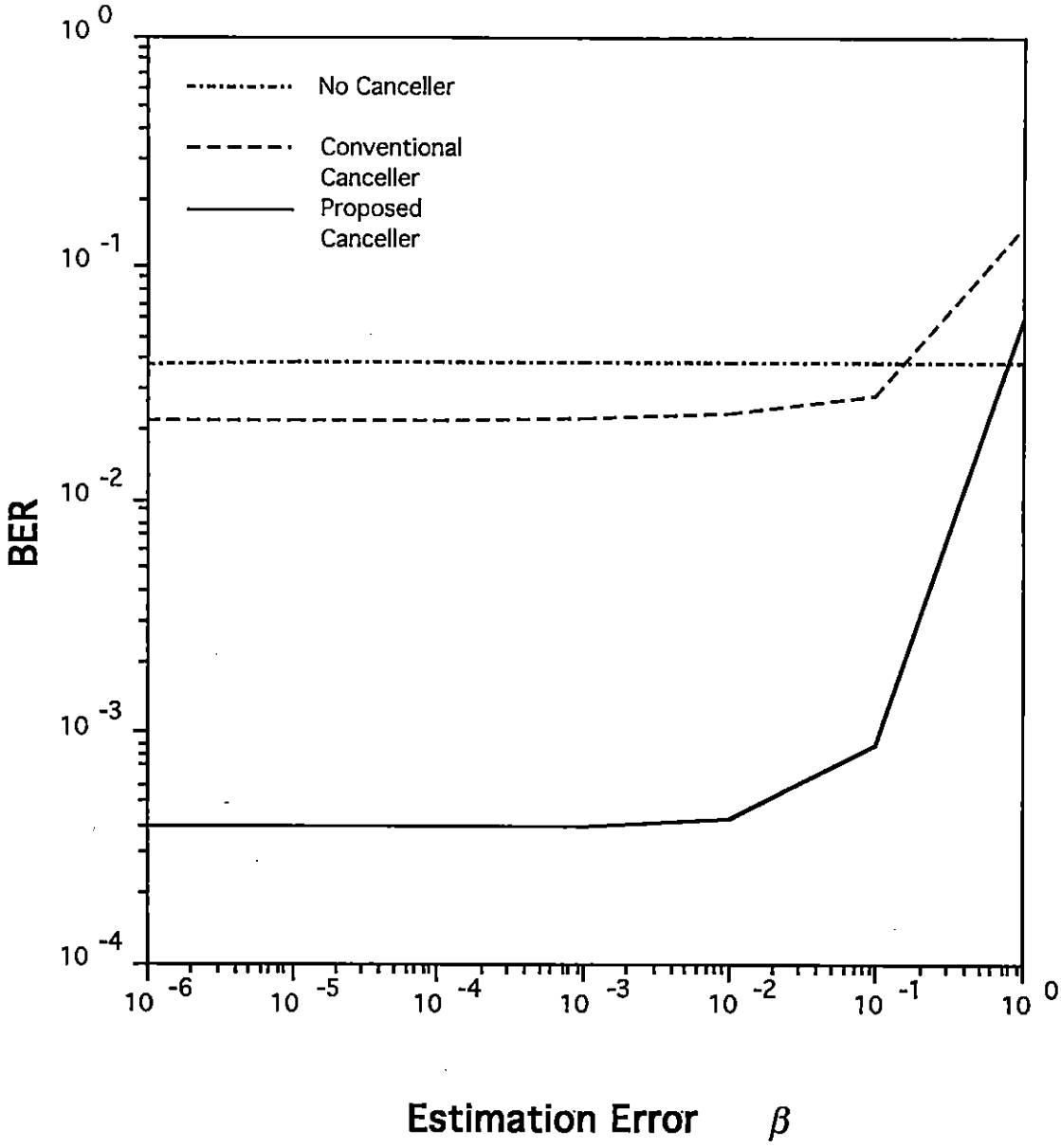

Figure 4.17 BER vs. Estimation Error

Number of Users=40, Number of Paths=1,
SNR/symbol=10dB, Code Rate=1/3,
Constraint Length=9.

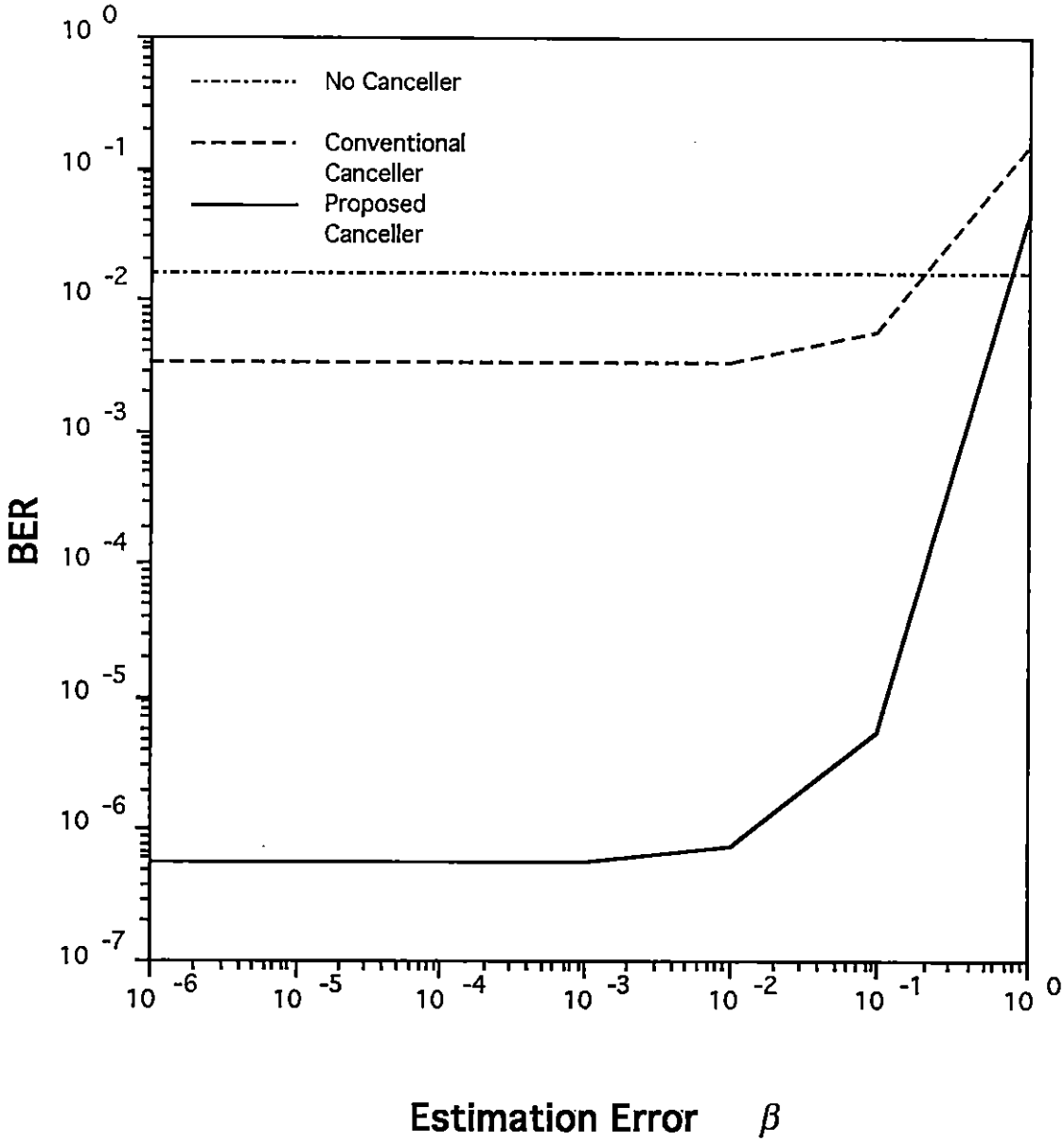

Figure 4.18 BER vs. Estimation Error,

Number of Users=40, Number of Paths=3,
SNR/symbol=15dB, Code Rate=1/3,
Constraint Length=9.

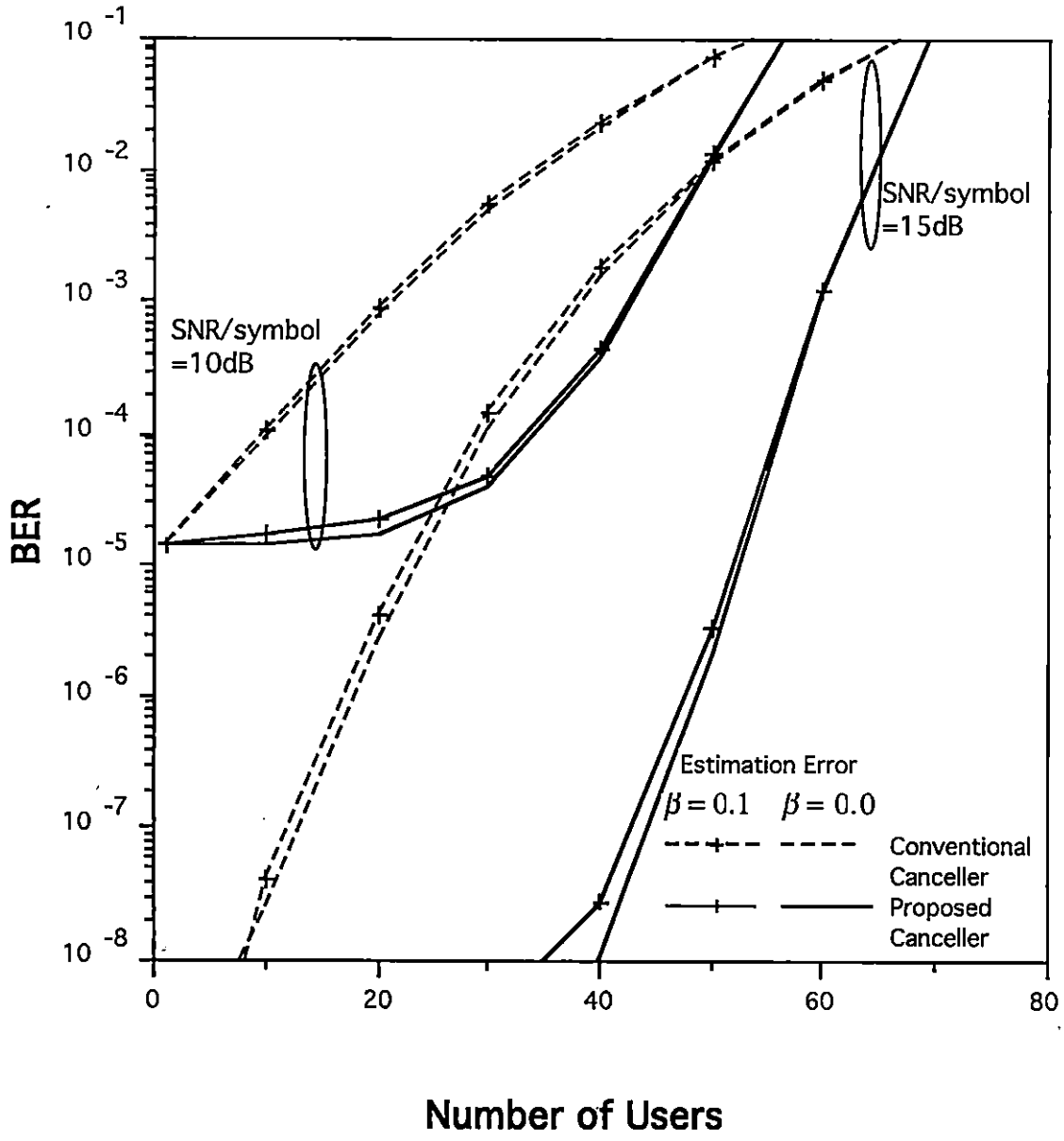

Figure 4.19 BER vs. Number of Users with Estimation Error,

Number of Paths=1, Coding Rate=1/3,
Constraint Length=9.

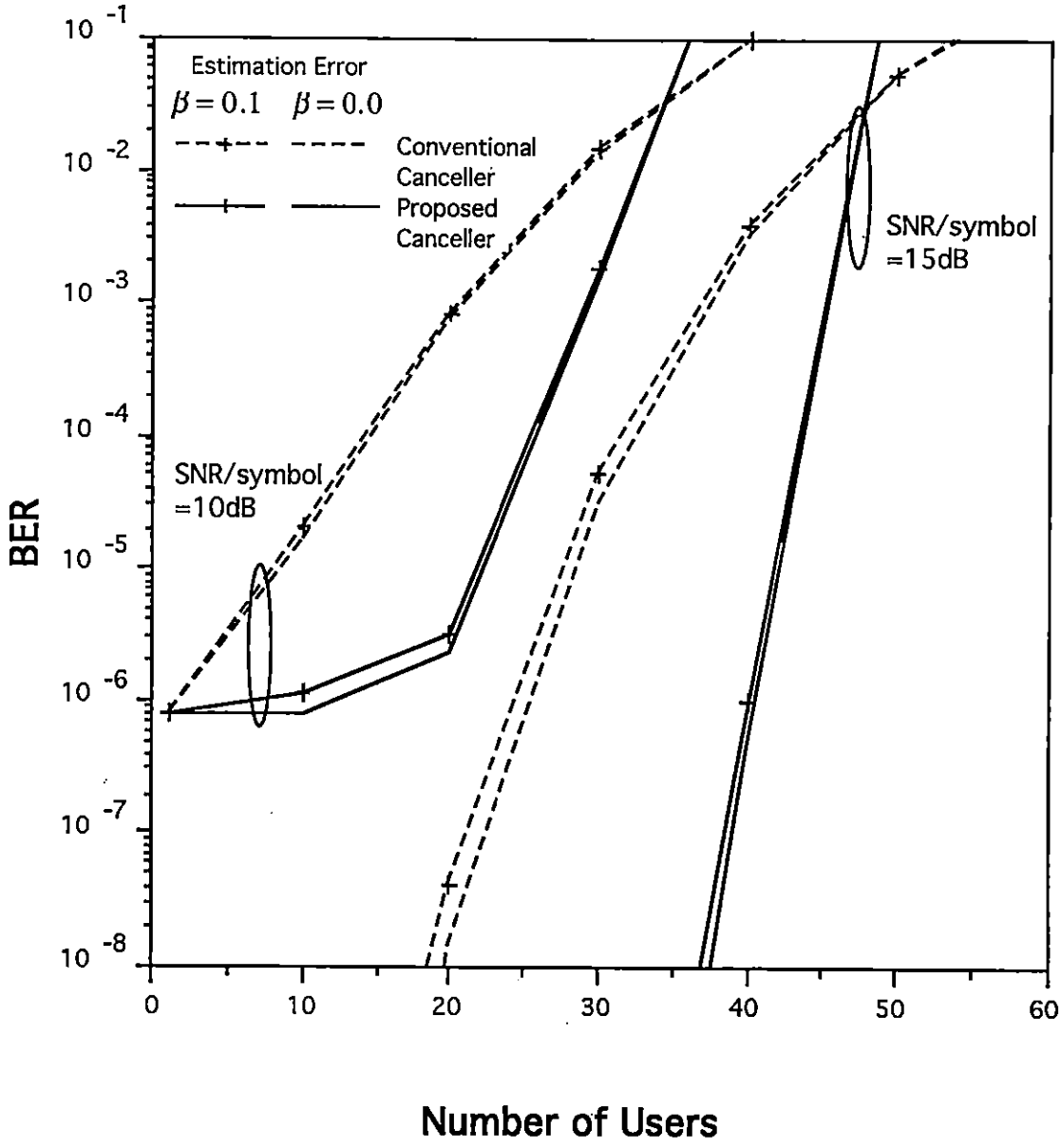

Figure 4.20 BER vs. Number of Users with Estimation Error,

Number of Paths=3, Coding Rate=1/3,
Constraint Length=9.

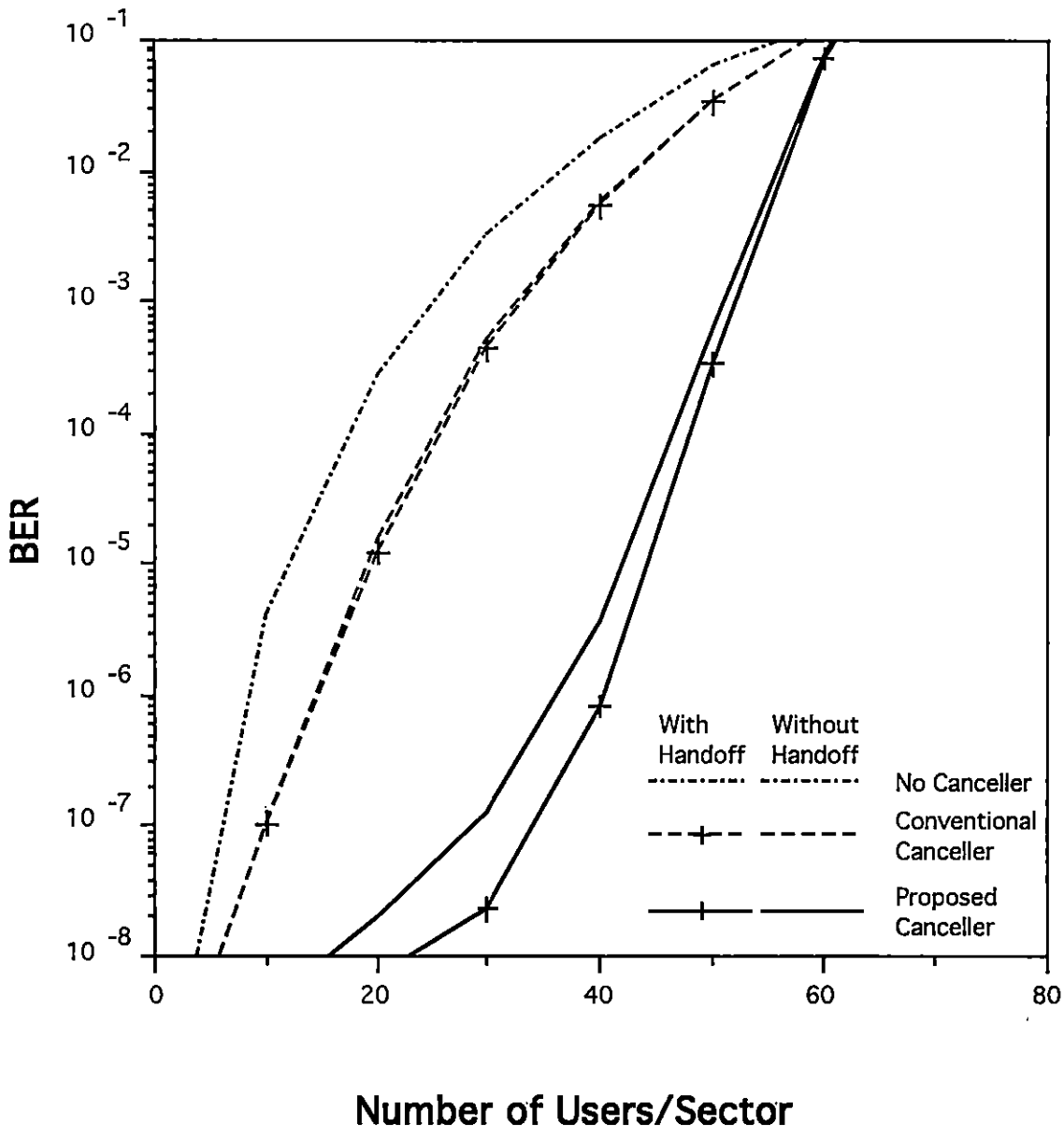

Figure 4.21 BER vs. Number of Users/Sector,

Number of Paths=1, SNR/symbol=15dB,
Code Rate=1/3, Constraint Length=9,
Handoff Probability=0.087.

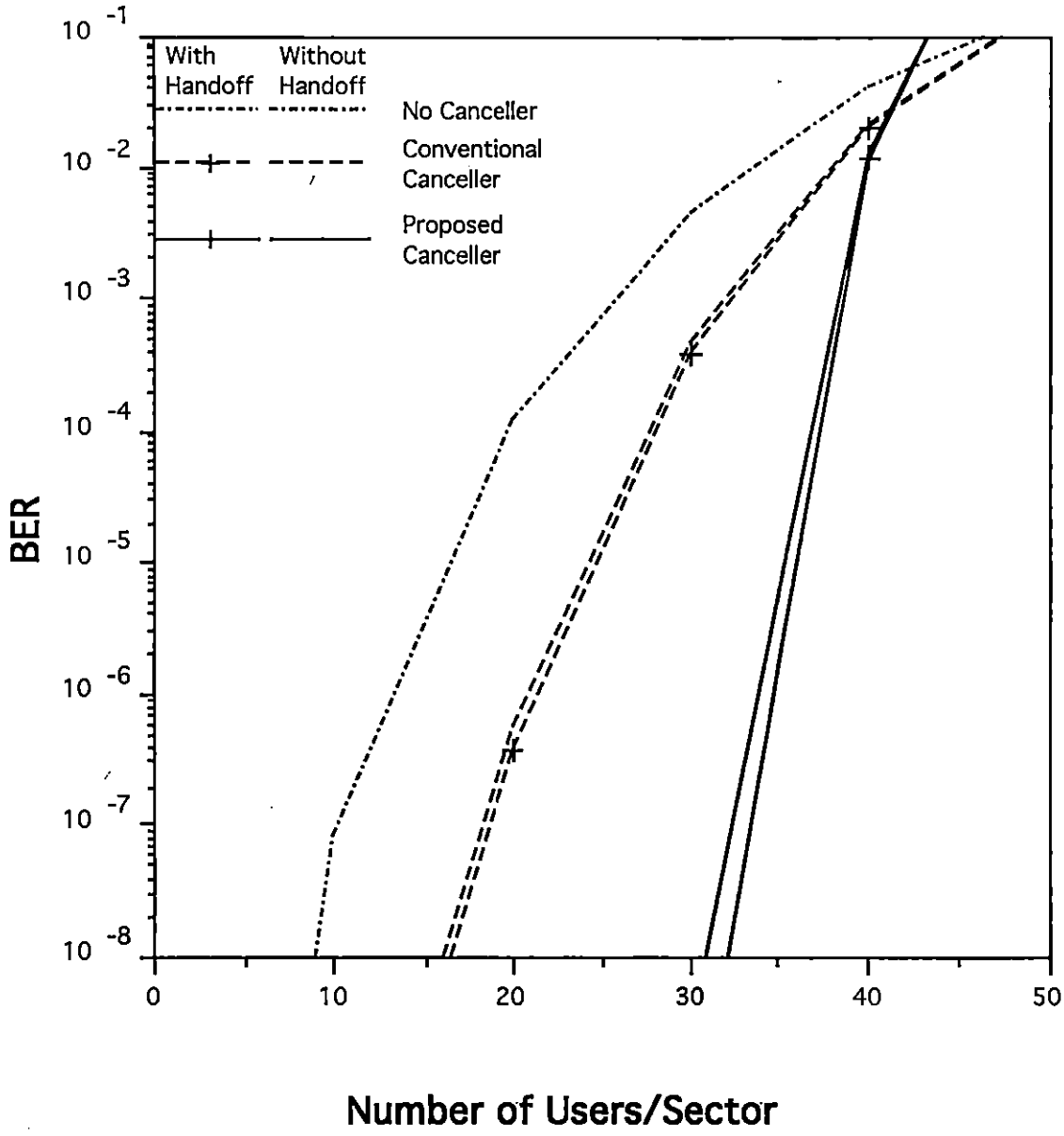

Figure 4.22 BER vs. Number of Users/Sector,

Number of Paths=3, SNR/symbol=15dB,
Constraint Length=9, Code Rate=1/3,
Handoff Probability=0.087.

4.4. Summary

In this chapter, the performances of the proposed co-channel interference cancellation technique on a multipath Rayleigh fading channel were investigated. It was shown that the proposed canceller offered one and a half to three times higher user capacity than the conventional canceller. It was also shown that the canceller significantly benefited from the use of the orthogonal convolutional code with a large constraint length. For the same performance as the conventional CCI canceller, the proposed canceller could effectively reduce the decoding complexity. The proposed canceller worked even in the presence of the interference due to imperfect cancellation. In the multicell configuration, the proposed canceller was shown to improve capacity by employing soft handoff.

Chapter 5: Conclusions and Future Research

5.1 Summary of the Thesis

In this thesis, a new parallel co-channel interference cancellation technique has been proposed. The proposed canceller improves the accuracy of the initial decision by utilizing the error correction capability of orthogonal convolutional codes. The performance of the proposed canceller has been investigated by theoretical analysis and computer simulation, and compared with the conventional canceller.

On both an AWGN channel and a multipath Rayleigh Fading channel, the proposed canceller offers 1.5 to 3 times higher user capacity than the conventional canceller. For up to about 40 users on the AWGN channel and about 20 users on the fading channel, the proposed CCI canceller cancels nearly all multiuser interference. It has also been shown that the canceller can significantly benefit from the use of a code with a large constraint length. For the same performance, the proposed canceller can effectively reduce the decoding complexity.

Moreover, the performance of the proposed canceller has been calculated in the presence of interference due to imperfect cancellation. Both the conventional and the proposed canceller work even if 10% of the CCI is left in the channel. Furthermore, the proposed canceller has been applied for the multicell system. In the multicell configuration, the proposed canceller has been shown to improve capacity improvement by employing soft handoff.

Since decoding of the orthogonal convolutional codes increases the processing delay, this system is primarily intended for data communications like the power line LAN system or wireless packet communications.

5.2 Suggestions for Future Work

In this thesis, only ideal interleaving has been assumed for simplicity of the analysis. However, non-ideal interleaving is more realistic on the fading channel. Therefore, analysis of the proposed canceller with non-ideal interleaving on the fading channel should be investigated.

Also, there are many kinds of coding schemes for CDMA systems. The performances of the proposed canceller with various coding schemes should be considered.

Finally, the proposed canceller is basically designed for the reverse link. To improve the overall capacity, it is also desirable to increase the bandwidth efficiency of the forward link. Although it is not practical to apply the proposed canceller directly to the mobile because of the complexity requirement, a simplified version of the proposed canceller might be employed.

References

[1] J. Zou, R. Pichna, Q. Wang, and V. K. Bhargava, "Efficient Methods for High Rate Data Transmission in Mobile and Personal Communications," Proc. of Memoria Technica of Mexicon '94, pp. 140-145, February 1994.

[2] M. K. Simon, J. K. Omura, R. A. Scholtz and B. K. Levitt, *Spread Spectrum Communications*- Vol. 1,2,3, Computer Science Press, 1985.

[3] K. S. Gilhousen, I. M. Jacobs, R. Padovani, A. J. Viterbi, L. A. Weaver, Jr., and C. E. Wheatley III, "On the Capacity of a Cellular CDMA System," IEEE Trans. on Vehi. Tech., Vol. 40, No. 2, pp. 303-312, May 1991.

[4] V. H. MacDonald, "The Cellular Concept," Bell System Technical Journal, Vol. 58, No. 1, pp. 15-45, January 1979.

[5] W. C. Y. Lee, "Overview of Cellular CDMA," IEEE Trans. on Vehi Tech., Vol. 40, No. 2, May 1991

[6] S. Verdu, "Adaptive Multiuser Detection, " Proc. of ISSSTA '94, pp. 43-50, July 1994.

[7] S. Verdu, "Minimum Probability of Error for Asynchronous Gaussian Multiple-Access Channels," IEEE Trans. Inform. Theory, Vol. IT-32, No. 1, pp. 85-96, January 1986.

[8] Z. Xie, C. K. Rushforth, and R. T. Short, "Multiuser Signal Detection Using Sequential Decoding," IEEE Trans. on Commun., Vol. 38, No. 5, pp. 578-583, May 1990.

[9] K. S. Schneider, "Optimum Detection of Code Division Multiplexed Signals," IEEE Trans. Aerosp. Electron. Syste., Vol. AES-15, pp. 181-185, January 1979.

[10] R. Lupas and S. Verdu, "Linear Multiuser Detectors for Synchronous Code-Division Multiple-Access Channels," IEEE Trans. Inform. Theory, Vol. IT-35, No. 1, pp. 123-136, January 1989.

[11] R. Lupas and S. Verdu, "Near-Far Resistance of Multiuser Detectors in Asynchronous Channels," IEEE Trans. on Commun., Vol. 38, No. 4, pp. 496-508, April 1990.

[12] A. Kajiwara and M. Nakagawa, "Microcellular CDMA System with a Linear Multiuser Interference Canceler," IEEE J. Select. Areas Commun., Vol. 12, No. 4, pp. 605-611, May 1994.

[13] A. Duel-Hallen, "Decorrelating Decision-Feedback Multiuser Detector for Synchronous Code-Division Multiple-Access Channel," IEEE Trans. on Commun., Vol. 41, No. 2, pp. 285-290, February 1993.

[14] Z. Xie, R. T. Short, and C. K. Rushforth, "A Family of Suboptimum Detectors for Coherent Multiuser Communications," IEEE J. Select. Areas Commun., Vol. 8, No. 4, pp. 683-690, May 1990.

[15] M. K. Varanasi and B. Aazhang, "Multistage Detection in Asynchronous Code-Division Multiple-Access Communications," IEEE Trans. on Commun., Vol. 38, No. 4, pp. 509-519, April 1990.

[16] Y. C. Yoon, R. Kohno and H. Imai, "A Spread-Spectrum Multiaccess System with Cochannel Interference Cancellation for Multipath Fading Channels," IEEE J. Select. Areas Commun., Vol. 11, No. 7, pp. 1067-1075, September 1993.

[17] Telecommunication Industry Association, TIA/EIA/IS-95, "Mobile Station-Base Station Compatibility Standard for Dual-Mode Wideband Spread Spectrum Cellular System," July 1993.

[18] B. D. Trumpis, "Convolutional coding for M-ary channels," Ph.D. dissertation, UCLA, 1975.

[19] P. Dent, B. Gudmundson, and M. Ewerbring, "CDMA-IC: A Novel Code Division Multiple Access Scheme based on Interference Cancellation," Proc. of PIMRC '92, pp. 4.1.1-4.1.5, October 1992.

[20] R. Kohno, H. Imai, M. Hatori, and S. Pasupathy, "An Adaptive Canceller of Cochannel Interference for Spread Spectrum Multiple-Access Communication Networks in a Power Line," IEEE J. Select. Areas Commun., Vol. 8, No. 4, pp. 691-699, May 1990.

[21] S. Tachikawa, "Performance of M-ary / Spread Spectrum Multiple Access Communication Systems using Co-Channel Interference Cancellation Techniques," Proc. of IEEE ISSSTA '92, pp. 5.4, December 1992.

[22] S. Tachikawa, "Characteristics of M-ary / Spread Spectrum Multiple Access Communication Systems using Co-Channel Interference Cancellation Techniques," IEICE Trans. on Commun., Vol. E76-B, No. 8, pp. 941-946, August 1993.

[23] A. J. Viterbi, "Very Low Rate Convolutional Codes for Maximum Theoretical Performance of Spread-Spectrum Multiple-Access Channels," IEEE J. Select. Areas Commun., Vol. 8, No. 4, pp. 641-649, May 1990.

[24] M. B. Pursley, "Performance Evaluation for Phase-Coded Spread-Spectrum Multiple-Access Communications - Part 1:System Analysis," IEEE Trans. on Commun. Vol. 25, No. 8, pp. 795-799, August 1977.

[25] J. Proakis, *Digital Communications,* New York, McGraw-Hill, 1989.

[26] S. Lin and D. Costello, Jr., *Error Control Coding: Fundamentals and Applications*, Englewood Cliffs, N.J., Prentice-Hall, 1983.

[27] G. C. Clark, Jr., and J. B. Cain, *Error-Correcting Coding for Digital Communications*, Plenum Press, New York, 1981.

[28] K. I. Kim, "On the Error Probability of a DS/SSMA System with a Noncoherent M-ary Orthogonal Modulation," Proc. of IEEE Vehi. Tech. Conf. '92, pp. 482-485, May 1992.

[29] W. C. Lee, *Mobile Communication Engineering*, McGraw-Hill, New York, 1982.

[30] Q. Bi, "Performance Analysis of a CDMA Cellular System," Proc. of Vehi. Tech. Conf. '92, pp. 43-46, May 1992.

[31] Q. Bi, "On Performance Improvement of Asynchronous CDMA Systems Through the Use of Orthogonal Sequence Spreading," Proc. of ICC '93, pp. 147-150, May 1993.

[32] A. C. K. Soong, "A Multi-Stage Interference Cancellation Scheme for CDMA Wireless Systems," Proc. of Wireless '94, pp. 729-736, July 1994.

[33] K. I. Kim, "CDMA Cellular Engineering Issues," IEEE Trans. on Vehi. Tech., Vol. 42, No. 3, pp. 345-350, August 1993.

[34] M. Gudmundson, "Analysis of Handover Algorithms," Proc. of Vehi. Tech. Conf. '91, pp. 537-542, May 1991.

[35] J. M. Wozencraft and I. M. Jacobs, *Principles of Communication Engineering*, John Wiley & Sons, New York, 1965.

Appendix

A. Interference

The self interference on the output of the I-channel's m-th correlator is

$$I_{I,I}^{k\lambda,k\lambda} = \sqrt{\frac{P}{T_s}} \int_0^{T_s} \gamma_{k\lambda}(t-\tau_{k\lambda}) W^r(t-T_d-\tau_{k\lambda}) W^m(t-\tau_{k\lambda}) \cdot c_k(t-T_d-\tau_{k\lambda}) c_k(t-\tau_{k\lambda}) p_Q(t-T_d-\tau_{k\lambda}) p_I(t-\tau_{k\lambda}) \frac{\sin\theta_{k\lambda}}{2} dt \quad . \tag{A1}$$

The interference due to the other paths of the same user is

$$I_{I,I}^{k\lambda,kj} = \sqrt{\frac{P}{T_s}} \sum_{\substack{j=1 \\ j\neq\lambda}}^{L_k} \int_0^{T_s} \gamma_{kj}(t-\tau_{kj}) [W^r(t-\tau_{kj}) W^m(t-\tau_{k\lambda}) \cdot c_k(t-\tau_{kj}) c_k(t-\tau_{k\lambda}) p_I(t-\tau_{kj}) p_I(t-\tau_{k\lambda}) \frac{\cos\theta_{kj}}{2} + W^r(t-T_d-\tau_{kj}) W^m(t-\tau_{k\lambda}) c_k(t-T_d-\tau_{kj}) c_k(t-\tau_{k\lambda}) \cdot p_Q(t-T_d-\tau_{kj}) p_I(t-\tau_{k\lambda}) \frac{\sin\theta_{kj}}{2}] dt \quad . \tag{A2}$$

The interference due to the other users is

$$I_{I,I}^{k\lambda,ij} = \sqrt{\frac{P}{T_s}} \sum_{\substack{i=1 \\ i\neq k}}^{K} \sum_{j=1}^{L_i} \int_0^{T_s} \gamma_{ij}(t-\tau_{ij}) [W^r(t-\tau_{ij}) W^m(t-\tau_{k\lambda}) \cdot c_i(t-\tau_{ij}) c_k(t-\tau_{k\lambda}) p_I(t-\tau_{ij}) p_I(t-\tau_{k\lambda}) \frac{\cos\theta_{ij}}{2} + W^r(t-T_d-\tau_{ij}) W^m(t-\tau_{k\lambda}) c_i(t-T_d-\tau_{ij}) c_k(t-\tau_{k\lambda}) \cdot p_Q(t-T_d-\tau_{ij}) p_I(t-\tau_{k\lambda}) \frac{\sin\theta_{ij}}{2}] dt \quad . \tag{A3}$$

The thermal noise is

$$N_{I,I}^{k\lambda} = \frac{1}{\sqrt{T_s}} \int_0^{T_s} \frac{n_c(t)}{2} c_k(t-\tau_{k\lambda}) p_I(t-\tau_{k\lambda}) W^m(t-\tau_{k\lambda}) dt \quad . \tag{A4}$$

Next the statistics of the interference are considered. It is assumed that the PN sequences are independent and identically distributed binary sequences and the chip pulse shape is rectangular.

From [28][30][31], the variance of the interference due to the other paths is (the variances of $I_{I,Q}^{k\lambda,kj}$, $I_{Q,I}^{k\lambda,kj}$, and $I_{Q,Q}^{k\lambda,kj}$ are the same as that of $I_{I,I}^{k\lambda,kj}$.)

$$Var\{I_{I,I}^{k\lambda,kj}\} = \sum_{\substack{j=1 \\ j\neq\lambda}}^{L_k} \bar{\gamma}_{kj} \frac{2}{3} \cdot \frac{E_s}{4Gp} = \sum_{\substack{j=1 \\ j\neq\lambda}}^{L_k} \bar{\gamma}_{kj} \frac{E_s}{6Gp} \tag{A5}$$

where $\bar{\gamma}_{ij}$ is the average attenuation for the *j-th* path of the *i-th* user's channel. Also the variance of the interference due to the other users is (the variances of $I_{I,Q}^{k\lambda,ij}$, $I_{Q,I}^{k\lambda,ij}$, and $I_{Q,Q}^{k\lambda,ij}$ are the same as that of $I_{I,I}^{k\lambda,ij}$.)

$$Var\{I_{I,I}^{k\lambda,kj}\} = \sum_{\substack{i=1 \\ i\neq k}}^{K} \sum_{j=1}^{L_k} \bar{\gamma}_{ij} \frac{E_s}{6Gp} \quad . \tag{A6}$$

Due to the quadrature modulation, the variance of the self interference is half of the other interference in terms of the same attenuation $\tilde{\gamma}_{ij}$. Therefore (the variances of $I_{I,Q}^{k\lambda,k\lambda}$, $I_{Q,I}^{k\lambda,k\lambda}$, and $I_{Q,Q}^{k\lambda,k\lambda}$ are the same as that of $I_{I,I}^{k\lambda,k\lambda}$.)

$$Var\{I_{I,I}^{k\lambda,k\lambda}\} = \bar{\gamma}_{k\lambda} \frac{E_s}{12Gp} \quad . \tag{A7}$$

Since the self interference is small compared to the other interference, it is assumed as in [28] that they are negligible.

The variance of the thermal noise is (the variances of $N_{Q,Q}^{k\lambda}$, $N_{I,Q}^{k\lambda}$, and $N_{Q,I}^{k\lambda}$ are the same as that of $N_{I,I}^{k\lambda}$.)

$$Var\{N_{I,I}^{k\lambda}\} = \frac{N_o}{4} \quad . \tag{A8}$$

Then assuming the thermal noise terms and the interference terms are uncorrelated, $N_{I,I}^{k\lambda} + N_{Q,Q}^{k\lambda} + I_{I,I}^{k\lambda,kj} + I_{I,I}^{k\lambda,ij} + I_{Q,Q}^{k\lambda,kj} + I_{Q,Q}^{k\lambda,ij}$ is Gaussian distributed with zero mean and variance

$$\frac{\sum_{i=1}^{K} \sum_{j=1}^{L_i} \bar{\gamma}_{ij} E_s - \bar{\gamma}_{k\lambda} E_s}{3Gp} + \frac{N_o}{2} = N_t \quad . \tag{A9}$$

Similarly $N_{I,Q}^{k\lambda} - N_{Q,I}^{k\lambda} + I_{I,Q}^{k\lambda,kj} + I_{I,Q}^{k\lambda,ij} - I_{Q,I}^{k\lambda,kj} - I_{Q,I}^{k\lambda,ij}$ is Gaussian distributed with zero mean and variance

$$SNR_{\kappa\lambda} = \frac{\bar{\gamma}_{\kappa\lambda} E_s}{\frac{2\left(\sum_{i=1}^{K}\sum_{j=1}^{L_i} \bar{\gamma}_{ij} E_s - \bar{\gamma}_{\kappa\lambda} E_s\right)}{3Gp} + N_o} \quad . \tag{A10}$$

B. Probability of Selecting the Incorrect Path

From Equation (4.13), the decision variable for the κ-th user on the m-th correlator is

$$S^{\kappa}(m) = \sum_{j=1}^{L_\kappa} \{[Z_{I,I}^{\kappa j}(m) + Z_{Q,Q}^{\kappa j}(m)]^2 + [Z_{I,Q}^{\kappa j}(m) - Z_{Q,I}^{\kappa j}(m)]^2\} \quad . \tag{B1}$$

Thus $S^{\kappa}(m)$ has a chi-square probability distribution with $2L_\kappa$ degrees of freedom. Assuming there are $L_\kappa = L$ paths and d is the distance of the coded sequence along the wrong path in the state diagram from the coded sequence along the correct path, the decision variable between paths has a chi-square probability distribution with $2dL$ degrees of freedom

$$\sum_{j=1}^{dL} \{[Z_{I,I}^{\kappa j}(m) + Z_{Q,Q}^{\kappa j}(m)]^2 + [Z_{I,Q}^{\kappa j}(m) - Z_{Q,I}^{\kappa j}(m)]^2\} = \sum_{l=1}^{2dL} \{r_l\}^2 \quad . \tag{B2}$$

Therefore, the probability of choosing a wrong path is

$$Pd(d,L) = P\left[\sum_{l=1}^{2dL} \{r_l'\}^2 > \sum_{l=1}^{2dL} \{r_l\}^2\right] \tag{B3}$$

where r_l is the output of a matched filter corresponding to the correct path while r_l' corresponds to the wrong path. Therefore $\{r_l\}$ and $\{r_l'\}$ are statistically independent zero-mean Gaussian random variables with variance

$$\overline{\{r_l\}^2} = \frac{E[\gamma E_s] + N_o + I_{co}}{2} \cong \sigma^2 \quad , \tag{B4}$$

$$\overline{\{r_l'\}^2} = \frac{N_o + I_{co}}{2} \cong \sigma'^2 \tag{B5}$$

where N_o is the noise and I_{co} is the co-channel interference. The density function of a chi-square distribution with $2dL$ degrees of freedom is[35, pp. 542]

$$p(\alpha)=\frac{1}{(dL-1)!}\frac{\alpha}{\sigma^2}\left(\frac{\alpha^2}{2\sigma^2}\right)^{dL-1}\exp\left(-\frac{\alpha^2}{2\sigma^2}\right) \quad , \tag{B6}$$

$$p'(\beta)=\frac{1}{(dL-1)!}\frac{\beta}{\sigma'^2}\left(\frac{\beta^2}{2\sigma'^2}\right)^{dL-1}\exp\left(-\frac{\beta^2}{2\sigma'^2}\right) \quad . \tag{B7}$$

The probability of selecting the wrong path is

$$Pd(d,L)=\int_{-\infty}^{\infty}p(\alpha)d\alpha\int_{\alpha}^{\infty}p'(\beta)d\beta \quad . \tag{B8}$$

Carrying out the integrations of Equation (B8) by parts, first

$$\int_{\alpha}^{\infty}p'(\beta)d\beta=\exp\left(-\frac{\alpha^2}{2\sigma'^2}\right)\left[1+\frac{\alpha^2/2\sigma'^2}{1!}+\frac{(\alpha^2/2\sigma'^2)^2}{2!}+\cdots+\frac{(\alpha^2/2\sigma'^2)^{dL-1}}{(dL-1)!}\right] \tag{B9}$$

and then

$$Pd(d,L)=\left(\frac{\sigma'^2}{\sigma'^2+\sigma^2}\right)^{dL}\left[1+\binom{dL}{1}\left(\frac{\sigma^2}{\sigma'^2+\sigma^2}\right)+\binom{dL+1}{2}\left(\frac{\sigma^2}{\sigma'^2+\sigma^2}\right)^2+\cdots+\binom{2dL-2}{dL-1}\left(\frac{\sigma^2}{\sigma'^2+\sigma^2}\right)^{dL-1}\right] \quad . \tag{B10}$$

The error probability depends on the average received signal energy $\overline{E_s}=E[\gamma E_s]$ through the parameters

$$p=\frac{\sigma'^2}{\sigma'^2+\sigma^2}=\frac{1}{2+\overline{E_s}/(N_o+I_{co})} \tag{B11}$$

and

$$1-p=\frac{\sigma^2}{\sigma'^2+\sigma^2} \quad . \tag{B12}$$

Therefore,

$$Pd(d,L)=p^{dL}\sum_{h=0}^{dL-1}\binom{dL-1+h}{h}(1-p)^h \quad . \tag{B13}$$

VITA

Surname: Sanada **Given Names:** Yukitoshi
Place of Birth: Tokyo, Japan **Date of Birth:** 12 July, 1969

Educational Institutes Attended:

Keio University 1988 to 1992

Degrees Awarded:

B.Eng. Keio University 1992

Publications:

[1] Yukitoshi Sanada, Akihiro Kajiwara, Masao Nakagawa, "Adaptive RAKE Receiver for Mobile Communications," IEICE Transactions on Communications, Vol. E76-B, pp. 1002-1007, August 1993.

[2] Yukitoshi Sanada, Qiang Wang, "Co-Channel Interference Cancellation Technique using Orthogonal Convolutional Codes," IEEE Transactions on Communications (Revised and Resubmitted).

[3] Yukitoshi Sanada, Qiang Wang, "A Co-Channel Interference Cancellation Technique using Orthogonal Convolutional Codes on Multipath Rayleigh Fading Channel," submitted to IEEE Transactions on Vehicular Technology.

[4] Kazuhiko Seki, Yukitoshi Sanada, Qiang Wang, Shuzo Kato, and Vijay K. Bhargava, "A Wireless Multimedia Network on a Time Division Duplex CDMA/TDMA," submitted to IEICE Transactions on Communications, Japan.

[5] Yukitoshi Sanada, Kazuhiko Seki, Qiang Wang, Masao Nakagawa, Shuzo Kato, and Vijay K. Bhargava, "A Transmission Power Control Technique on a TDD-CDMA/TDMA system for Wireless Multimedia Networks," submitted to IEICE Transactions on Communications, Japan.

[6] Yukitoshi Sanada, Kazuhiko Seki, Qiang Wang, Masao Nakagawa, Shuzo Kato, and Vijay K. Bhargava, "A Channel Equalization Technique on a Time Division Duplex CDMA/TDMA system for Wireless Multimedia Networks" submitted to IEICE Transactions on Communications, Japan.

[7] Yukitoshi Sanada, Akihiro Kajiwara, Masao Nakagawa, "Adaptive RAKE System for Mobile Communications," Proc. of International Conference on Selected Topics in Wireless Communications, Session 10.4, June 1992.

[8] Yukitoshi Sanada, Qiang Wang, "Co-Channel Interference Cancellation Technique using Orthogonal Convolutional Codes," Proc. of IEEE ISSSTA '94, pp. 176-180, July 1994.

[9] Yukitoshi Sanada, Qiang Wang, "A Co-Channel Interference Cancellation Technique using Orthogonal Convolutional Codes on Multipath Rayleigh Fading Channel," accepted to IEEE International Conference on Communication '95, June 1995.

[10] Kazuhiko Seki, Yukitoshi Sanada, Qiang Wang, Shuzo Kato, and Vijay K. Bhargava, "A Wireless Multimedia Network on a Time Division Duplex CDMA/TDMA," accepted to Pacrim '95, May 1995.

Partial Copyright License

I hereby grant the right to lend my thesis to users of the University of Victoria Library, and to make single copies only for such users or in response to a request from the Library of any other university, or similar institution, on its behalf or for one of its users. I further agree that permission for extensive copying of this thesis for scholarly purposes may be granted by me or a member of the University designated by me. It is understood that copying or publication of this thesis for financial gain shall not be allowed without my written permission.

Title of Thesis: A Co-Channel Interference Cancellation Technique using Orthogonal Convolutional Codes

Author: [redacted]
Yukitoshi Sanada

Date: January 27, 1995